

**Photothermal Experiments on Condensed Phase
Samples of Agricultural Interest:
Optical and Thermal Characterization**

Promotoren: **dr. J. Reuss**
emeritus hoogleraar in de molecuul- en laserfysica
Katholieke Universiteit Nijmegen

dr. G.P.A. Bot
hoogleraar in de technische natuurkunde
Landbouwuniversiteit Wageningen

Co-promotor: **dr. D. Bicanic**
universitair hoofddocent,
departement Agro-, Milieu en Systeemtechnologie
Landbouwuniversiteit Wageningen

NN02201, 2337

**Photothermal Experiments on Condensed Phase
Samples of Agricultural Interest:
Optical and Thermal Characterization**

Jan Paul Favier

proefschrift
ter verkrijging van de graad van doctor
op gezag van de rector magnificus
van de Landbouwniversiteit te Wageningen,
dr. C.M. Karsen,
in het openbaar te verdedigen
op vrijdag 31 oktober 1997
des namiddags te vier uur in de Aula.

Jan Paul Favier
1997

CIP-Data Koninklijke Bibliotheek, DEN HAAG

Favier J.P.

Photothermal Experiments on Condensed Phase Samples of Agricultural Interest:
Optical and Thermal Characterization / J.P. Favier.

[S.I. : s.n.]

Thesis Wageningen Agricultural University. -With ref. - With summary in Dutch

ISBN 90-5485-768-4

Cover: Nazca lines in Peru, the spider (46 meters), the monkey (90 meters) and the
humming bird (110 meters)

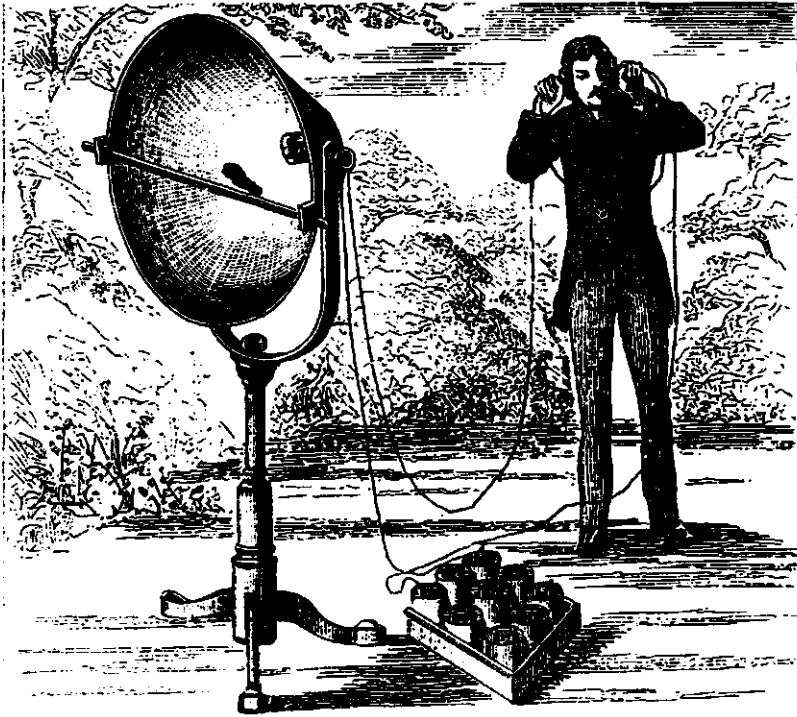
BIBLIOTHEEK
LANDBOUWUNIVERSITEIT
WAGENINGEN

Stellingen

- 1 De standaard fotopyroelektrische techniek maakt het mogelijk om snel en nauwkeurig de warmtevereffeningscoëfficiënt (m^2s^{-1}) te bepalen van zowel vaste stoffen, vloeistoffen als pasta's.
Daderlat *et al.*, *Chem. Phys. Lipids* **82**, 115-123 (1996)
dit proefschrift
- 2 Het concept van het optothermisch venster levert een elegante en eenvoudige methode om vloeistoffen spectroscopisch te analyseren.
dit proefschrift
- 3 Fotothermische technieken zullen in combinatie met moderne scheidings-technieken de detectielimieten aanscherpen.
Tran C.D. *et al.*, *Anal. Chem. Acta* **299**, 361-369 (1995)
Franko M. *et al.*, ingediend *Chromatography* (1997)
- 4 Indien entropie intuïtief wordt gedefinieerd als maat voor de hoeveelheid wanorde, is dit in tegenspraak met het harde bollen systeem, aangezien de entropie van dit model, bij voldoende hoge dichtheid, in de geordende kristallijne fase groter is dan in de wanordelijke vloeistoffase.
B.J. Alder and T.E. Wainwright, *J. Chem. Phys.* **27**, 1207 (1957)
M. Dijkstra, proefschrift Universiteit Utrecht (1995)
R. van Roij, proefschrift Universiteit Utrecht (1996)
- 5 Door de lage structuurstabiliteit van het Fc fragment en de relatief hoge structuurstabiliteit van het F(ab')₂ fragment zal de bindingsactiviteit van geadsorbeerd IgG voor hCG behouden blijven onder verschillende adsorptie omstandigheden.
J. Buijs, proefschrift Landbouwniversiteit Wageningen (1995)
- 6 Differential Scanning Calorimetry is een "cantankerous device" dat onderzoekers meer problemen geeft dan oplost.
V.E. Sweat, Chapter 2, *Engineering properties of foods*, M.A. Rao and S.S.H. Rizvi (1994)

- 7 Volgens Felicia Huppert hebben vrouwen een beter geheugen dan mannen. Dat betekent dat bij verdergaande emancipatie het fenomeen "verstrooide professor" zal verdwijnen.
Intermediair 20-2-1997
- 8 In de toekomst zal bodemverontreiniging vooral aangepakt worden door gefundeerd niets doen.
- 9 Als het aantal dodelijke slachtoffers van malaria in de Westerse wereld een voelbare fractie zou zijn van dat in de tropen, dan zou er harder naar een oplossing worden gezocht.
- 10 Voetbal zou een stuk aantrekkelijker worden als men met dezelfde frequentie regelwijzigingen zou doorvoeren als bij het hockey.
- 11 Erkennen dat men zich heeft vergist, is slechts constateren dat men vandaag meer inzicht heeft dan gister.
- 12 Kindertelevisie is volwassen geworden en volwassenentelevisie kinds, dat betekent dat televisie in ieder geval met zijn tijd mee gaat.

Stellingen behorend bij het proefschrift "Photothermal Experiments on Condensed Phase Samples of Agricultural Interest: Optical and Thermal Characterization" van Jan Paul Favier, Landbouwwuniversiteit Wageningen, 31 oktober 1997



The Articulating Photophone. The Selenium Receiver

Contents

1	Introduction to Photothermal Science	1
2	Photoacoustic Spectroscopy for Optical Characterization of Different Samples	9
2.1	Photoacoustic Characterization of Different Food Samples	11
2.2	New and Versatile Photoacoustic Cell for Studies of Powdered Specimens Across Broad Spectral Range	21
2.3	Organic Compounds Measured with Infrared (3.39 μm) Photoacoustics	29
3	Optothermal Window Spectroscopy for Optical Characterization of Different Samples	35
3.1	Detection of Total Trans Fatty Acids Content in Margarine: an Intercomparison Study of GLC, GLC + TLC, FTIR, and Optothermal Window (Open Photoacoustic Cell)	37
3.2	CO ₂ Laser Infrared Optothermal Spectroscopy for Quantitative Adulteration Studies of Extra Virgin Olive Oil in Binary Mixtures	49
3.3	Optothermal Detection of Infrared Radiation-Induced Absorption in Aqueous Solutions of Carbohydrates: Lactose and Corn Starch	57
3.4	Compact, Open and General Purpose Cell of Variable Effective Pathlength: Direct Absorption Measurement of SO ₄ ²⁻ in Water	65
4	Thermal Characterization of Different Samples	69
4.1	Thermal Diffusivity of Hard Boiled Candy Obtained by Photothermal Beam Deflection and Standard Photopyroelectric Method	71
4.2	Photopyroelectric (PPE) Measurement of Thermal Diffusivity in Low Density Polyethylene (LDPE) and Polyvinyl Chloride (PVC) Foils	83
	Summary	97
	Samenvatting	101
	Dankwoord	105
	Curriculum Vitae	107
	List of Publications	109

1 Introduction to Photothermal Science

History

Photothermal (PT) science is a cumulative name for a class of phenomena that involve the generation of heat caused by the absorption of modulated or pulsed radiation. The first report on photoacoustic (PA) effect, the oldest among PT phenomena, dates back to 1880.¹ The discoverer Alexander Bell and his coworker Tainter were ahead of their time when using the photophone to transmit the 'speech' by modulated light over a distance of 213 meter. Rayleigh, Röntgen, Mercadier, and Tyndall were among the scientists who were also involved in studying the new phenomena. Due to practical limitations of hearing tubes used as detectors in the early experiments, the PA effect remained a scientific curiosity, but some interesting conclusions could be made. For example, Mercadier who performed PA spectroscopic studies on various materials, came to the conclusion that "the maximum effect was found to be produced by the red rays and by the invisible ultra-red rays". Likewise, Röntgen stated that "the sounds in question are due to the bending of the plates under unequal heating".

It was only at the beginning of the 1970s that the PA effect was rediscovered mainly due to the event of lasers (well defined and strong radiation sources) and the development in electronics (microphones, diodes etc.). The introduction of the Rosencwaig-Gersho theory^{2,3} that has described the PA effect and the concept of the 'thermal wave' led to numerous, new PT detection schemes and various applications. In general one distinguishes two classes of PT methods, i.e. those for optical characterization and thermal characterization of a sample.

The photothermal experiment

In the November 4 1880 issue of Nature one reads the following:

"A beam of light from the sun or from a powerful artificial source, such as an electrical lamp, falls upon a mirror and is reflected through a large lens, which concentrates the rays to a focus. Just at the focus is interposed a disk pierced with holes, forty or so in number, arranged in a circle. This disk can be rotated so that the light is interrupted from one to five or six hundred times a second. The intermittent beam thus produced is received by a lens, or a pair of lenses upon a common support, whose function is to render the beam once more parallel, or to concentrate it upon the disk of ebonite placed immediately behind, but not quite touching them. From the disk a tube conveys the sound to the ear. We may remind our readers here that this apparent direct conversion of light into sound takes place, as Prof. Bell found, in disks of all kinds of substances hard rubber, zinc, antimony, selenium, ivory,

parchment, wood, and that he has lately found that disks of carbon and of thin glass, which he formerly thought exceptions to this property, do also behave the same way.”

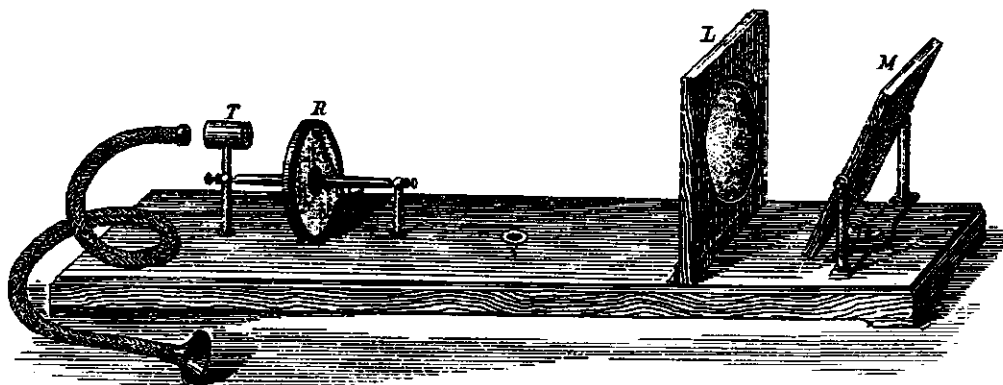


Figure 1 Photophone used by Bell and Tainter where light was reflected by mirror M on a large lens L which focused the light on a rotating disk with holes R. The lens system T concentrated the beam on the sample (not in figure)¹

Modern experimental set-up for PA studies resembles Bell's photophone; the radiation source is either a powerful lamp (with a monochromator) or a laser, the pressure wave is detected by a sensitive transducer and the modulated signal processed by a phase sensitive lock-in amplifier.

Recent PT trends in agricultural and environmental sciences

Worldwide developments of new PT detection schemes have also had a substantial impact in the field of agricultural and environmental sciences.⁴⁻⁸ In the Netherlands most significant progress was made in highly sensitive and on-line PA concentration measurements of atmospheric and biological gases.^{5,9-11} The concept of intermodulated Stark PA spectroscopy⁹ proved the unique and elegant approach to suppress the unwanted interferences without the loss in sensitivity.

Further development of PT techniques and their applications for optical as well as thermal characterization of condensed phase samples seemed the next logical step. The generally recognized lack of data about thermal properties and in particular their temperature dependence is another important topic worth investigating.

To what it concerns the choice of condensed phase samples, foods in general deserve considerable attention. At the moment numerous (analysis) techniques are under development and existing techniques optimized. Analysis and quantitative testing of product composition

represent an important research area in the analysis of (food) compounds. Another active research area is that associated with the quality and safety of foods.

Target samples like powders, opaque liquids and gels of special interest as they are generally difficult to study with available techniques. There are the high absorption and the scattering resulting in low amount of radiation throughput, that constitute major problems in transmission spectroscopy because the information about absorbance of the sample is derived from the measurement of transmitted energy. The essential feature of PT techniques is that the signal is proportional to the energy absorbed by the sample and therefore PT techniques don't have this problem.

Photothermal techniques can be regarded as instrumental methods for investigation of material physical properties. In this research new photothermal methods have been proposed and tested as candidate techniques for obtaining thermal and optical properties of agricultural products. Exploitation of qualitative and quantitative photothermal studies was concentrated on (food) samples not easily amenable (e.g. high scattering and strong absorption) to traditional methods. Examples include trace analysis, studies of liquids and solids, non-destructive sampling, adulteration etc. The new techniques and instrumentation are characterized by their reliability, sensitivity, ease of operation, speed, compactness, small quantity of sample needed for analysis and a relatively low cost. Recent progress in the development of new radiation sources, transducers and data acquisition justified the studies described in this thesis. It is anticipated that in the near future photothermal methods will be generally accepted as a valuable analytical tool.

This PhD thesis describes the applications of several new PT techniques to condensed phase samples. Spectroscopic studies were made on flours, oils, fatty acids (margarine), aqueous solutions of carbohydrates and water pollutants. Thermal investigations concerned mainly concentrated sugar systems (candies) and polymer materials used for food packaging.

Two different PA techniques were used here for optical characterization are described in following two chapters. In chapter 2 PA spectroscopy was used for investigation of powdered and liquid samples. Initially, spectra of various flours (differing in color and grain size) and spices were studied in the visible part of the electromagnetic spectrum. Then, a new PA cell for infrared measurements was constructed and a spectrum of Bovine Serum Albumin was recorded in the 10P wavelength range of the CO₂ laser. The same PA cell was used with an infrared He-Ne laser (wavelength 3.39 μm) to study various compounds (alcohols, liquid and solid carboxylic acids) as a function of the chain length.

The concept of optothermal window, an elegant and new approach to obtain the absorption coefficients of "difficult" to study specimens (such as optically opaque and highly viscous samples), is discussed in chapter 3. The feasibility of the new technique was demonstrated and the results compared to these obtained by other established techniques such as FTIR and GLC. In this thesis, the use of optothermal window was extended to 5-6 μm and 9-11 μm spectral regions both rich in characteristic absorption bands of different molecules. Initially, the content of trans fatty acids in margarine was determined. Then, the extent of adulteration (with known adulterants) in virgin olive oil was measured. Since most biological systems contain water, optothermal measurements were also performed on aqueous solutions (i.e. sulfate and carbohydrates). Traditional infrared analysis of such systems is precluded due to an intrinsically strong absorption of water in the same region.

The standard photopyroelectric method (PPE), a newly proposed technique for thermal characterization of condensed phase samples is described in chapter 4. Its usability was demonstrated by obtaining thermal diffusivity over a wide temperature range (including the region of glass transitions) for a hard boiled candy and different polymer foils used for food packaging. Finally, the PTBD zero crossing method was used as an alternative and non-destructive technique to determine thermal diffusivity of a hard boiled candy at room temperature.

Basic facts about of PT methods

As stated already the PT phenomena rely on the conversion of absorbed excitation energy into heat. Although initial absorption of the energy can be selective (spectroscopy), the non-radiative relaxation rises the temperature of the sample. The magnitude and nature of the generated PT signal depend upon many parameters, among which sample's absorption coefficient, the excitation power, the efficiency of radiation to heat conversion and thermo-physical properties of the sample.^{5,12-14}

Common to all PT phenomena is that the strength of PT signal is directly related to the energy absorbed by the sample. Changes in temperature, pressure and density may occur simultaneously due to optical absorption are the basis for the PT methods. The choice of a most suitable PT technique and detection scheme depends on the nature of the sample and the purpose of the measurement.

In PA, the oldest among the PT techniques, periodic heating and cooling of the sample causes a consequent heating and cooling of the surrounding gas layer. The subsequent expansion and contraction of the gas gives rise to an acoustic wave, which is detected with a microphone.

Before considering the PT signal in more detail, it is useful to introduce the concept of thermal diffusion length μ defined as $(2\alpha\omega)^{-1/2}$ where α is the thermal diffusivity (m^2s^{-1}) and

ω (rads^{-1}) is the modulation frequency. Due to the dissipative character of diffusion, the amplitude of PT signal decreases with increasing distance from the heat source. At a distance μ away from the source, the amplitude of the thermal wave is attenuated to e^{-1} of its initial value and therefore heat originating in a depth layer larger than μ will not contribute substantially to the signal.

In general, mathematical relations describing the amplitude and phase of the PT signal are knotty and their interpretation is neither straightforward nor simple. However, physical insight may be gained by examining some special cases resulting in simpler equations. These are classified according to optical opaqueness of the samples as determined by the relation of the optical absorption length $l_\beta = \beta^{-1}$ (β is the optical absorption coefficient (m^{-1})) to the physical thickness of the sample l_s . Three cases are distinguished for each category of optical opaqueness depending on the relative magnitude of μ as compared to l_s and l_β .³ For example, if $\mu < l_s$, the sample is said to be thermally thick, while for $\mu > l_s$, the sample becomes thermally thin. A analogy applies for optical opacity and transparency.

The amplitude R and the phase φ of a PT signal predicted by the general Rosencwaig-Gerscho theory in a case of thermally thick sample can be approximated by the expressions

$$R = \frac{AI_0\sqrt{2}\beta\mu}{\sqrt{(\beta\mu)^2 + (\beta\mu + 2)^2}} \quad (1)$$

and

$$\varphi = \tan^{-1}\left(\frac{1}{\beta\mu + 1}\right) \quad (2)$$

In Eq. (1) I_0 is the intensity of incident radiation and A is the instrumental constant that depends on both sample and the geometry. From Eq. (1) it is obvious that PT response, non-linear in $\beta\mu$, can be influenced by changing μ through variation of frequency f (chapter 3).

The potential of PT method, for sensitive trace analysis (weak absorption) in gases and liquids follows from Eq. (1) that in such a case ($\beta\mu < 1$) reduces to

$$R = \frac{AI_0\beta\mu}{\sqrt{2}} \quad (3)$$

indicating a linear relationship between R and β (and hence also the concentration of the sample). At another extreme i.e. $\beta\mu > 1$, the PT signal saturates and R becomes independent of the sample's absorption, since

$$R = AI_0 \quad (4)$$

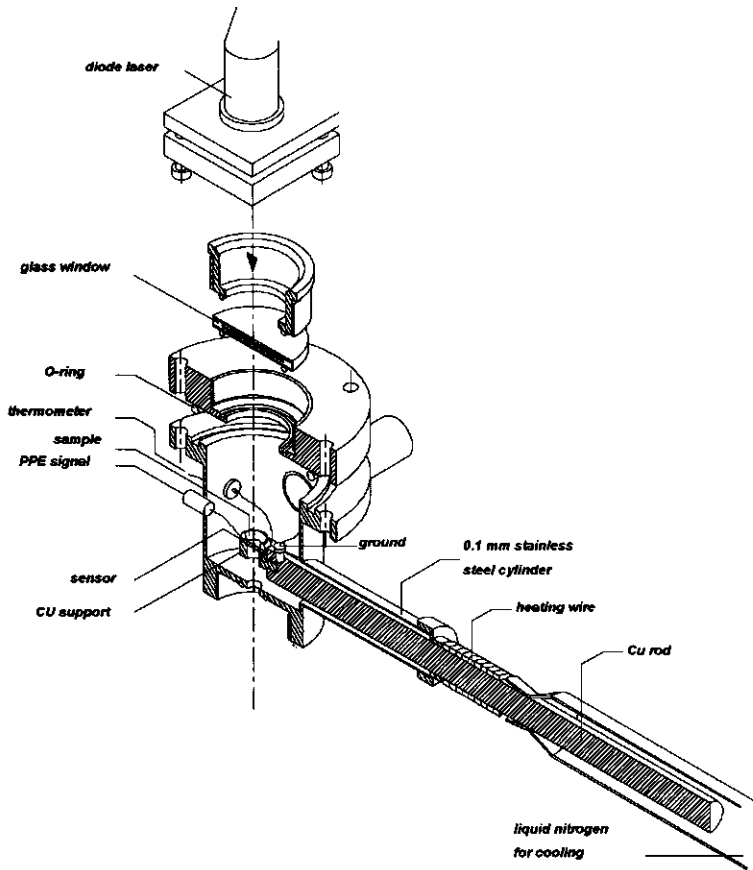


Figure 2 PPE set-up used in chapter 4

An example of a PT method that directly measures the temperature rise in the sample is the photopyroelectric calorimetry (PPE) the use of which is described in chapter 4 (Fig. 2). The periodic temperature rise induced in a sample is detected by a pyroelectric sensor being in intimate thermal contact with the sample. Depending on the configuration used, the sensor can be irradiated either from a front or a rear side. When pyroelectric materials, exhibiting a permanent internal dipole moment are periodically heated, the induced temperature fluctuations cause a corresponding polarization change, a variation of the surface charge and hence the current change. The average temperature rise $\langle \Delta T \rangle$ of the sensor is given by

$$\langle \Delta T \rangle = \frac{1}{L_p} \int_0^{L_p} T(x, t) dx \quad (5)$$

where $T(x,t)$ is the time dependent one dimensional temperature distribution in the sensor, and L_p is the thickness of the sensor. Due to its ability to provide the temperature dependence of the thermal parameters, the PPE method can also be used to detect phase and glass transitions as well as other anomalous behavior of materials.^{5,12}

Photothermal beam deflection (PTBD) makes use of a heating pump laser (Gaussian profile) and probing of the changes in the refractive index n induced in the sample or the contacting fluid (Fig. 3). Since the refractive index of a medium is itself temperature dependent, a refractive index gradient is generated. The latter is probed by a second (probe) laser beam and the deflection D is measured by a position sensitive detector. The deflection of the probe beam is related to the amount of absorbed pump beam radiation and can be calculated from

$$D = -\frac{1}{n} \frac{dn}{dt} \int_{-\infty}^{\infty} \nabla T(\vec{r}, t) \times dl \quad (6)$$

where $T(\vec{r}, t)$ is the radial temperature distribution and l is the distance over which pump and probe beam overlap.¹²⁻¹⁴ A variant of PTBD, the zero crossing method was used in chapter 4 for thermal characterization.

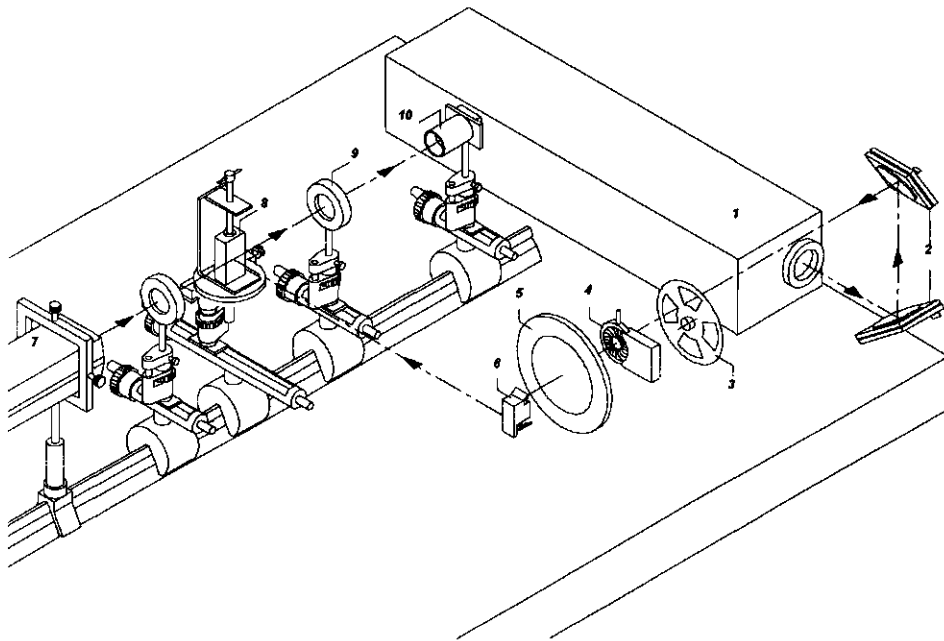


Figure 3 PTBD set-up: 1 Ar laser pump beam, 2 mirrors, 3 chopper, 4 diaphragm, 5 lens, 6 movable mirrors, 7 He-Ne laser probe beam, 8 sample, 9 lens, 10 quadrant diode

References

- 1 Bell's Photophone, *Nature* **23**, 15-19 Nov. 4 (1880)
- 2 Rosencwaig A. and Gersho A., Theory of the Photoacoustic Effect in Solids, *J. Appl. Phys.* **47**, 64-69 (1976)
- 3 Rosencwaig A., Photoacoustics and Photoacoustic Spectroscopy, John Wiley & Sons, New York (1980)
- 4 Mandelis A., Principles and Perspectives of Photothermal and Photoacoustic Phenomena, Progress in Photothermal and Photoacoustic Science and Technology, Vol. I, Elsevier Science Publishing Co., New York (1992)
- 5 Mandelis A., Non-Destructive Evaluation, Progress in Photothermal and Photoacoustic Science and Technology, Vol. II, PTR Prentice-Hall, New Jersey (1994)
- 6 Mandelis A. and Hess P., Progress in Photothermal and Photoacoustic Science and Technology, Vol. III: Life and Earth Sciences, SPIE Optical Engineering Press, Washington DC (1997)
- 7 Bicanic D. (Ed.), Photoacoustic and Photothermal Phenomena III, Springer Series in Optical Sciences **69**, Springer Verlag Heidelberg, Berlin (1992)
- 8 Bicanic D., Chirtoc M., Asselt K. van, Gerkema E., Jalink H., Sauren H., Groot T., Torfs T. and Haupt K., New Trends and Perspectives of Photoacoustic and Photothermal Spectroscopies in Agricultural and Environmental Sciences, *Acta Chemica Slovenica* **40**, 175-202 (1993)
- 9 Sauren J.J.A.M., Ammonia Monitor Based on Intermodulated CO₂ Laser Photoacoustic Stark Spectroscopy, PhD thesis, Wageningen Agricultural University (1992)
- 10 Vries H.S.M. de, Local Trace Gas Measurements by Laser Photothermal Detection: Physics Meets Physiology, PhD thesis, Nijmegen University (1994)
- 11 Bijnen F.G.C, Refined CO-Laser Photoacoustic Trace Gas Detection: Observation of Anaerobic Processes in Insects, Soil and Fruit, PhD thesis, Nijmegen University (1995)
- 12 Amond D.P. and Patel P.M., Photothermal Science and Techniques, Chapman & Hall, London (1996)
- 13 Bialkowski S.E., Photothermal Spectroscopy Methods for Chemical Analysis, Chemical Analysis: A Series of Monographs on Analytical Chemistry and Its Applications Vol. 134, John Wiley & Sons, New York (1996)
- 14 Sell J.A., Photothermal Investigation of Solids and Fluids, Academic Press, London (1989).

2 Photoacoustic Spectroscopy for Optical Characterization of Different Samples

2.1 Photoacoustic Characterization of Different Food Samples

2.2 New and Versatile Photoacoustic Cell for Studies of Powdered Specimens Across Broad Spectral Range

2.3 Organic Compounds Measured with Infrared (3.39 μm) Photoacoustics

2.1 Photoacoustic Characterization of Different Food Samples

based on

Jan Paul Favier, Jos Buijs, András Miklós, András Lőrincz and Dane Bicanic

Zeitschrift für Lebensmittel-Untersuchung und-Forschung **199**, 59-63 (1994)

Abstract

Photoacoustic spectroscopy in the 350-700 nm range proved a useful tool for discriminating between a variety of opaque, light-scattering samples. Spectral features originating from powdered food specimens of different colour and grain size were observed. These results suggest the feasibility of photoacoustics for quality control in the food-processing industry.

Photoakustische Charakterisierung von verschiedenen Lebensmitteln

Zusammenfassung

Die photoakustische Spektroskopie im Wellenlängenbereich von 350-700 nm hat sich als nützliches Instrumentarium zur Unterscheidung verschiedener undurchsichtiger, Licht streuender Proben erwiesen. Spektrale Eigenschaften pulverisierter Nahrungsmittelproben unterschiedlicher Korngrößen und Farbe wurden beobachtet. Die Ergebnisse zeigen, daß der Einsatz der Photoakustik in der Qualitätskontrolle für die Nahrungsmittelindustrie vielversprechend ist.

Introduction

In the past photoacoustic spectroscopy (PAS) was used in studies of inhomogeneous and light-scattering powdered samples.¹⁻⁵ Since de-excitation processes in these samples proceed along non-radiative channels, thermal excitation spectra of powders correlate well with their absorption spectra.⁶

Biological specimens (such as food products) are complex mixtures of either chemically diverse compounds or chemically related molecules, often possessing significant differences in physical properties. As many food products are also powders, PAS might be useful for quality control in the food-processing industry.^{3,7-9} Establishing more objective selection and characterization criteria for flours is an example of potential PAS application in practice. Likewise, cosmetic qualities of foods have become increasingly important during recent years. As a result colour (just as quality and nutritional factors) has achieved a more pre-eminent position for the consumer.¹⁰ New techniques and instrumentation for color measurements are therefore considered as useful additions to the laboratory.

It is well-known^{1,6,11,12} that the magnitude of the PA signal is directly proportional to the fraction of energy absorbed by a sample. The absorbed energy in its turn is a function of light intensity distribution in the sample, which, when multiple scattering plays an important role, might differ from that predicted by Beer's law. Light scattering, which is also wavelength-dependent, reduces the optical penetration depth of the radiation into the sample.¹³ In photoacoustics (PA), light scattering affects the PA signal in two different ways. In the first place there is a scattering on the cell walls that leads to correspondingly increased intensity of light in the cell and gives rise to an acoustic signal. Moreover, light intensity distribution is influenced by internal scattering due to reflections and scattering on the surface of grains. When grain particles are loosely packed and relatively big, the light can reach deeper layers (under the sample surface) at distances that exceed the effective illumination depth (or effective optical penetration depth) of powdered samples (i.e. thickness across which the light intensity has decreased to a practically negligible value). It is the effective illumination depth that characterizes the intensity distribution in the cell. Although this parameter is important whenever comparison of PA spectra of powdered samples of different grain size is anticipated, surprisingly no reliable method for its determination has been proposed so far. The main objective in undertaking the study described in this paper was to obtain PA spectra (350-700 nm range) of different flour and other powdered food specimens and to collect more data on parameters involved in the process of PA signal generation.

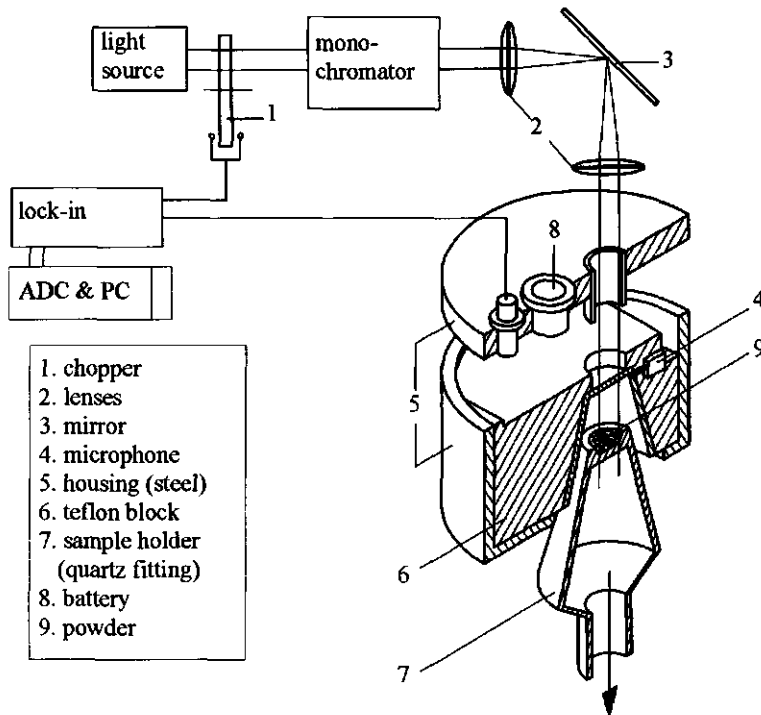
Materials and methods

Figure 1 The set-up used for measuring photoacoustic (PA) spectra of powdered flour samples: ADC, analogue to digital converter; PC, IBM compatible computer

The experimental set-up used to record the spectra of flours (all specimens were kindly provided by Gabona Tröszt, Budapest, Hungary) and samples of commercially available instant coffee and spices is shown in Fig. 1. It comprises a 400 W Xenon lamp (ILC Technology) the polychromatic beam was mechanically chopped (1) before it entered Jobin-Yvon H-20 monochromator (spectral resolution of 8 nm). The beam was focused into a quartz cell (see detail in Fig. 1) by means of two glass lenses (2) and a plane mirror (3). The sample holder (7) is a cup 10 mm in diameter and 2 mm deep (distance measured from the bottom). The cell window and sample window are separated by a distance of 2 mm. The cell design allows easy loading (quantity of sample used in each measurement was kept as constant as possible) and enables removal of sample (9) without a need to change the position of the cell. This greatly facilitated performance of the measurements since no problems associated with alignment were experienced. Pressure fluctuations were measured with a Knowles EA-1954 microphone (4) powered by a battery (8). The signal was fed into Stanford Research SRS preamplifier, the output of which was connected to a Stanford

Research SR510 lock-in amplifier. The output signal of the lock-in was interfaced to a IBM-compatible computer. The scan speed of the step motor was 1 nm/s; 40 data points were taken each second. The arithmetic averages of these 40 points were used to construct the spectra displayed in Figs. 4-8. The chopping frequency used in all the measurements was 70 Hz because the signal to noise ratio was found optimal at that value. The thermal diffusion lengths (μ) of carbon black powder, air and flours at this frequency are 640, 313 and 20 μm , respectively. For carbon black the thermal diffusion length is much larger than the dimension of the grains whereas for flours it is of the same order of magnitude.

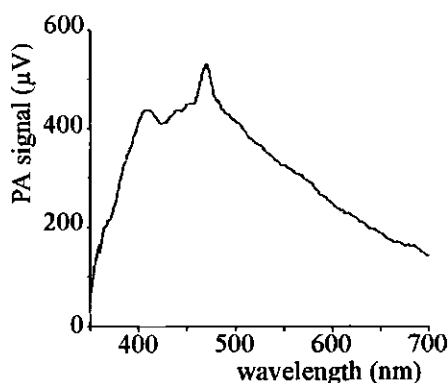


Figure 2 Photoacoustic spectrum of carbon black

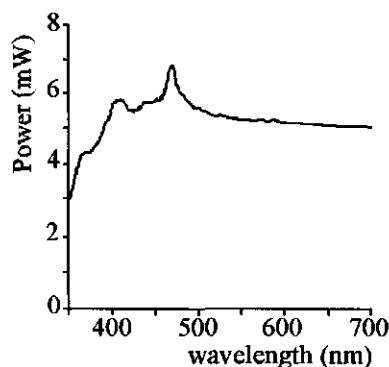


Figure 3 Power spectrum of radiation incident onto the PA cell (used for normalization of the PA signal)

In photoacoustics it is customary to normalize the PA spectra in order to eliminate wavelength dependence of the source. In previous studies,^{2-5,7-9,11,12} the PA spectra of powders were normalized to the PA spectrum of carbon black taken as a reference sample. The basic idea behind such an approach is the assumption that carbon black absorbs equally strongly throughout the entire spectral range. However our own measurements indicate (Figs. 2 and 3) that the PA signal of carbon black and the power spectrum of the lamp show the same trend for wavelengths shorter than 500 nm. Above this wavelength the PA signal of carbon black decreases (Fig. 2) whereas the power of the xenon lamp (showing several peaks between 400 and 500 nm) remains nearly constant (Fig. 3). Below 350 nm the measurements are no longer accurate because of a substantially reduced signal to noise ratio due to lens absorption. The PA spectra (Figs. 5, 7 and 8) were normalized by ratioing their magnitudes (recorded at 5 nm increments) directly to the power spectrum of xenon lamp. The reproducibility of the set-up before each measurement was tested consistently by measuring the PA signal from carbon black at two preselected (maxima at 400 and 467 nm) wavelengths.

Results

Barium sulphate (a white powder) was investigated first. For such a sample the effective gas volume is very close to that used in actual measurements. The spectrum (normalized to a power spectrum of the xenon source) is wavelength independent in the spectral range 350-700 nm (Fig. 4A), in contrast to that normalized to the PA spectrum (Fig. 4B) of carbon black (conventional normalization). Since wavelength dependence in Figs. 4 resembles that expected for the white sample, the normalization procedure suggested here seems justified.

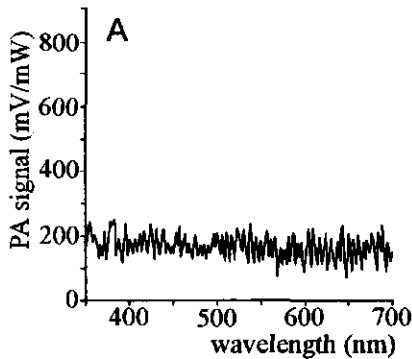


Figure 4A Spectra of BaSO₄ powder normalized to the method proposed here

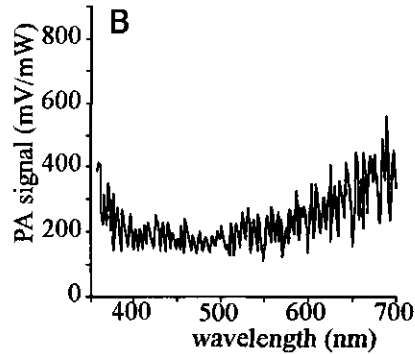


Figure 4B Spectra of BaSO₄ powder normalized ratioed to carbon black

Powder spectra of flours

The flour specimens investigated all differed in colour and grain size. There were a few white flours such as fine and normal bread, pastry and rice flours. The soya flour, corn grits and corn flour are yellow, whereas whole wheat flour, wheat flour and rye flour contained some brown coloured grains. Finally, dried pea flour has a greenish colour.

Figure 5A shows PA spectra of white bread flours; all had absorption bands around 370, 385 and 410 nm. Above 410 nm the PA signal decreases rapidly and drops to a nearly zero at 700 nm. The grain size affects the magnitude of the signal; as an example normal bread flour can be discriminated from fine bread flour (Fig. 5A). The signal from fine bread flour is lower than that obtained with normal bread flour because the grain diameter (d) is smaller than the thermal diffusion length ($d < \mu$); therefore less heat is deposited into grains. Figure 5B shows the PA spectra of yellow coloured specimens. Again, absorption bands common to all specimens were observed near 370, 385 and 410 nm. In general, the overall spectral features of yellow flours appeared broader than for white flours. The effect of different grain size on amplitude of the PA signal can also be seen when inspecting spectra of corn grits and corn flour. If the grain size is (much) larger than the thermal diffusion length, i.e. $d \gg \mu$ (such as for

corn grits), the signal decreases because fewer grains are irradiated. In addition the surface/volume ratio decreased with increasing grain size. Figure 5C shows the PA spectra of three differently coloured (yellow, green and brown) flours. The dried pea flour is the only sort that has a maximum signal at 410 nm. Soya flour exhibits a broader spectrum whereas rye flour resembles that of the bread flour and also produced the highest signal of all the samples.

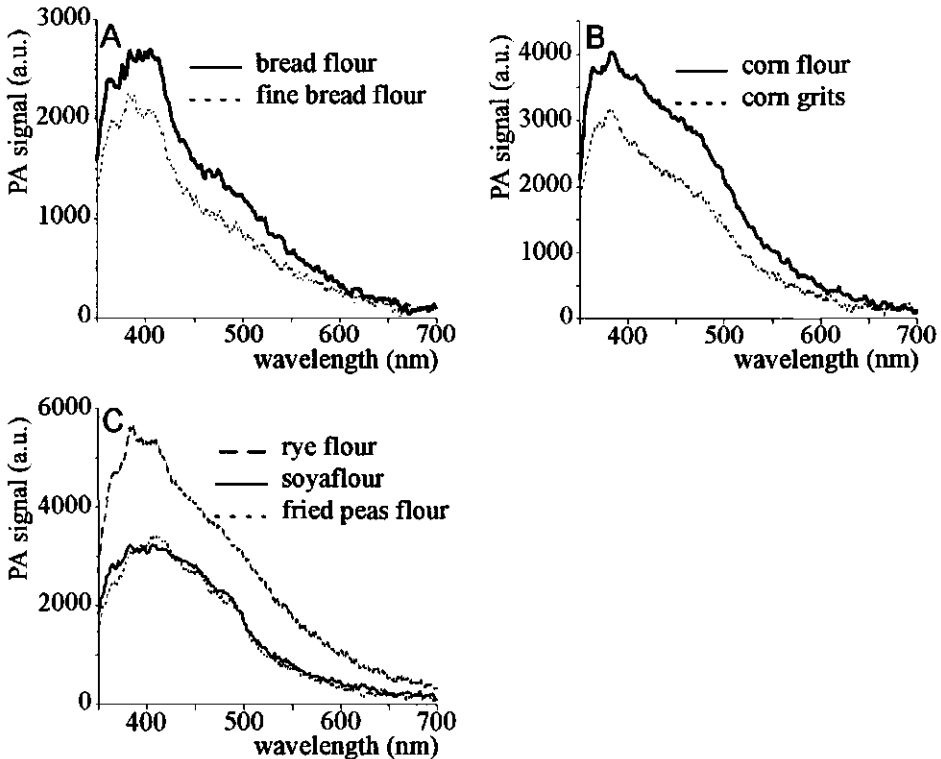


Figure 5 Photoacoustic spectra of flours. (A) Bread flour and fine bread flour. (B) Corn flour and corn grits. (C) Rye flour, soya flour and dried pea flour: a.u., PA signal divided by the power of the xenon lamp (Fig. 3)

In order to quantitatively compare different flours, the magnitude S of the PA signals at 385, 410 and 475 nm were normalized to the signals obtained with normal bread flour at the same wavelengths, yielding the dimensionless ratios (S') shown in the first three columns of Table 1. Careful inspection of all the spectra suggests that most differences are observed near 475 nm.

Table 1 Results of the measurements on powdered flour samples. The magnitude of the signals (S') and their relative magnitudes at three different wavelengths (385, 410, 475 nm) are given.

No.	flour brand (color)	S'_{385} (-)	S'_{410} (-)	S'_{475} (-)	$\frac{S'_{385}}{S'_{475}}$	$\frac{S'_{410}}{S'_{475}}$	$\frac{S'_{385}}{S'_{410}}$
1	bread flour (w)	1.00	1.00	1.00	1.00	1.00	1.00
2	fine bread flour (w)	0.85	0.77	0.71	1.20	1.08	1.10
3	pastry flour (w)	0.59	0.61	0.53	1.11	1.15	0.97
4	wheat flour (b)	0.61	0.58	0.59	1.03	0.98	1.05
5	rye flour (b)	2.13	2.02	2.46	0.87	0.82	1.05
6	whole wheat flour (b)	1.59	1.40	1.59	1.00	0.88	1.14
7	corn flour (y)	1.54	1.39	1.90	0.81	0.73	1.11
8	corn grits (y)	1.19	0.99	1.30	0.92	0.76	1.20
9	soya flour (y)	1.22	1.22	1.58	0.77	0.77	1.00
10	dried peas flour (g)	1.18	1.29	1.50	0.79	0.86	0.91
11	rice flour (w)	0.52	0.43	0.44	1.18	0.98	1.21

w, white; b, brown; y, yellow; g, greenish

From Table 1 there is a direct relationship between the magnitude of the PA signal and the colour of the flour: compare, for example, corn powders (7 and 8) to wheat (4) and rice (11) flours. Compared to coloured flours, white flours yielded only a small signal. The spectrum shape also provides some information about the colour of samples. For example yellow-coloured flours (corn and soya) can be discriminated from other coloured specimens (columns 4 and 5). The ratio S'_{385}/S'_{475} , (column 4 in Table 1) decreases according to the colour of the sample. The reproducibility of the measurements was satisfactory (error was typically within 5%).

The light distribution in powders

Both internal reflections within the grains as well as the wavelength dependent reflectance (R) at the surface of flour grains affected¹⁴ the magnitude of the PA signal significantly (as shown in Table 2).

Table 2 The wavelength-dependent reflectance (R) for a typical flour specimen¹⁴

wavelength (nm)	R (-)
400	0.75
500	0.87
600	0.94
700	0.97

Next, the role that the effective illumination depth of the radiation plays in the generation of PA signal in various flour specimens was explored in more detail. This was done by

comparing the PA signals measured with the cell loaded with a specific flour to those obtained from a thin layer (≈ 0.5 mm) of the very same flour specimen placed on top of a relatively thick backing layer of carbon black. Pure carbon black produced typically a maximum PA signal of $500 \mu\text{V}$ at 467 nm (Fig. 2) whereas the signal originating from pure flours at the same wavelength varied from 10 to $20 \mu\text{V}$ (Fig. 6).

In a two layer sample (flour on top of a carbon black) an increase in the PA signal is expected for larger effective illumination depths. Even a minor fraction of transmitted light is sufficient to produce a PA signal with a magnitude that might be comparable to that of the flour. The contribution of carbon black to the signal may be estimated by comparing the non-normalized signals from pure flour to signals obtained from the very same flour on top of a the carbon black. Two spectra are depicted in Fig. 6. For soya flour (Fig. 6A), the differences were not very obvious at shorter wavelengths and the contribution of carbon black (trace a) became significant above 500 nm. For larger grains, carbon black strongly prevailed (trace a in Fig. 6B) over that of wheat-meal (trace b in Fig. 6B). The largest PA signal due to the contribution of carbon black (approx. $50 \mu\text{V}$ at 467 nm) was about 10% smaller than that obtained when the cell was loaded with pure carbon black. For small grains (Fig. 6.A) the amplitude decrease was substantially lower (about 2%). Scattering also reduces the optical penetration depth and at shorter wavelengths scattering is larger than at longer wavelengths as seen in Fig. 6.

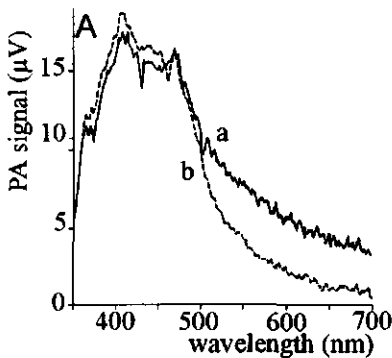


Figure 6A Photoacoustic spectra of carbon black covered by a thin layer of soya flour (a) and of soya flour (b)

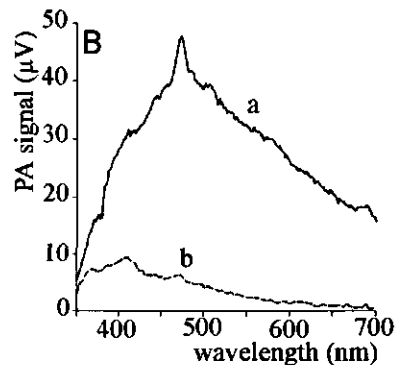


Figure 6B Photoacoustic spectra of carbon black covered by a thin layer of flour wheat (a) and of the flour wheat (b)

The above measurements suggest that due to a short effective illumination depth the PA signal is generated in the uppermost layer (0.5 mm) of powdered sample (the effective illumination depth increases for larger grains as concluded by careful inspection of traces a and b (Fig. 6)). This implies that with the present cell design radiation does not reach the cell

walls; which has two important consequences. First, the contribution of the cell walls is minimal and secondly, only small quantities of flour are needed to produce satisfactory spectra.

Photoacoustic spectra of spices and coffee

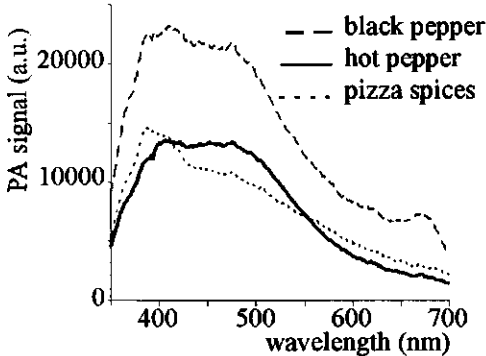


Figure 7 Photoacoustic spectra of three different spices

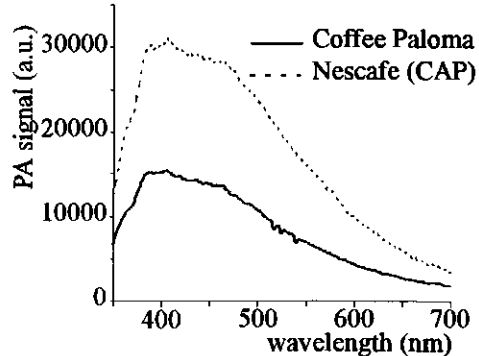


Figure 8 Photoacoustic spectra of two different instant coffees

In order to demonstrate the practicability of the PA method, spectra of a few more food products were measured. Figure 7 features spectra of hot pepper, black pepper and pizza spices whereas Fig. 8 shows PA spectra of two instant coffee brands: Paloma, Compact Budapest and Nescafe (CAP) Collombie (100% arabica beans). On visual inspection, the samples appear very much alike, but their PA spectra are quite different. We conclude that the PA technique appears capable of producing reproducible spectra of powdered food samples (discrimination of different flours based on origin, colour and grain size is possible), demonstrating its usefulness for quality control purposes.

It was shown that light intensity distribution near the surface increases due to the scattering and that a large fraction of incident light is reflected and leaves the sample. For this reason no energy can reach the bottom of the sample; in addition only small quantities of sample are required. The use of quartz optics will further improve the sensitivity of the PA method. This might eventually also allow the use of PA method for determination of basic amino acids, present in almost all biological samples.

Acknowledgements. Credit is due to dr. Otto Dóka for his advices and help during this work. We also thank László Détári for his suggestions in making the computer programme operational. The skilled drawing work of Kees Rijpma and Mees Schimmel from the Illustration Dept. (WAU) is gladly acknowledged.

References

- 1 Zafer A.Y., Jackson W.B. and Amer N.M., Photothermal Spectroscopy of Scattering Media, *Appl. Opt.* **21**, 21-31 (1982)
- 2 Dóka O., Biró T., Lőrincz A., High-exposure Dosimetry with LiF (TLD-100) by Photoacoustic Spectroscopy, *Appl. Phys. D* **21**, 820-825 (1988)
- 3 Dóka O., Kispeter J. and Lőrincz A., Potential Value of Photoacoustic-Spectroscopy for determining Iron Content Determination of Milk Protein-Concentrates, *J. of Dairy Research* **58**, 453-460 (1991)
- 4 Alebić-Juretić A., Güsten H., and Zetzch C., Absorption Spectra of Hexachlorobenzene Absorbed on SiO₂ Powders, *Fresenius J. Anal. Chem.* **340**, 380-383 (1991)
- 5 Moreira-Nordemann L.M., Lucht L.A.M., Muniz R.P.A., Photoacoustic Spectroscopy and Surface Temperature Measurements of Tropical Soils, *Soil Science* **139**, 538-546 (1985)
- 6 Rosencwaig A., Photoacoustics and Photoacoustic Spectroscopy, Chemical Analysis Vol 57, Wiley, New York (1980)
- 7 Martel R., N'Soekpoe-Kossi C.N., Paquin P. and Leblanc R.M., Photoacoustic analysis of some Milk Products in Ultraviolet and Visible Light., *J. Dairy Sci.* **70**, 1822-1827 (1987)
- 8 Sadler A.J., Horsh J.G., Lawson E.Q., Hamatz D., Brandau D.T. and Middaugh C.R. Near Infrared Photoacoustic Spectroscopy of Proteins., *Anal. Biochem.* **138**, 44-51 (1984)
- 9 N'soukpoé-Kossi C.N., Martel R., Leblanc R.M. and Paquin P., Kinetic Study of Maillard Reactions in Milk Powder by Photoacoustic Spectroscopy, *J. Agric. Food Chem.* **36**, 497-501 (1988)
- 10 Clydesdale F.M., Food Analysis, Chapter 3 Colour measurement, Dekker M inc. New York (1984)
- 11 Helander P. and Lundström I. Light Scattering Effects in Photoacoustic Spectroscopy, *J. Appl. Phys.* **51**, 3841-3847 (1980)
- 12 Monchalin J.P., Bertrand L. and Rousset G., Photoacoustic Spectroscopy of Thick Powdered or Porous Samples at Low Frequency, *J. Appl. Phys.* **56**, 190-210 (1984)
- 13 McGovern S., Royce B.S.H. and Benziger J.B., The Importance of Interstitial Gas Expansion in Infrared Photoacoustic Spectroscopy of Powders, *J. Appl. Phys.* **57**, 1710-1718 (1985)
- 14 Dwight E.G. (ed), American Institute of Physics Handbook, 3rd ed., McGraw-Hill Book Company (1982).

2.2

New and Versatile Photoacoustic Cell for Studies of Powdered Specimens Across Broad Spectral Range

based on

Jan Paul Favier, András Miklós and Dane Bicanic

Acta Chimica Slovenica 40, 115-122 (1993)

Abstract

Photoacoustic spectroscopy (PAS) is insensitive to scattering since the generated photoacoustic signal (PA) is proportional only to the fraction of energy absorbed by the sample. It is therefore suitable for the analysis of powdered samples. A new PA-cell for application within a broad spectral range was developed and its design optimized in terms of both, performance and the user aspects.

Provizetok

Fotoakustična spektroskopija (PAS) ni občutljiva na sipanje, ker je nastali fotokustični (PA) signal sorazmeren le z delom energije, ki jo absorbira vzorec. Zato je metoda primerna za analizo praškastih vzorcev. Avtorji so razvili novo PA-celico, uporabno v širokem spektralnem območju, ter jo optimirali tako s stališča učinkovitosti kot praktičnosti pri uporabi.

Introduction

Photoacoustic spectroscopy is one of techniques for studying the absorption features of gases, liquids and solids in the wide spectral range.¹ The method proved uniquely suitable for strongly scattering and opaque samples (e.g. powdered and porous specimens) often intractable for other spectroscopies. The traditional methods for spectral analysis of inhomogeneous and light scattering samples provide satisfactory results only under certain limited conditions.²⁻⁴ The majority of spectroscopic data for powders reported so far in the scientific literature were collected in the UV, visible and the near infrared region.

As many food products are powders, the PAS could potentially be useful for quality control in the food industry; one example is the processing of milk (to control directly the presence of protein peak in dairy products or to determine the concentration of protein and moisture content in skimmed milk⁵⁻⁷). Other PA work on powdered samples includes applications in studies of high exposure dosimetry⁸, adsorption⁹ as well as the structural investigations of biological¹⁰ and soil science specimens.¹¹ In the work described here, a new and versatile cell is being proposed and its feasibility demonstrated (in the 10 microns region) with protein as a specimen under investigation.

The heart of each PA based instrument is the cell, actually a chamber that accommodates both, the sample and the microphone. The incident periodically chopped radiation of a suitable wavelength is coupled into the cell, where upon interaction with the absorbing sample, heat is generated and eventually an acoustical signal produced. In order to increase the sensitivity of the apparatus, it is important to minimize the effect of various noise sources. This implies the suppression of unwanted, non-sample contributions to the PA signal, finding of the optimal position for the microphone and finally the optimization of the cell size, shape and degree of the acoustic tightness. Some of these are discussed below in more detail.

The non-sample contributions to the PA signal

There are several sources of the non-sample PA signals; for example scattered radiation (directly and indirectly) and the absorption of radiation by the cell windows all are sensed by the microphone. Indirectly scattered radiation reaches the cell wall by means of diffuse light reflections in the sample and produces a PA signal. In order to eliminate this effect it is recommended to use transparent material in the cell construction. Metals having favourably large thermal diffusivities are frequently being used as cell construction materials. Nevertheless, relatively large background signals have been measured (for example in case of stainless steel) in the near infrared;⁷ in addition cells fabricated from metals are not easy to clean. Finally, it is also advantageous to use the windows exhibiting high transmission in the wavelength region of interest.

The position of the microphone

To avoid scattered radiation from reaching the microphone membrane, it is necessary to separate the microphone from the sample volume. This is usually done by connecting the microphone and the cell via a small circular opening. Ensuring a proper degree of acoustic matching between the microphone and sampling volume offers an opportunity to improve the signal to noise ratio considerably.

The size, shape and the acoustic tightness of the cell

Numerous experiments have established that the magnitude of the PA signal is inversely proportional to the cell volume. However, the cell dimensions may not be decreased unlimitedly, as the cell must always be larger than the thermal diffusion length of the gas in the cell. Whenever designing a PA cell, one should consider the aspects such as loading and replacement of the sample as well as, the ease of cleaning and the maintenance. Sealing of the cell should be done in a quick, simple, reliable and reproducible manner. The cell must be acoustically insulated from the ambient in order to reduce the effect of external noise. However, the sealing must not be too tight, so that an equilibrium between the external and the internal pressure can exist avoiding thereby a pressure buildup at the microphone.

Experimental

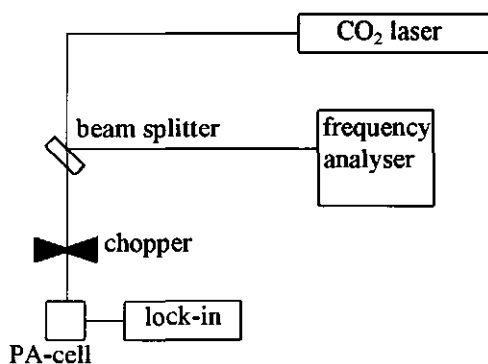


Figure 1 Set-up used for PA measurements of powder samples

The experimental setup used for the measurements of powder spectra is shown in Fig. 1. It consists of a home made cw CO₂-laser in conjunction with the PA cell (Fig. 2), the chopper and the electronics needed for processing of the microphone signal (Fig. 1). The ZnSe beam splitter inserted into the radiation path served simultaneously to reduce the power of the laser beam and to couple a fraction of laser radiation into the spectrum analyzer (Optical Engineering) for identification of laser emission. The radiation was mechanically chopped

(PTI 4000 Optical Chopper) and focussed into the cell by means of an off-axis parabolic reflector (6) (Melles Griot 02 POA 015). The output of the microphone was fed into the Princeton Applied Research lock-in amplifier (model 128A) for synchronous detection at the modulation frequency. The cell mounted on a revolving drum (4) was affixed to the magnetic foot (1) so that cell position could be maintained unchanged during the measurements.

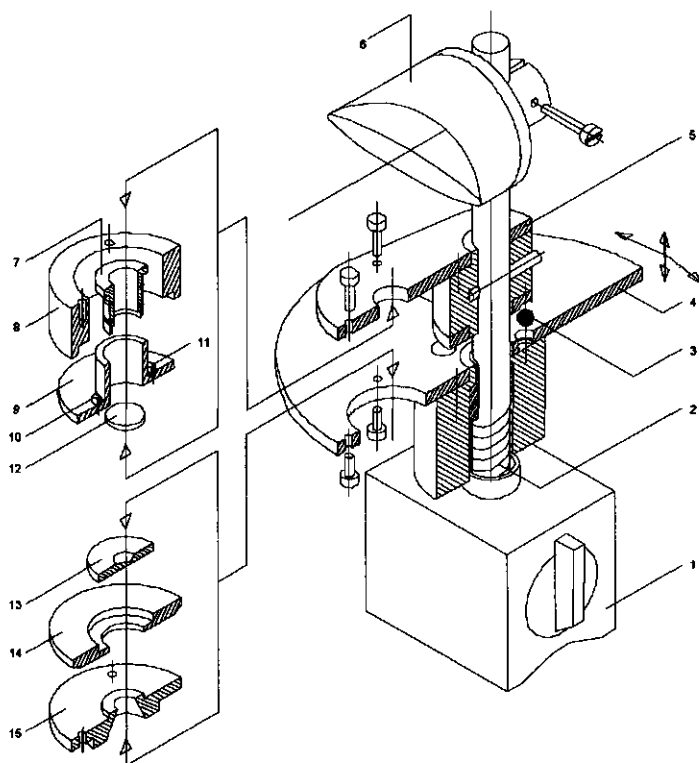


Figure 2 Exploded view of the PA-cell, see the text for explanation

The exploded view of the cell is shown in Figure 2. The revolving drum (4) and detection unit (7-15) are the two major parts of the PA cell. The drum is an aluminum circular platform that carries three identical and symmetrically distributed sample holders. Each holder consists of a cup (13) that accommodates the sample (the cup is actually a ZnSe flat (25.4 mm diameter, thick 3 mm) provided with the central spherical cavity (13 mm diameter and 2 mm deep)) resting in the retaining teflon ring (14) supported by a metal plate (15). The plate is bolted to the platform by means of three screws.

The detection unit includes the metal adapter (7) fitting closely (by two "O" rings) into the microphone assembly (9) that on its turn is glued to the aluminum housing (8). The adapter

(7) is terminated by a ZnSe flat (12) window (12 mm diameter and 2 mm thick). Detection unit as a whole is screwed against the fixed auxiliary plate (15). When put together, the detection unit and one single sample holder form the PA cell. The detection unit actually serves as a cover for the above described sample holder leaving a layer of air 300 μm thick in between. The acoustic wave is negligibly damped across 300 μm length while the heating of the microphone is prohibited.

The radiation of appropriate wavelength is collected by the Rhodium electroformed paraboloidal reflector (6) with the clear aperture of 50 mm, deflected and focused (distance from reflector mechanical axis to the focal point is 66 mm) into the sample holder (13).

The microphone assembly is equipped with the two miniature electret microphones for sensing of pressure fluctuations. One of them, the "signal" microphone (11) is mounted in a distant channel (2 mm diameter, height 4 mm) 13 mm from the vertical symmetry axis of the cell. Another transducer (10), the "reference" microphone, was used in a differential arrangement (for suppression of acoustical and electrical noise). Such a configuration allowed the automatic subtraction of the background signal. The metal housing (8) shields the microphones from the possible sources of electrical noise.

Such cell design allowed an easy (un)loading of the sample and the replacement of the cup (13-14) and of the entrance window (12) whenever needed the cell suitable for studies at other wavelengths as well. The three sample holders on the drum permit to complete more measurements within a given time interval, since the cleaning of the cup (removed from the supporting plate) can take place simultaneously with the investigation of the new specimen.

With the position of the detection unit unchanged all the time, the drum can be manually revolve around the vertical rod. The spring load (2) helps to lock the drum in any of three distinct positions. The lock is achieved by three stainless steel balls (3) fixed in the drum that fit into semispherical cavities drilled in the body (5).

As to the measurements themselves, the acoustic characteristics of a differential PA cell was determined first using the Brüel&Kjær dual channel signal analyzer 2032. The major objective of this study was to obtain information about the intrinsic sensitivity and the frequency response of both microphones. This is important since proper functioning of a differential arrangement is ensured only if the sensitivity figures and the response curves for both microphones are comparable. The results indicate the presence of response peaks near 3136 Hz and the second harmonic of this frequency. However, the sensitivities of both microphones differed substantially (the ratio of microphone signal magnitude to that recorded by the reference microphone was three). Presumably, this is due to the fact that the microphones used were not of the same origin.

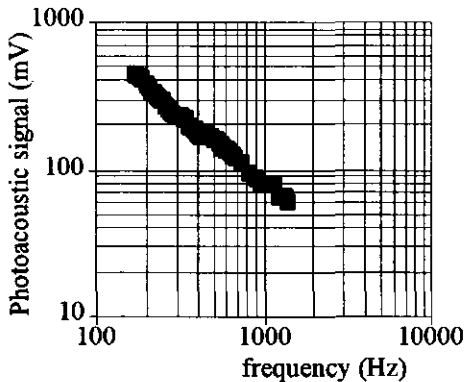


Figure 3 The frequency dependence of the amplitude of the PA signal of BSA

As the next step, few preliminary experiments served only to illustrate the versatility of this new PA cell design were performed. Figure 3 shows $1/f$ the frequency dependence of the PA-signal amplitude obtained from BSA (bovine serum albumin) with the CO_2 -laser tuned to a 9P(10) transition at $9.473 \mu\text{m}$. The system performed well and in a reproducible manner up to the frequencies as high as 1500 Hz. With the laser blocked the noise never exceeded $2 \mu\text{V}$.

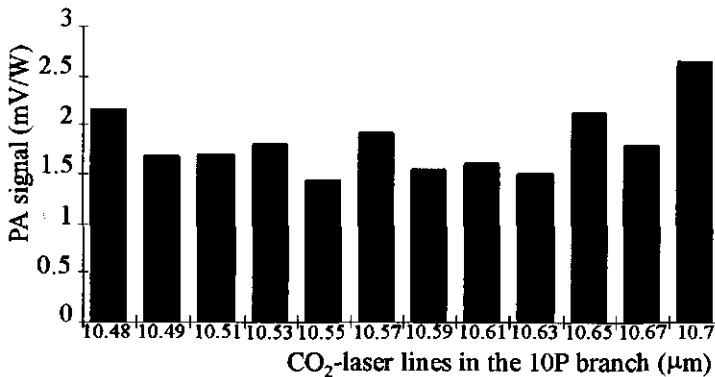


Figure 4 Measured PA spectrum of BSA at different CO_2 laser lines

Figure 4 shows the PA spectrum of BSA ratioed to the incident laser power (in the 10P branch of the CO_2 -laser). This latter was determined by an independent measurement using the power meter (Photon Control model 35502) placed in front of the PA cell. The true power reaching the cell is, however, not known because the potentially present reflection and absorption losses (paraboloid mirror and of the entrance window), were not considered here. With the laser blocked the noise in this experiment was $1 \mu\text{V}$ (chopping frequency of 233 Hz and t_c of 300 ms).

In conclusion, the usefulness of the new PA cell for spectroscopic studies of powders in the middle infrared was demonstrated. The use of microphone preamplifiers could not only further improve the sensitivity of a system but also assist in matching the sensitivities of both microphones. In addition to the above discussed factors (that influence the power), an attempt must also be made to determine experimentally the amount of radiation reflected directly from the surface of the sample, so that the actual level of radiation input power used in generating the PA signal could be calculated.

An improved PA device could eventually become a low cost, multiwavelength, and sensitive instrument suitable for non-destructive analysis of powdered samples over a wide wavelength range. Work on this matter is currently in progress.

References

- 1 Rosencwaig A., Photoacoustics and Photoacoustic Spectroscopy, Chemical Analysis Vol 57, Wiley, New York (1980)
- 2 Helander P. and Lundström I. Light Scattering Effects in Photoacoustic Spectroscopy, *J. Appl. Phys.* **51**, 3841-3847 (1980)
- 3 Monchalín J.P., Bertrand L. and Rousset G., Photoacoustic Spectroscopy of Thick Powdered or Porous Samples at Low Frequency, *J. Appl. Phys.* **56**, 190-210 (1984)
- 4 McGovern S., Royce B.S.H. and Benziger J.B., The Importance of Interstitial Gas Expansion in Infrared Photoacoustic Spectroscopy of Powders, *J. Appl. Phys.* **57**, 1710-1718 (1985)
- 5 Martel R., N'Soekpoe-Kossi C.N., Paquin P. and Leblanc R.M., Photoacoustic Analysis of Some Milk Products in Ultraviolet and Visible Light., *J. Dairy Sci.* **70**, 1822-1827 (1987)
- 6 N'soukpoé-Kossi C.N., Martel R., Leblanc R.M. and Paquin P., Kinetic Study of Maillard Reactions in Milk Powder by Photoacoustic Spectroscopy, *J. Agric. Food Chem.* **36**, 497-501 (1988)
- 7 A.Miklós and D.D.Bicanic, (submitted 1993).
- 8 Dóka O., Biró T., Lőrincz A., High-exposure Dosimetry with LiF (TLD-100) by Photoacoustic Spectroscopy, *Appl. Phys. D* **21**, 820-825 (1988)
- 9 Alebić-Juretić A., Güsten H., and Zetzch C., Absorption Spectra of Hexachlorobenzene Absorbed on SiO₂ Powders, *Fresenius J. Anal. Chem.* **340**, 380-383 (1991)
- 10 Sadler A.J., Horsh J.G., Lawson E.Q., Hamatz D., Brandau D.T. and Middaugh C.R. Near Infrared Photoacoustic Spectroscopy of Proteins., *Anal. Biochem.* **138**, 44-51 (1984)
- 11 Moreira-Nordemann L.M., Lucht L.A.M., Muniz R.P.A., Photoacoustic Spectroscopy and Surface Temperature Measurements of Tropical Soils, *Soil Science* **139**, 538-546 (1985).

2.3 Organic Compounds Measured with Infrared (3.39 μm) Photoacoustics

based on

Jan Paul Favier, Dane Bicanic, Kees van Asselt and András Miklós

Journal de Physique IV 4, 495-497 (1994)

Abstract

A variety of carboxylic acids, alcohols and alkanes were studied using photoacoustic spectroscopy (PAS) with an excitation wavelength of 3.39 μm . The analytical potential of this method was estimated with different organic compounds dissolved in chloroform. A detection limit of 0.25%, with a signal to noise ratio of 6, was achieved.

Introduction

The high infrared absorption coefficients of (semi-)liquid samples such as edible oils, fats and alkanes make their quantitative analysis by means of transmission spectroscopy a difficult task. They are normally examined in very thin layers, either neat or dissolved in an infrared inactive solvent. The thickness of such layers, and therefore the pathlengths investigated, are often difficult to determine accurately. The development of more reliable methods is therefore desirable.

Experimental

In this work, the photoacoustic (PA) signals from various carboxylic acids, alcohols and alkanes were compared at an excitation wavelength of $3.39 \mu\text{m}$. Additionally, the analytical potential of PA at that wavelength was estimated by varying the concentrations of these chemicals in chloroform. The measurements were performed by exciting the C-H stretch bond at 2967 cm^{-1} with a 2 mW HeNe laser and using a chopping frequency of 82 Hz. The cell has been employed as described in chapter 2.2¹; it can be applied over a wide spectral range on either liquid or powdered samples. Its design facilitates easy and reproducible sample positioning and uses a parabolic mirror to couple the incident laser radiation into the PA cell.

Results

Figures 1 and 2 show the dependence of the PA signal on carbon length. Although the signal itself was not linear with the number of C-H bonds (Fig. 1), after it was normalized to the number of molecules a stronger linear tendency was observed (Fig. 2).

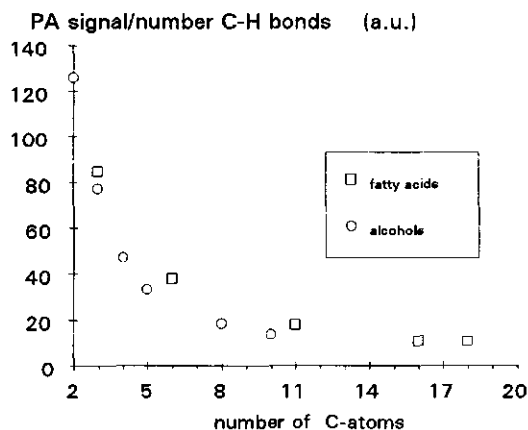


Figure 1 Photoacoustic signal, normalized to the number of C-H bonds, versus number of C-atoms in the sample molecule

As shown in Fig. 1, the ratio of PA signal to number of C-H bonds, decreased with increasing number, n , of C-atoms in the molecules being investigated. For $n > 10$ the ratio reached a constant value. The signal was then normalized to the number of molecules by multiplying it by the samples' molecular weight and dividing it by its density and is shown in Fig. 2 (this was done because the volume of all samples was constant). The normalized PA signal has a linear dependence on the increasing number of C-H bonds.

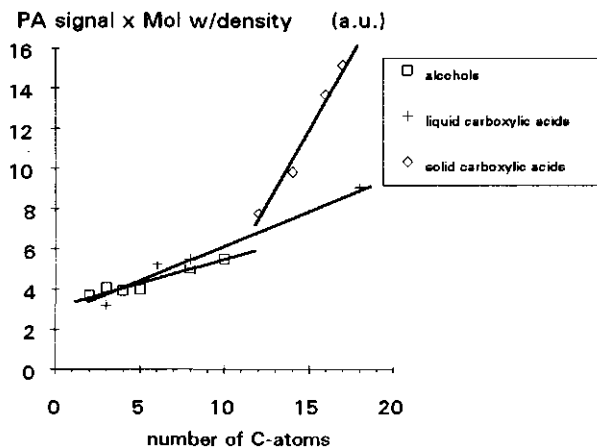


Figure 2 Photoacoustic signal normalized to the number of molecules versus the number of C-atoms in the samples

Figure 3 indicates the analytical potential of the PA method. The relationship between PA signal and the concentration of organic/chloroform solutions was linear ($R=0.997$) in the 0-10% concentration range. PA signal from alcohols and carboxylic acids showed maxima at around 25% concentration. This was due to dimer formation in the solutions, resulting in a shift of the absorption band it unresolvable from the hydrogen bonded O-H...O band.² For octane, the signal increased up to 100% concentration, since there was no influence from the OH band. At high concentrations the curve flattened as the PA signal became saturated due to the large absorption coefficients ($>1000 \text{ cm}^{-1}$) as expected from theory.³

Additionally, the thermal properties of the solutions change over such a large concentration range. Differences in the thermal properties of the organic compounds and chloroform could cause differences in the PA signals as large as 200-300% (calculated from the thermal conductivity, heat capacity and density of the compounds^{3,4}).

Similar behaviour was found for an optothermal sensor as described in ref. 5; the signal exhibited pronounced linearity for concentrations up to 25% and saturation at higher concentrations.⁶ The PA method was found superior (detection limit for oleic acid 0.25% with $S/N=6$) to the optothermal method (detection limit for C18:1 0.35% $S/N=3$). The optothermal

method, however, is often more convenient because its measurements are independent of the amount of sample.

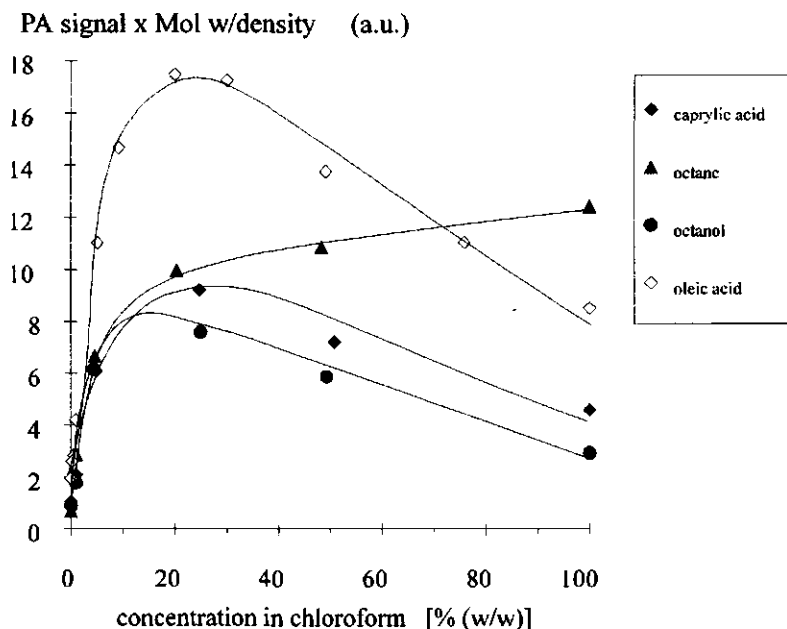


Figure 3 Photoacoustic signal normalized to the number of molecules versus concentration of octane, octanol, and caprylic and oleic acids

Conclusions

These experiments show the feasibility of a photoacoustic study of organic liquids and solids in the infrared. It forms an important addition to optical spectroscopy, as it allows measurement of absorption coefficients two or three orders of magnitude greater than is accessible by conventional spectrometers. The possible use of different radiation sources would improve the usefulness of the technique.

References

- 1 Favier J.P., Miklós A., and Bicanic D, New and Versatile Photoacoustic Cell for Studies of Powdered Specimens Across Broad Spectral Range, *Acta Chem. Slov.* **40**, 117-122 (1993)
- 2 O'Conner R.T., Field E.T. and Singleton W.S., The Infrared Spectra of Saturated Fatty Acids with Even Number of Carbon Atoms from Caproic, C6, (Hexanoic), to Stearic, C18 (Octadecanoic), and their Methyl and Ethyl Esters, *J. Amer. Oil Chem. Society* **28**, 154-160 (1951)

- 3 Rosencwaig A., Photoacoustics and Photoacoustic Spectroscopy, John Wiley & Sons, inc. (1980)
- 4 Parry J.H, Chemical Engineers' Handbook 4th edition, McGraw-Hill book company New York (1963)
- 5 Helander P., A Reliable Optothermal Sensor, Photoacoustic and Photothermal Phenomena III, Springer Series in Optical Sciences 69 ed. D. Bicanic, 562-564 (1992)
- 6 Bicanic D., Chirtoc M., Chirtoc I., Veldhuizen B., Favier J.P. and Helander P., New Technique for Measuring Absorption Coefficients of Strongly Absorbing Liquids: Optothermal Study of Sunflower Oil, Oleic Acids and Its Chloroform Solutions at 3.39 Microns, Spec. Lett. 28, 101-110 (1995).

3

Optothermal Window Spectroscopy for Optical Characterization of Different Samples

- 3.1 Detection of Total Trans Fatty Acids Content in Margarine: an Intercomparison Study of GLC, GLC + TLC, FTIR, and Optothermal Window (Open Photoacoustic Cell)**
- 3.2 CO₂ Laser Infrared Optothermal Spectroscopy for Quantitative Adulteration Studies of Extra Virgin Olive Oil in Binary Mixtures**
- 3.3 Optothermal Detection of Infrared Radiation-Induced Absorption in Aqueous Solutions of Carbohydrates: Lactose and Corn Starch**
- 3.4 Compact, Open and General Purpose Cell of Variable Effective Pathlength: Direct Absorption Measurement of SO₄²⁻ in Water**

3.1

Detection of Total Trans Fatty Acids Content in Margarine: an Intercomparison Study of GLC, GLC + TLC, FTIR, and Optothermal Window (Open Photoacoustic Cell)

based on

Jan Paul Favier, Dane Bicanic, Peter van de Bovenkamp, Mihai Chirtoc and Per Helander
Analytical Chemistry **68**, 729-733 (1996)

Abstract

Four techniques, i.e., gas-liquid chromatography, gas-liquid chromatography + thin-layer chromatography, and two spectroscopic methods, Fourier transform infrared spectroscopy and optothermal window, a variant of the open photoacoustic cell, were intercompared to determine their potential to detect the total trans fatty acid content in margarine. At the same time, this study represents a first application of the optothermal window technique at long wavelengths (10 μm). The total trans fatty acid data obtained by different methods show good mutual agreement. Besides offering several attractive advantages above conventional methods, the optothermal window also proved suitable for measuring total trans fatty acid content as low as 2%.

Introduction

Oils and fats are primary sources of lipids that provide a major portion of the energy supply in the human diet. The unsaturated constituents of most natural vegetable and marine oils contain only nonconjugated or isolated double bonds in *cis* configuration; a sizable fraction of these are converted to *trans* isomers during the process of hydrogenation needed to give fats and margarine a better consistency and stability.¹

Since the importance of monounsaturated fatty acids in reducing saturated fat intake, thereby lowering the serum level of the atherogenic low-density lipoprotein cholesterol, has been emphasized by various studies,² the content of total *trans* fatty acids in edible oil is regarded as an important issue. It was shown that the effect of *trans* fatty acids (TFA) on the serum lipoprotein profile is at least as unfavorable as that of the cholesterol-raising saturated fatty acids. The TFA not only raise the low-density lipoprotein cholesterol levels, but also lower the high-density lipoprotein cholesterol levels.² The recommended reduction of saturated fatty acids might lead to increased consumption of TFA. Since the TFA are the best substitute for saturated fatty acids in a production process of semisolid and solid fats in the edible oil industry,² the demand for the availability of a reliable and rapid on-line method capable of determining TFA is self-evident. At present, most commonly used methods to detect TFA in margarine utilize chromatography and infrared spectroscopy, each having its own specific pros and cons.

In their infrared spectra, oils and fats feature several characteristic, absorbing bands with large absorption coefficients β (m^{-1}); the one centered at 966 cm^{-1} is recommended and widely used for measurements of TFA.³ This in turn requires the use of a cell with short ($<10\text{ }\mu\text{m}$) and difficult to reproduce path lengths, thereby often complicating quantitative studies of such samples by means of traditional transmission spectroscopy. However, this problem can be circumvented by using the novel concept of optothermal window (OW) spectroscopy. This paper reports on the first application of the OW technique for measurement of TFA content in samples of margarine and compares its performance to that of existing methods.

Theory

With the exception of the OW method, all other methods used here are well-established laboratory techniques; for this reason, only OW is discussed in more detail. The operational principle of the OW technique, actually a variant of conventional photoacoustic spectroscopy, is as follows: a modulated (laser) radiation passes through the OW cell before impinging on the sample. The OW cell is actually an optically transparent disk (window), having a large thermal expansion coefficient. Its rear side is provided with an annular piezoelectric transducer. Due to the absorption of radiation, the sample's temperature rises

and the generated heat diffuses into the disk (being in a good thermal contact with the sample), which expands. The induced stress is then detected at the modulation frequency by the piezoelectric transducer in conjunction with the lock-in amplifier.

When compared to conventional photoacoustic spectroscopy, the OW method offers some attractive features.^{4,7} At first, accommodating the sample in the sealed cell is no longer an impetus. The OW signal remains unaffected by thermal expansion of the sample and in addition is also less susceptible to the effect of other sample's thermal parameters. Finally, as long as it exceeds the sample's thermal diffusion length μ (m), the thickness d (m) of the sample is not relevant, making the OW technique more practical for quantitative infrared (1700 cm^{-1}) analysis of strongly absorbing fluids and semifluids.^{8,9}

At a given modulation frequency f (s^{-1}), the magnitude of the OW signal was shown⁵ to be proportional to the amplitude of the temperature oscillation originating one thermal diffusion length below the sample-window interface. In general, thermal diffusion length μ is related to the modulation frequency f via

$$\mu = \sqrt{\frac{\kappa}{f\pi\rho c}} \quad (1)$$

where κ ($\text{Wm}^{-1}\text{K}^{-1}$), ρ (kgm^{-3}) and c ($\text{Jkg}^{-1}\text{K}^{-1}$) are thermal conductivity, density, and specific heat, respectively.

For an optically opaque ($\beta^{-1} < d$) and thermally thick ($\mu < d$) sample, making good thermal contact with a thermally thick ($\mu_{\text{window}} < d_{\text{window}}$) window, the amplitude of the normalized, dimensionless optothermal signal S is related⁵ to the product of $\beta\mu$:

$$S = \frac{\beta\mu}{\sqrt{(\beta\mu + 1)^2 + 1}} \times \frac{1}{1 + \frac{e}{c_{\text{window}}}} \quad (2)$$

where e ($\text{Ws}^{-1/2}\text{K}^{-1}\text{m}^{-2}$) is the thermal effusivity, defined in general as $e = \sqrt{\kappa\rho c}$. The plot of S from Eq. 2 versus $\beta\mu$ shown in Fig. 1 was computed for distilled water used as a test specimen and the window made of zinc selenide.

As concluded from Eq. 2, the sensitivity $dS/d(\beta\mu)$ increases for decreasing $\beta\mu$. Consequently, when studying strongly absorbing (large β) samples by the OW method, short μ (high modulation frequencies) are required. One has to bear in mind, however, that the magnitude of the photothermal signal decreases with increasing modulation frequency.

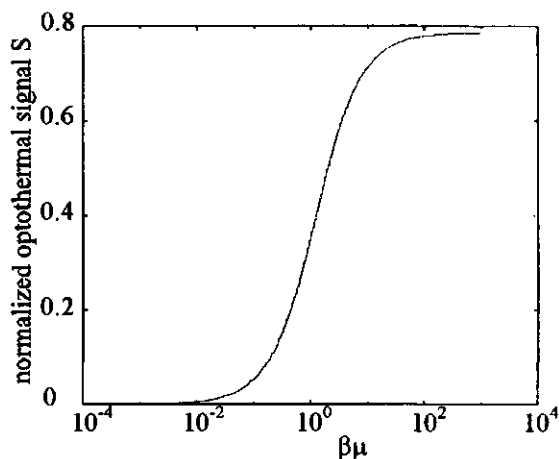


Figure 1 Plot of S calculated from eq 2 of $\beta\mu$ for distilled water ($e = 1577 \text{ W s}^{-1/2} \text{ K}^{-1} \text{ m}^{-2}$) used as a sample and the ZnSe optothermal window ($e_{\text{window}} = 5800 \text{ W s}^{-1/2} \text{ K}^{-1} \text{ m}^{-2}$, respectively).

Expressing $\beta\mu$ from Eq. (2) as a function of S one obtains

$$\beta\mu = \frac{2}{\sqrt{2 \times S^{-2} \times \left(1 + \frac{e}{e_{\text{window}}}\right)^{-2} - 1 - 1}} \quad (3)$$

This equation constitutes the basis for obtaining the absorption spectrum of the sample under investigation, provided optical and thermal properties of the reference sample at a given wavelength and modulation frequency are known. To do so, S in Eq. 3 is replaced by

$$S = \frac{S_{\text{ref}} V}{V_{\text{ref}}} \quad (4)$$

In Eq. 4 S_{ref} is the calculated (Eq. 2) OW signal for a reference substance having known values for β at selected wavelength and μ at a given modulation frequency. The V_{ref} is the measured signal at the same wavelength and modulation frequency as S_{ref} and normalized to the incident laser power. Likewise, V is the measured signal (normalized to laser power) obtained from an arbitrary sample under identical conditions. Upon substitution of Eq. (4) in Eq. (3) one can compute β if μ is known. By repeating this procedure at other laser wavelengths, the absorption spectrum of the sample under investigation can be constructed.

Experimental Section

Samples

The samples of margarine used for the intercomparison study all contained relatively high TFA (40-60%) content (mainly elaidate). They were originally prepared for the purpose of another independent experiment aimed at studying the influence of high TFA concentrations on low-density lipoprotein and high-density lipoprotein cholesterol levels in healthy subjects.¹⁰ In order to reduce the effect of spectral interferences, the triglycerides in the margarine were first converted into the methyl esters of their component fatty acids (FAME).¹¹ The calibration curves were prepared using methyl elaidate (C18:1 trans) and methyl oleate (both Nu-Chek-Prep Inc., Elysian, MN), and results expressed as a percentage of methyl elaidate in methyl oleate. In the actual experiment, 200 mg of the oil fraction (prepared from margarine samples containing both trans and cis bonds) was dissolved in 2 ml of hexane. In the final phase of our study, two different margarines (one with a low (3%) and another with a high (40%) TFA content) were investigated using only the OW method. All spectroscopic studies were carried out according to the instructions specified in AOAC method 964.34.³

Gas-Liquid Chromatography

The gas-liquid chromatography (GLC) analysis of margarine was performed on a Hewlett-Packard 5890 2 plus, with a flame ionization detector and the split injector (1 μ L of 7 mg of FAME/mL of petroleum ether; split flow 200 ml/min). The separation was achieved using a SIL88 column (100 m \times 0.25 mm Chrompack No. 007488).¹² The temperature of the injector was consistently maintained at 275°C; that of the detector was 250°C. The inlet pressure of the hydrogen carrier gas was 167 kPa. The initial temperature (150°C) was raised to 155°C using a fixed heating rate (2°C/min) and was maintained constant for 60 min. Then, a 40°C/min heating rate was applied to reach and keep the temperature at 200°C. The time of a single run was 89 min.

Ag-Thin-Layer Chromatography

Thin-layer chromatography (TLC) was carried out by depositing 200 μ L of solution (7 mg of FAME/mL of petroleum ether) on a 10% silver nitrate-coated silica plate (20x20 cm, 500 μ m Alltech Silicagel GF No. 729012) and eluting with petroleum ether/diethyl ether 19:1 (v/v). After drying, the plates were sprayed with Rhodamine 6G (25 mg/100 mL of ethanol) and examined under UV light. Three bands associated with cis fatty acids, trans fatty acids, and saturated fatty acids were observed; these were removed and separated, and the FAME eluted with diethylether before GLC examination. The temperature program was identical to that for the GLC detection mentioned above. Recovery values of 90% from the silica plate were found; the complete description is given elsewhere.¹³

Fourier transform infrared spectroscopy

Fourier transform infrared spectroscopy (FTIR) is a powerful technique that has gained much in popularity during the last ten years.^{14,15} The Biorad BST-7 FTIR spectrophotometer (resolution 4 cm^{-1}) with $12\text{ }\mu\text{m}$ thick NaCl cell was used here for spectral studies of margarine samples in a $880\text{--}1040\text{ cm}^{-1}$ range. All samples exhibit an absorption peak with a maximum at 966 cm^{-1} . The regression coefficient of the calibration graph (prepared with methylelaidate) was 0.9998.

Optothermal window cell

The experimental arrangement for OW studies (Fig. 2) comprises a homemade c.w. CO_2 waveguide laser, the radiation of which was modulated (typically 223 Hz) by a chopper (EG&G Model 179). Moveable mirrors (MM) were inserted to divert the laser radiation toward the spectrum analyzer (SA) and the homemade $25\text{ }\mu\text{m}$ thick PVDF pyroelectric detector (P_1), with a typical response of 1.5 V/W at 500 Hz . A diaphragm ($\approx 1.5\text{ mm}$ diameter) was used to reduce the size of the laser beam, so that it could enter (from below) and pass unobstructedly through the uncoated ZnSe disc (thickness 1.5 mm , diameter 20 mm) that served as the OW cell. The annular lead-zirconate-titanate PZT piezotransducer (impedance $3\text{ M}\Omega$ at 100 Hz) ring was glued to the bottom of the ZnSe window. A droplet of sample (thickness typically exceeding 3 mm) was deposited on the rear side of the ZnSe disc.

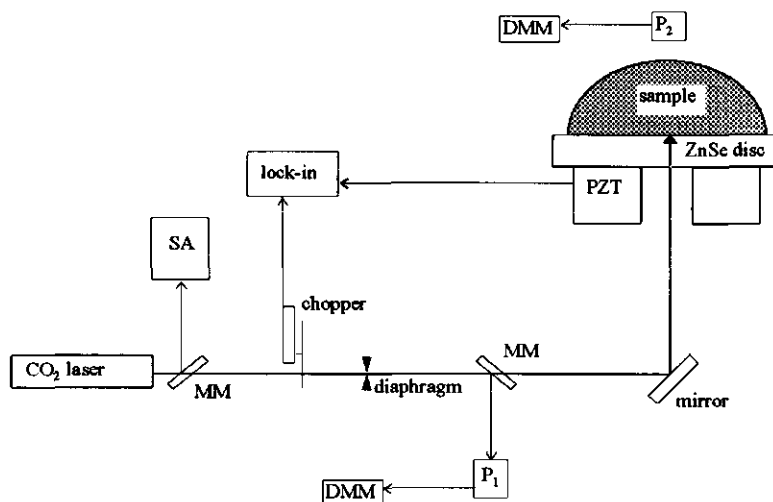


Figure 2 Experimental arrangement used for in this OW study: with moveable mirrors (MM), pyroelectric detectors (P_1 and P_2), PZT piezotransducer, spectrum analyzer (SA), and digital multimeter (DMM)

The strength of the OW signal was measured via current to voltage amplifier using a two-phase lock-in amplifier (Stanford Research Model SR850 DSP) and then normalized to the

incident power measured by P_1 placed behind the iris diaphragm (Fig. 2). A similar pyroelectric detector (P_2) mounted above the OW cell was used to monitor the power transmitted through the sample (for strongly absorbing samples, no power is transmitted). The signals from P_1 and P_2 were read off the digital multimeter (DMM). Cleaning the OW cell is easily accomplished by wiping out the sample (using cotton swabs and a paper towel) and removing residual oil deposits by washing with pure chloroform.

The optical alignment of the OW cell is relatively easy to perform. While positioning the OW assembly (mounted on a adjustable x-y-z-platform), one attempts to minimize the signal from an empty OW, or alternatively, the OW loaded with a weakly absorbing liquid such as chloroform, while maximizing the radiation throughput behind the ZnSe disc as measured by P_2 . The alignment and the signal level were regularly checked between successive measurements and following each cleaning of the cell.

As explained previously, normalized OW signals allow in the principle for direct calculation (eq 3 and 4) of the sample's β and thus for recording of its absorption spectrum. However, it was experimentally verified that the uncoated front surface of the ZnSe disk occasionally could lead to the occurrence of undesirable wavelength-dependent effects, such as multiple interferences for example, and hence false peaks in the spectrum. It is for this very reason that with our present OW the measurements were performed only at a single wavelength (966 cm^{-1} corresponding to the 10R6 CO_2 laser line).

Results

Distilled water (with well-known thermal properties¹⁶) was used as a reference sample at 293 K to calibrate the OW cell at $f = 223\text{ Hz}$ ($\mu_{\text{water}} \approx 14\text{ }\mu\text{m}$). Since no accurate β of water at 966 cm^{-1} was available in the literature, the nearest¹⁷ value $\beta = 79200\text{ m}^{-1}$ at the 10P10 (953 cm^{-1}) CO_2 laser line was used instead; this gives $S_{\text{ref}} = 0.377$ from eq 1 and 2. The calibration curve (see Experimental Section) was constructed by computing the normalized lock-in signals V (series of standard reference solutions containing 0-60% TFA) and V_{ref} (distilled water), followed by calculation (eq 3 and 4) of $\beta\mu$ for TFA-containing samples. For distilled water one obtains $\beta = 65800\text{ m}^{-1}$ at 966 cm^{-1} : a decrease of β at shorter wavelength is in agreement with the expected general trend.¹⁷ The calibration curve is characterized by the average regression coefficient of 0.9993 ($\sigma = 0.004$). The limit of detection for the present system, calculated as a ratio of three times the standard deviation obtained from the blank solution, i.e., methyl oleate in hexane, and the slope of the calibration curve is 2%.

As an illustrative example, at a laser power of 300 mW (signal from P_1 measured on DMM was 0.173 mV), the normalized signal strength V (for sample containing 32.7% TFA) was 2.061 ($\sigma = 0.028$ and lock-in signal was 0.356 mV). For water, one obtained $V_{\text{ref}} = 10.05$ ($\sigma = 0.050$, lock-in signal was 1.658 mV) when DMM voltage was 0.165 mV. Under similar

conditions, the empty cell produced a normalized signal of 0.657 ($\sigma = 0.040$). This value was consistently subtracted from the readings obtained from both samples and reference when calculating $\beta\mu$.

Table 1 TFA Content (%) in different samples of margarine by various methods

margarine sample (code)	FTIR	OW	GLC	GLC+ TLC
6337	59.3	62.2	50.5	58.3
6338	64.9	63.6	53.6	62.7
6339	42.9	42.0	35.9	41.8
6340	41.8	42.4	39.8	41.0

Table 1 displays the percentage of the total TFA content found in different samples of margarine (each datum represents the arithmetic mean of average values obtained from duplicate measurements, and each of these in turn implied a series of three consecutive measurements) by various methods. The corresponding concentrations were derived from the calibration graph by interpolation. Data obtained by different methods are generally in a good mutual agreement: some minor discrepancies are explainable. For example, the TFA content determined by GLC is usually lower than that obtained by other methods: presumably this is because some of the trans peaks are masked by cis peaks and hence cannot be resolved. Consistently higher values found by spectroscopic methods (OW and FTIR) are probably due to the presence of polyunsaturated fatty acids in the sample (spectroscopic measurements provide an estimate of the total number of trans bonds in the sample). Thus, if knowledge of the total TFA content is a priority, OW and FTIR are preferred. When, however, the profile of TFA is desired, the combined GLC+TLC method, capable of detecting constituents in the mixture (including various stereo and positional isomers) is a proper choice. A disadvantage of GLC+TLC is its time- and labor-consuming character. The relative error in all techniques is typically 2%.

Table 2 TFA Content (%) in different samples of margarine measured on different days

sample	sample age (days)		
	0	6	13
A	6.1	6.3	6.3
3×A+C	15.7	15.7	15.7
A+C	27	27.2	28
C	42	44.6	45.7

As a next step, the potential of the OW method to detect total TFA in margarine at concentration levels more likely to occur in practice was investigated. Two (arbitrarily called

A and C) different samples of margarine and their combinations (A:C mixed in mass proportionality ratios 1:1 and 3:1) were studied. Based on results of the GLC measurements, sample A has a low (3%) TFA content while sample C is a high-TFA (40%) mixture. A new calibration graph (0-40% TFA) was prepared in the same way as described above. Since one of objectives of our studies was also to check the repeatability and reproducibility of the OW method (measurements were performed on different days), samples were stored at 5°C (to avoid evaporation). As seen in Table 2, expected and measured (each datum represents the arithmetic average of three consecutive measurements) values compare well (e.g., $(44.6+6.3)/2=25.5\%$ is close to a measured TFA content of 27.2%); this is also true in the lower TFA concentration range. Minor differences might be due to the fact that the mixing of samples was not homogeneous (only ≈ 200 mg was taken from the mixed margarine). The TFA content in all samples shows a tendency to increase slightly with age, which is probably caused by uncontrollable evaporation of the hexane.

Conclusions

The feasibility of the OW method as a candidate technique for quantitative analysis (at 966 cm^{-1}) of total TFA content (2-60%) in realistic margarine samples was demonstrated in this intercomparison study. Compared to other well-established methods, the OW concept offers intrinsically some economic and practical advantages such as ease and speed of operation, as well as simple and rapid sample loading and cleaning of the cell. Current detection limit (2% TFA) for OW is restricted by the slope of the calibration curve rather than by the relative experimental error ($0.028/2.061 = 0.13\%$); the reproducibility of the measurement was very good. Further enhancement of detection sensitivity is anticipated by reducing the level of background absorption (proper choice as well as specific treatment (e.g., coating) of the window material). Changing the modulation frequency could also lead to an improved sensitivity.

In conclusion, unlike in traditional IR analysis where cell thickness is the restricting factor in dealing with strongly absorbing samples, the magnitude of the OW signal depends solely on the product $\beta\mu$, which, in principle, can be manipulated by the choice of the modulation frequency. At this stage, wavelength-dependent multiple interference effects in the currently used ZnSe window (it was not possible to mount it at a Brewster angle) preclude the accurate determination of absolute optical absorption coefficients β for our samples over a broader spectral range (see chapter 3.2). Nevertheless, the OW method is thought useful for potential applications in many other research areas including absorption-concentration studies in analytical chemistry, process control, and analytical studies of intact specimens in the life sciences.

Acknowledgments

M.C. expresses his gratitude to NWO (Dutch Organization for Scientific Research) for a fellowship received. Credit is to B. van Veldhuizen (Department Organic Chemistry WAU), for his advise and assistance provided in the FTIR experiments and to H. Boshoven for manufacturing components used in the experimental setup. Gratitude is to Mrs. J. Bos and Mrs. Kosmeijer-Schuil (both Department of Human Nutrition) for preparing the samples and provided valuable help during GLC and GLC+TLC measurements.

References

- 1 Osborne B.G., Fearn T. and Hindle P.H., Practical NIR Spectroscopy with Applications in Food and Beverage Analysis 2nd ed., Longman Scientific & Technical Singapore (1993)
- 2 Mensink R.P. and Katan M.B., Effect of Dietary Trans Fatty Acids on High-Density and Low-Density Lipoprotein cholesterol levels in healthy subjects, *New Engl. J. Med.* **323**, 439-445 (1990)
- 3 AOAC Method 965.34 Official Methods of Analyses of the Association of Official Analytical Chemists; AOAC Washington DC, Vol XV, 969-701 (1990)
- 4 Helander P., Signal Processing in Optothermal Spectroscopy, *J. Appl. Phys.* **59**, 3339-3343 (1986)
- 5 Helander P., A Method for the Analysis of Optothermal and Photoacoustic Signals, *Meas. Sci. & Technol.* **4**, 178-185 (1993)
- 6 Tam A.C., Applications of Photoacoustic Sensing Techniques, *Rev. Mod. Phys.* **58**, 381-427 (1986)
- 7 Wetsel G.C. Jr. and McDonald F.A., Photoacoustic Determination of Absolute Optical Absorption Coefficient, *Appl. Phys. Letts.* **30**, 252-254 (1977)
- 8 Bicanic D., Chirtoc M., Chirtoc I., Veldhuizen B., Favier J.P. and Helander P., New Technique for Measuring Absorption Coefficients of Strongly Absorbing Liquids: Optothermal Study of Sun Flower Oil, Oleic Acid and Its Chloroform Solutions at 3.39 Microns, *Spec. Letts.* **28**, 101-110 (1995)
- 9 Bicanic D., Chirtoc M., Chirtoc I., Favier J.P. and Helander P., Photothermal Determination of Absorption Coefficients in Optically Dense Fluids: Application to Oleic Acid and Water at CO Laser Wavelength, *Appl. Spec.* **49**, 1954-1959 (1995)
- 10 Zock P.L. and Katan M.B., Hydrogenation Alternatives: Effects of Trans Fatty Acids and Stearic Acid Versus Linoleic Acid on Serum Lipids and Lipoproteins in Humans, *J. Lipid Res.* **33**, 399-410 (1992)
- 11 Metcalfe L.D., Schmitz A.A. and Pelka J.R., Rapid Preparation of Fatty Acid Esters from lipids for Gas Chromatographic Analysis, *Anal. Chem.* **38**, 514-155 (1966)

- 12 Pfalzgraf A., Timm M. and Steinhart H., Content of Trans-Fatty Acids in Food, *Z. Ernährungswiss.* **33**, 24-43 (1994)
- 13 Morris L.J., Separations of Lipids by Silver Ion Chromatography, *J. Lipid Res.* **7**, 717-731 (1966)
- 14 Nyquist R.A., Chrzan V., Kirchner T., Yurga L. and Putzig C.I., Studies of Carbonyl-Containing Compounds in Mixed Solvent Systems by Application of Infrared Spectroscopy, *Appl. Spec.* **44**, 243-263 (1990)
- 15 Bertie J.E. and Eysel H.H., Infrared Intensities of Liquids I: Determination of Infrared Optical and Dielectric Constants by FT-IR using the Circle ATR Cell, *Appl. Spec.* **39**, 392-401 (1985)
- 16 Dwight E.G. (ed); American Institute of Physics Handbook, 3rd edition, McGraw-Hill Book Company, New York (1982)
- 17 Hale G.M. and Querry M.R., Optical Constants of Water in the 200-nm to 2000-nm Wavelength Region, *Appl. Optics* **12**, 555-63 (1973).

3.2

CO₂ Laser Infrared Optothermal Spectroscopy for Quantitative Adulteration Studies in Binary Mixtures of Extra Virgin Olive Oil

submitted to J. Amer. Oil Chem. Soc.

Jan Paul Favier, Dane Bicanic, Jan Cozijnsen, Beb van Veldhuizen and Per Helander

Abstract

Optothermal window spectroscopy at CO₂ laser infrared wavelengths, was used to detect the extent of adulteration of extra virgin olive oil by sunflower and safflower oils. A good linearity between the strength of optothermal signal and the concentration of each adulterating compound was found. Predicted limits of detection presently attainable by this new method are 6% (w/w) and 4.5% (w/w) for extra virgin olive oil adulterated with safflower oil and sunflower oil respectively, were confirmed experimentally; the corresponding relative errors were 0.3% and 0.18%. Interference effects are comparable to those encountered in other spectroscopic methods, at the same wavelength.

Keywords: adulteration, infrared, olive oil, optothermal spectroscopy, photoacoustic spectroscopy

Introduction

Consumption of olive oil has increased over the past few years, a trend which may be attributed to its characteristic flavor and potential health benefits. Olive oil is obtained from the fruit of the olive tree (*Olea europaea* L.) and may neither be manipulated nor subjected to any treatment not approved by the recognized international standards.¹

Substitution or adulteration of extra virgin olive oil by a cheaper ingredient is not only a major economic fraud, but can also have potential health implications.^{2,3} The authentication of extra virgin olive oil is a major analytical challenge, but is often time-consuming and laborious.³ Traditional analytical techniques used for characterizing extra virgin olive oil, such as determination of iodine and saponification values, measurement of density, viscosity, and refractive index, all require some kind of sample pretreatment.^{1,2}

Modern high performance liquid chromatography (HPLC) and gas-liquid chromatography (GLC) techniques provide adequate separation and good sensitivity,⁴ but require substantial know-how to interpret the results. As an example, adulteration of extra virgin olive oil by canola oil could be detected down to 7.5% (w/w).⁵ Likewise, mass spectrometry in combination with an artificial neural network was shown capable of detecting 5% (v/v) adulteration of extra virgin olive oil by soya, sunflower, corn and peanut oil.⁶

Spectroscopy, on the other hand, offers the possibility for direct and non-destructive analysis. For example, UV spectroscopy (at 210 and 315 nm) was successfully used to detect adulteration of extra virgin olive oil by refined oil at a level as low as 6%.³ Near infrared spectroscopy was recently utilized to estimate the level (5% (w/w)) of corn oil, sunflower oil and raw olive residue oil in virgin and extra virgin olive oils using principal component analysis techniques.⁷

Although mid infrared (MIR) spectroscopy (4000-400 cm^{-1} region) is often employed for studies of oils and fats, its application for detection of adulteration in olive oil has been rarely reported.³ In contrast to the IR spectra of other seed oils, the spectrum of olive oil is rather flat in the 900 to 1200 cm^{-1} spectral region.^{1,2} Recently performed⁸ quantitative analysis of extra virgin olive oil adulterated by walnut oil and refined olive oil using FT-IR spectroscopy combined with attenuated total reflection (ATR) yielded a detection limit of 2% (w/w).

In this paper, the optothermal window (OW) method, a spectroscopic technique related to photoacoustic spectroscopy, exploited to determine the levels of the adulterants safflower and sunflower oils in extra virgin olive oil.

Experimental section

Samples used in this study, were purchased fresh from a local store. A standard series of blends containing different proportions (analytical balance) of safflower and sunflower oils in extra virgin oil was prepared. During the initial phase of the research the percentage of adulterant in the mixture varied from 0-100% (w/w) in steps of 20%.

Fatty acid profiles of the methyl esters⁹ (Table 1) were obtained by GLC with splitless injection (Carlo Erba 4160 GLC, Carlo Erba Strumentazione Milano, Italy). The separation was achieved on a DB-225 (50% Cyanopropylphenyl-methyl polysiloxane) column (15m×0.53mm, film thickness 1.0 μm; J&W Scientific, Folsom, CA). The linear velocity of the helium carrier gas was 50 cms⁻¹. The initial temperature (150°C), was programmed to 210°C at a heating rate of 2.5°C/min. The injection temperature and the detector temperature were 250°C and 275°C, respectively.

Prior to the actual OW experiments, the spectra (900-1150 cm⁻¹) of all adulterated and pure samples were recorded on a Biorad BST-7 FT-IR (Digit Lab. Dev. Cambridge MA 02139) spectrophotometer (resolution 2 cm⁻¹) with a deuterated triglycine sulfate detector.

The basic principles behind the OW spectroscopy and a detailed description of the experimental set-up are given elsewhere.^{10,11} The optothermal window constituted a 1.5 mm thick ZnSe disk and the annular piezoelectric crystal (PZT) was bonded to the rear side of the disk. A liquid sample (≈50 μL) was deposited directly atop the disk, that on its turn was exposed to modulated CO₂ laser radiation. Following the absorption of radiation in the sample, the generated heat diffused into the disk causing its expansion that is sensed by a PZT.

The OW cell used in this study was an improved version of a previous design.¹¹ To avoid Fabry-Perot resonances in the ZnSe disk, the latter was provided with an antireflective coating on the side facing the incident laser beam. Additionally, to prevent laser radiation from directly striking the PZT detector which would give rise to false signals, a reflective gold layer (5 μm thick) was deposited onto the very same surface in such a way as to leave a clear, uncoated, central circular area about 4 mm in diameter.

Results and Discussion

The composition of pure extra virgin olive oil and of adulterated samples were investigated by GLC measurements and are shown in Table 1. The GLC data showed a linear relationship between the extent of adulteration and the content of oleic and linoleic acid. The peak areas were expressed as percentages of the total areas (response factors were not used) and a typical error for these measurements is 3% (for a content of 36% the error is 1.1%).

The FT-IR experiments were performed first in order to determine most appropriate excitation wavelengths of the CO₂ laser (emitting between 931-1084 cm⁻¹). The comparison of FT-IR absorption spectra obtained from adulterated samples and the pure olive, safflower and sunflower oil revealed only small differences. In the 900 to 1050 cm⁻¹ region olive oil featured a relatively flat absorption as expected.² The actual OW studies were carried out (at 293K) at five selected CO₂ laser wavelengths: 931 cm⁻¹, 953 cm⁻¹, 966 cm⁻¹, 1041 cm⁻¹ and 1079 cm⁻¹.

Table 1 The fatty acid profiles (determined by GLC) FAMES of olive and safflower oils and of their mixtures. The composition of sunflower oil is also given.

safflower oil (% w/w)	C16:0	C16:1	C18:0	C18:1	C18:2	C18:3	C20:0	C20:1
0%	13	1	2	73	9	1	<0.5	<0.5
20%	11	1	2	62	23	1	<0.5	<0.5
40%	11	<0.5	2	49	37	<0.5	<0.5	<0.5
60%	10	<0.5	2	36	51	<0.5	<0.5	<0.5
80%	8	<0.5	2	23	66	<0.5	<0.5	<0.5
100%	7	-	2	11	77	<0.5	<0.5	<0.5
sunflower oil	7	<0.5	4	18	70	<0.5	<0.5	<0.5

Because of its well known optical and thermal properties, distilled water was used to calibrate of the set-up for OW measurements.¹¹ The 953 cm⁻¹ and 1041 cm⁻¹ CO₂ laser lines were used for the calibration; the absorption coefficients β for water at these wavelengths are $7.92 \times 10^4 \text{ m}^{-1}$ and $5.94 \times 10^4 \text{ m}^{-1}$ respectively.¹² The optical alignment as well as the magnitude (typically < 1 μV) of a background signal obtained from the empty OW window were checked between successive measurements and after completing the cleaning procedure of the cell (with chloroform).

The plot showing the OW signals at 953 cm⁻¹ calculated from experimental data obtained from mixtures containing known proportions of the safflower oil in olive oil is displayed in Fig. 1. In order to calculate the absorption coefficients, the OW signals were first normalized to the laser power measured behind the OW cell.¹¹

Each data point in Fig. 1 represents an average of twenty successive measurements performed at 221 Hz with the CO₂ laser tuned to 953 cm⁻¹ line; at this particular wavenumber the relative error was 0.3%. In general, the later was found to depend on a power stability of the laser at a specific transition; i.e. 0.7% at 931 cm⁻¹, 0.4% at 966 cm⁻¹ and 0.2% at 1079 cm⁻¹. For olive oil adulterated with safflower oil, the limit of detection (LOD), here defined as the ratio of a threefold standard deviation obtained from the blank (olive oil) and the slope of the calibration curve, is 6% (w/w); the regression coefficient r for data in Fig. 1 is 0.9995.

The 8% (w/w) and 6% (w/w) LOD's (regression coefficients $r = 0.997$) obtained when studying the above test samples at 931 cm^{-1} and 966 cm^{-1} are ascribed to a poorer stability of the laser at these two lines. At 1079 cm^{-1} , as expected, no difference was between the OW signals obtained from safflower and olive oils. On the other hand, differences measured at other lines were found to be due to the optical, rather than thermal changes induced in the sample.

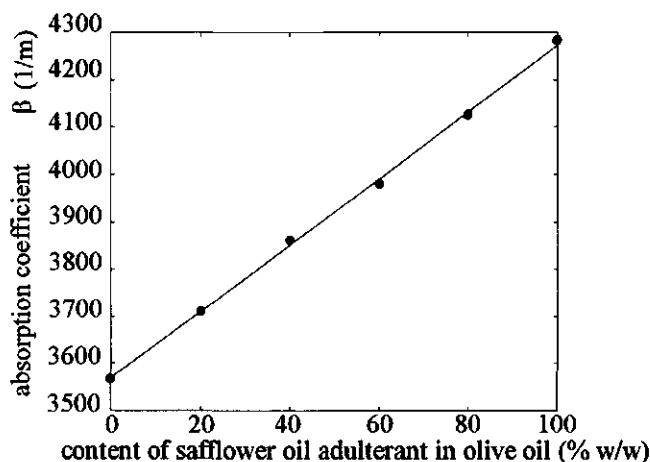


Figure 1 Experimentally determined absorption coefficient β for olive oil adulterated by safflower oil. The study was performed at 953 cm^{-1} transition of the CO₂ laser

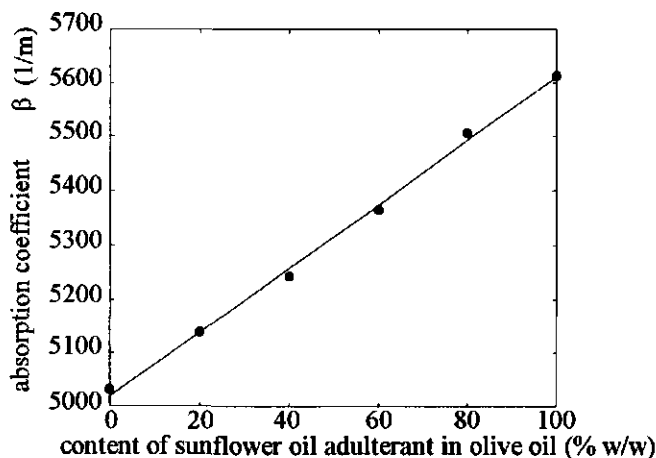


Figure 2 Experimentally determined absorption coefficient β for olive oil adulterated by sunflower oil. The study was performed at 1041 cm^{-1} transition of the CO₂ laser

Results for olive oil adulterated by sunflower oil shown in Fig. 2, were obtained in the same way as those shown in Fig. 1, but with the CO₂ laser tuned to the 1041 cm⁻¹ line instead. The relative error was 0.18%, giving a 4.5% LOD and a regression coefficient *r* of 0.999.

When deriving the above stated LOD's (Figs. 1 and 2), the concentration range between 0 and 20% (w/w) was originally extrapolated. This deficiency was later rectified by preparing extra standards (5% (w/w)) of each adulterant. Both of these samples produced measurable OW signals. As an example, for the extra virgin olive oil adulterated with 5% (w/w) safflower oil, absorption coefficient (at 953 cm⁻¹) calculated from calibration curve (Fig. 1) is 3604 m⁻¹, which is very close to experimentally found 3590 m⁻¹. Similarly, one finds 5059 m⁻¹ (at 1041 cm⁻¹) compared to expected 5051 m⁻¹ for a specimen containing 5% of sunflower oil in the extra virgin olive oil.

The OW method used here proved suitable to rapidly detect reasonably small amounts of known adulterants (safflower and sunflower oils) in the extra virgin olive oil; LOD's presently attainable are 5% (w/w). Generally, the obtained LOD's are of the same order of magnitude as those attainable for similar adulterants by traditional methods (FTIR, GLC, HPLC and the mass spectrometry). An enhancement of LOD is anticipated for a more stable, discretely tunable CO₂ laser. The level of a background noise for a OW device used in this study was significantly below that of the OW sensor used previously.¹¹ Manufacturing the thinner window from a material having better optical and thermal properties than currently used ZnSe (e.g. diamond), is expected to lead to an improvement of sensitivity.

In conclusion, it has to be emphasized here that the OW study was performed with a discretely tunable CO₂ laser on two binary mixtures containing only adulterants, the quantities and the identities of which were precisely known. Obviously, in order to identify and quantitate the adulterant of unknown nature in a complex mixture, one needs continuously tunable radiation. The presently emerging generation of compact and high power infrared diode lasers will therefore boost both the specificity and sensitivity of the OW method, simply because the excitation wavelengths characterized by the optimal spectral contrast will become available. As for the effect of unwanted spectral interferences at a selected wavelength in the OW approach, this latter is comparable to that normally encountered with any other spectroscopic technique.

One should also bear in mind that OW device represents a universal detection scheme, i.e. it is not wavelength limited. This means that one and the same device can be used within a wide range of wavelengths, provided window remains transparent to the exciting radiation.

When combined with other advantages of the OW technique (practicality, reasonably low cost, suitability for the on-line operation and intrinsic simplicity when loading, cleaning and operating the cell) the developments mentioned above could eventually make OW technique

a good candidate technique not only for rapidly quantifying presence of unknown adulterants in the extra virgin olive oil, but for many other applications as well.

As to this point, it is certainly worth noting the recent application of OW based instruments for the analysis of principal components (moisture, fat, protein, carbohydrates) of cheeses at the selected near and mid-infrared wavelengths. Its performance was shown superior to that of FTIR-ATR in terms of speed, accuracy and the ease of data analysis.^{13,14} Work on similar matter is in progress.¹⁵

Acknowledgments

The work described in this paper was partially supported by the European Community (Copernicus ERBIC15CT961003).

References

- 1 Recommended International Standard for Olive Oil, Virgin and Refined, and for Refined Olive-Residue Oil, FAO/WHO Food Standard Program, CAC/RS 33 Rome, Italy (1970)
- 2 Kiritsakis A. and Marakakis P. Essential Oils and Waxes, ed. Linskens H.F. & Jackson J.F., Springer Verlag, Heidelberg, Germany, Chapter 7 (1991)
- 3 Wilson R.H., New Physico-Chemical Techniques for the Characterization of Complex Food Systems, 1st ed. Dickinson E., Blackie Academic & Professional Chapman & Hall, Glasgow UK, Chapter 8 (1995)
- 4 Tsimidou M. and Macrae R., Detection and Quantitative Determination of Adulteration of Olive Oil, *Int. Analyst* **2**, 29-34 (1987)
- 5 Salivaras E. and McCrudy A.R., Detection of Olive Oil Adulteration with Canola Oil from Triacylglycerol Analysis by Reverse-Phase High-Performance Liquid Chromatography, *J. Amer. Oil Chem. Soc.* **69**, 935-938 (1992)
- 6 Goodacre R., Douglas B.K. and Bianchi G., Food Adulteration Exposed by Neural Networks, *J. Sci. Food Agric.* **63**, 297-307 (1993)
- 7 Wesley I.J., Barnes R.J. and McGill A.E.J., Measurement of Adulteration of Olive Oils by Near-Infrared Spectroscopy, *J. Amer. Oil Chem. Soc.* **72**, 289-292 (1995)
- 8 Lai Y.W., Kemsley E.K. and Wilson R.H., Quantitative Analysis of Potential Adulterants of Extra Virgin Olive Oil Using Infrared Spectroscopy, *Food Chem.* **53**, 95-98 (1995)
- 9 NEN 6304 Plantaardig en Dierlijke Oliën en Vetten. Gaschromatografische Analyse van Methylsters van Vetzuren met Capilaire Kolommen
- 10 Helander, P., A Method for the Analysis of the Optothermal and Photoacoustic Signals, *Meas. Sci. & Technol.* **4**, 178-185 (1993)
- 11 Favier J.P., Bicanic D., Bovenkamp P. van de, Chirtoc M. and Helander P., Detection of Total Trans Fatty Acids Content in Margarine: An Intercomparison Study of GLC, GLC +

- TLC, FT-IR and Optothermal Window (Open Photoacoustic Cell), *Anal. Chem.* **68**, 729-733 (1996)
- 12 Hale G.M. and Query M.R., Optical Constants of Water in the 200-nm to 200- μm Wavelength Region, *Appl. Optics* **12**, 555-563 (1973)
 - 13 McQueen D.H., Wilson R., Kinnunen A., Near and Midinfrared Photoacoustic Analysis of Principal Components of Foodstuffs, *Trends in Anal. Chem.* **14**, 482-492 (1995)
 - 14 McQueen D.H., Wilson R., Kinnunen A., Jensen E.P. Comparison of Two Infrared Spectroscopic Methods for Cheese Analysis, *Talanta* **42**, 2007-2015 (1995)
 - 15 Wilson R., Institute of Food Research, Norwich, England, Private communication 1997.

3.3

Optothermal Detection of Infrared Radiation-Induced Absorption in Aqueous Solutions of Carbohydrates: Lactose and Corn Starch

based on

Jan Paul Favier, Dane Bicanic, Otto Dóka, Mihai Chirtoc and Per Helander

Journal of Agricultural & Food Chemistry **45**, 777-780 (1997)

Abstract

The optothermal window method, a variant of photoacoustic spectroscopy, was used at 10 μm wavelength to explore its feasibility for direct investigation of aqueous solutions of lactose and corn starch. Present limits of detection attainable by this method are 0.19% (w/w) for lactose solution and 0.6% (w/w) for corn starch gel, respectively.

Keywords: Photoacoustics, infrared spectroscopy, non-destructive analysis

Introduction

Chemical-physical analyses are becoming steadily more important when the quality of raw agricultural products and foodstuffs is evaluated.¹⁻³ Most of these techniques not only require some kind of sample treatment before detection is attempted but are also time consuming. The need for a rapid analysis while maintaining simultaneously sample integrity has therefore stimulated development of non-destructive inspection methods, among which are also various spectroscopic techniques.^{3,4} In particular, the infrared (IR) region with specific absorption frequencies and their band intensities uniquely characterizing chemical compounds, was utilized for qualitative and quantitative studies of foods.⁵⁻⁸

As many foodstuffs contain water which has a strong absorption in the IR, accurate quantitative spectroscopic measurements on such samples are not trivial. The use of traditional transmission cells for studies of pasty or viscous samples also causes problems associated with filling and cleaning procedures. These were partially alleviated by the introduction of the attenuated total reflection technique (ATR).⁶

This paper exploits the prospects of a new technique, i.e., that of optothermal window (OW), used in combination with a CO₂ laser (emitting between 1100 and 900 cm⁻¹) for quantitative IR analysis of lactose and corn starch in water. A peculiar feature of this new technique, when compared to other methods, is the fact that the temperature variations induced in the sample by the absorption of radiation are sensed outside the area of the sample irradiated by the excitation source. Corn starch and lactose were selected as test samples because of their important role in foods.² Starch is a major food constituent of foods and serves as a model for many foodstuffs. In the infrared corn starch has strong absorptions at 1681, 1053-952 and 855 cm⁻¹.⁷ On the other hand, lactose is an important constituent of milk and dairy products.

A sample of real milk was also investigated to validate the feasibility of the OW technique. Infrared analysis of milk is currently performed by determining the content of lactose (1042 cm⁻¹), protein (1549 cm⁻¹), and fat (1745 cm⁻¹) using dedicated filter instruments.^{9,10}

All OW studies described here were carried out only at a few discrete wavelengths of the laser. However, the evaluation of results obtained in this experiment is important to estimate the prospects of a new, experimental technique based on a combined use of continuous tunable (powerful) infrared diode lasers as the radiation source and the OW concept. Finally, incorporating this new concept into that of FTIR spectrometry for quick scanning of spectra is worth considering.

Basic theoretical concepts of the OW method

The OW technique is a variant of photoacoustic spectroscopy.^{11,12} The heat, produced in a condensed phase sample by the absorption of modulated frequency f (s^{-1}) radiation, diffuses into the disk supporting the sample. Expansion of the disk generates an acoustic wave which is detected by a piezoelectric transducer (PZT). A decisive parameter is the thermal diffusion length (μ) of the sample, defined as $\mu = \sqrt{\frac{\alpha}{\pi f}}$ with α (m^2s^{-1}) being the thermal diffusivity of the sample. Physically, μ is the distance across which the amplitude of a generated thermal wave is reduced to e^{-1} of its initial value. Only the heat originating from a layer of μ deep is detected by the PZT.

When the thickness of the sample is larger than its thermal diffusion length, the sample is termed as "thermally thick". For such a sample that, in addition, is in a good thermal contact with the disk, the normalized OW signal $S(\beta)$ ¹¹ is given by

$$S(\beta) = \frac{\sqrt{2}\mu\beta}{\sqrt{(\mu\beta)^2 + (\mu\beta + 2)^2}} \quad (1)$$

where β is the wavelength dependent absorption coefficient (m^{-1}) of the sample. In general, the OW signal decreases at higher frequencies; this is also true for the sensitivity of the PZT sensor. The absorption coefficient β of the sample can be obtained from Eq. (1) provided the OW cell is properly calibrated. In principle, recording the OW signal at varying wavelengths of incident laser radiation enables one to construct an absorption spectrum. The optical penetration depth must be larger than the thermal diffusion length, i.e., $\beta^{-1} > \mu$, if the OW spectrum is to coincide with the true absorption spectrum.

Experimental Procedures

The OW experimental arrangement (Fig. 1) comprised a homemade c.w. CO₂ waveguide laser which was modulated (here 221 Hz) by a chopper (EG&G model 179). A 2 mm diameter diaphragm (1), was used to reduce the size of the unfocused laser beam, so that it could pass from below (at a normal incidence) through a 20 mm diameter and 1.5 mm thick ZnSe disk (4) (Janos Technology, Inc.) with the annular PZT (3) (impedance 3M Ω at 100 Hz) bonded to the lower surface. To avoid Fabry-Perot resonances, the disk was provided with the antireflective coating on the side facing the incident laser beam. In order to prevent radiation striking the PZT directly, which would give rise to unwanted false OW signals, a reflective gold layer (5 μ m thick) was deposited on the surface of the disk bonded to the PZT, in such a way as to leave a clear (uncoated), central circular area about 4 mm in diameter. A droplet of the sample (200 μ L for lactose) or a small quantity of starch gel was deposited directly atop the disk. The strength of the preamplified OW signal (after current to voltage amplifier

conversion) was measured by a lock-in amplifier (Stanford Research model SR850 DSP) and normalized to the incident intensity measured with a power detector (Spectra Physics model 407A) placed above the empty OW cell. The emission wavelength of the laser was determined by inserting a movable mirror to divert the laser radiation toward the spectrum analyzer.

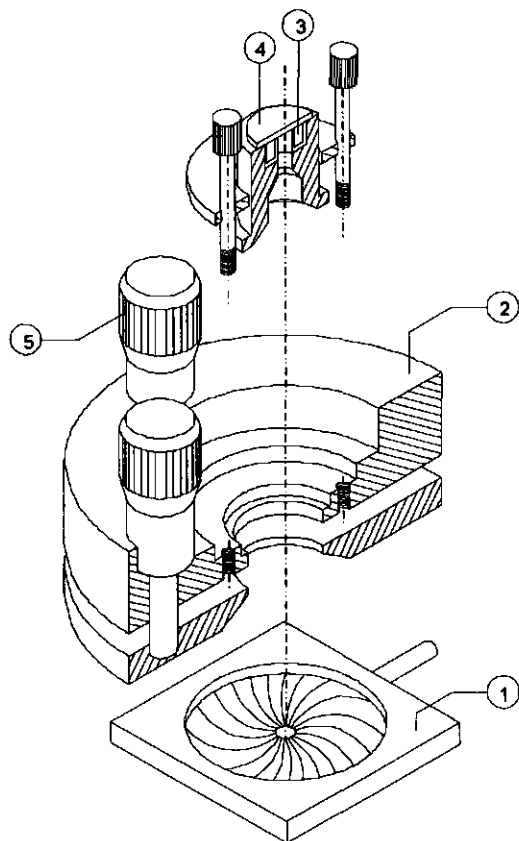


Figure 1 Heart of the experimental OW set-up, displaying an adjustable diaphragm (1), gimbal mount (2), piezoelectric transducer (3), ZnSe disk (4), and adjusting micrometer screws (5)

The alignment of the OW cell (the disk and PZT assembly) was relatively easy to perform. With the empty OW cell in a gimbal mount (2) (Microcontrole), the lock-in signal was minimized (typically $0.7 \pm 0.4 \mu\text{V}$) by adjusting the micrometer (5) and maximizing the laser power throughput (typically 30-100 mW depending on the laser line) measured behind the cell. Both the alignment and the level of the OW signal were regularly checked between successive measurements as well as after completing the disk-cleaning procedure (simply wiping out the sample using cotton swabs and a paper towel).

Results

Standard solutions varying from 2.5% to 20 % (w/w) lactose (Merck CAS-No. 10039-26-6 7660) and from 2.5% to 10 % (w/w) corn starch (Merck CAS-No. 9005-25-8 11686) were prepared by dilution in distilled water. The starch solutions were shaken vigorously after heating (30 seconds at 80°C) in a microwave oven; the gel was then formed on cooling down to room temperature.

Initially, the spectrum of 10% lactose was recorded with a FTIR spectrophotometer (Biorad BST-7, resolution 4 cm^{-1}) to determine appropriate excitation wavelengths of the CO_2 laser needed for OW studies. The maximal absorption of the lactose solution was found at 1041 cm^{-1} . The limit of detection (LOD), calculated as a ratio of 3 times the standard deviation obtained from the blank (water) and the slope of the fitted calibration curve, is 0.1% for this FTIR experiment. The spectra of 2.5% and 5 % corn starch samples were recorded using a ZnSe ATR accessory. Difficulties were experienced when trying to evenly spread a layer of gel along the flat surface of the ATR crystal (the gel tends to fractionate easily). The FTIR-ATR spectra of the corn starch samples were only qualitative indicating the absorption peaks around 1053 cm^{-1} .

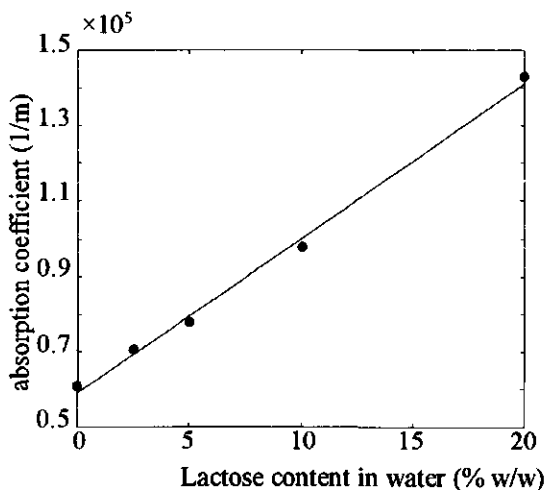


Figure 2 Absorption coefficient β for aqueous solutions containing a varying lactose content. The measurement was performed at the 9P26 (1041 cm^{-1}) line of the CO_2 laser

The calibration of the experimental set-up was performed¹³ with distilled water because of its well-known optical and thermal properties. The 9P26 (1041 cm^{-1}) line of the CO_2 laser (nearly coinciding with the recommended analytical wavelength for lactose) was used for calibration; the absorption coefficient β for water at this wavelength is $5.94 \times 10^4 \text{ m}^{-1}$.¹⁴ The

calibration curve for lactose was linearized (Eq. 1) and the calculated absorption coefficients are shown in Fig. 2; each data point is an average of four measurements.

The average regression coefficient of the calibration curve in Fig. 2 is 0.9992, and the calculated LOD of lactose in water is 0.19% (w/w). The 0.4% relative error for distilled water (the ratio of the standard deviation $\sigma = 0.03$ to the normalized OW signal of 6.70) was higher than 0.2% ($\sigma = 0.01$ divided by 7.45) and 0.3% ($\sigma = 0.02$ divided by 7.89) obtained for 2.5% and 5% lactose solutions, respectively. The LOD of 0.19% (w/w) is substantially below the average lactose content found in milk. The straight line intercepts the y-axis at $5.92 \times 10^4 \text{ m}^{-1}$ which is very close to the absorption coefficient of pure water at 1041 cm^{-1} . Finally, a commercial milk sample was used to test the feasibility of the OW technique. The 5.5% lactose content found in milk is 1% above the expected value, which is not surprising as no correction was made for the contribution to the OW signal due to absorption of protein and fat. For comparison a FTIR apparatus yielded a LOD of 0.05-0.1% for lactose in milk.¹⁰

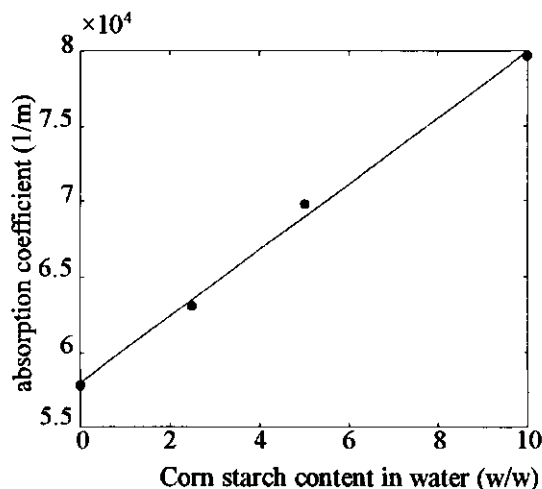


Figure 3 Absorption coefficient β for a varying content of corn starch in water. The measurement was performed at the 9P12 (1053 cm^{-1}) transition of the CO_2 laser

The results of measurements on corn starch samples are shown in Fig. 3; at the 9P12 (1053 cm^{-1}) line of the CO_2 laser, the LOD in water is 0.6 % (w/w) and the regression coefficient is 0.999. The procedure in deriving these value was the same as described above for lactose. The intercept in Fig. 3 gives $5.83 \times 10^4 \text{ m}^{-1}$ which corresponds well with the β of water at 1053 cm^{-1} .¹⁴ The larger relative error (0.5-1%) for measurements of corn starch gels is ascribed to the power instability of the laser. To check the reliability of the OW technique, the same samples were also examined at the 10P10 line of the CO_2 laser (953 cm^{-1}) where their absorption is expected to be negligible. The OW signal was found independent of the

concentration, and the relative error was 0.6%. The difference between the OW signal strengths observed at 9P12 and 10P10 laser transitions is due to optical characteristics of the sample (gel) rather than to thermal ones.

Conclusions

The OW method with the CO₂ laser here was used for quantitative and direct determination of lactose and corn starch contents in water. Presently attainable LOD's are 0.19% (w/w) for lactose and 0.6% (w/w) for corn starch gels. For the OW sensor described here, the physical condition (liquid or gel) of the sample is irrelevant, since a good thermal contact between sample and sensor is the only condition to be met.

Apparently the FTIR method is slightly more sensitive for determination of lactose than OW, although the relative error (0.02%) is comparable to that of the OW method. For precise determination of lactose in milk, the OW is at present inadequate due to the availability of only a limited number of wavelengths which precludes the application of multiple linear regression. For corn starch gels only qualitative studies could be made with FTIR-ATR. The effect of gel fractionation was less pronounced in the OW approach because the area that must be covered is much smaller.

Contrary to ATR and the enzymatic methods (used to determine incorporated starch), which both are very expensive,¹⁵ the low-cost OW device is easy to clean and moreover offers the possibility for on-line studies of optically opaque and thermally thick samples that are otherwise not accessible by other techniques.

At present, due to a limited tunability of the CO₂ laser, it is not possible to obtain the whole spectrum of the samples with the OW method. In the near future continuously tunable infrared diode lasers (gradually emerging on the market) are expected to provide power levels (strength of the OW signal is proportional to the power density) sufficient to generate an acceptable signal to noise ratio. Therefore, such a device when combined with the FTIR technique might be regarded as a new, candidate method for rapid analysis of realistic food samples throughout the entire infrared region. Additional potential practical applications of the OW method include the on-line control of processes (hydroponic growth) and the quality control in the food industry, for example, trans fatty acids content in margarine¹³ and phosphate sensor for soft drinks.¹⁶

The performance of other thin IR transparent materials characterized by large values of thermal conductivity and thermal expansion coefficients might eventually surpass that of the ZnSe disk used in this experiment. Additional enhancement of the sensitivity is expected from a differential OW concept.

References

- 1 Alexander R.J. and Zobel H.F., *Developments in Carbohydrate Chemistry*, American Association of Cereal Chemists, St. Paul, MN (1992)
- 2 Belitz H.D. and Grosch, W., *Food Chemistry*, Springer-Verlag, New York, Berlin, Heidelberg (1987)
- 3 Chang S.K.C., Holm E., Schwartz J. and Rayas-Duarte P., *Food, Anal. Chem.* **67**, 127R-153R (1995)
- 4 Osborne B.G., Fearn T. and Hindle P.H., *Practical NIR Spectroscopy with Applications in Food and Beverage Analysis*, 2nd ed, Longman Scientific & Technical, Singapore (1993)
- 5 Belton P.S. and Tanner S.F. Determination of the Moisture Content of Starch Using Near Infrared Photoacoustic Spectroscopy, *Analyst* **108**, 591-596 (1983)
- 6 Belton P.S., Saffa A.M. and Wilson R.H., Use of Fourier Transform Infrared Spectroscopy for Quantitative Analysis: A Comparative Study of Different Detection Methods, *Analyst*, **112**, 1117-1120 (1987)
- 7 Kochhar S.P. and Rossell J.B., Applications of Infrared Absorption Spectroscopy in Food Industry, *Spectroscopy* **4**, 34-40 (1989)
- 8 Wilson R.H. and Belton P.S., A Fourier-Transform Infrared Study of Wheat Starch Gels, *Carbohydr. Res.* **180**, 339-344 (1988)
- 9 Biggs D.A., Performance Specifications for Infrared Milk Analysis, *J. Assoc. Off. Anal. Chem.* **62**, 1211-1214 (1979)
- 10 Luinge H.J., Hop E., Lutz E.T.G., Hemert J.A. and Jong E.A.M. de, Determination of the Fat, Protein and Lactose Content of Milk using Fourier Transform Infrared Spectroscopy, *Anal. Chem. Acta* **284**, 419-433 (1993)
- 11 Helander P., A Method for the Analysis of Optothermal and Photoacoustic Signals, *Meas. Sci. Technol.* **4**, 178-85 (1993)
- 12 Bicanic D., Chirtoc M., Chirtoc I., Favier J.P. and Helander P., Photothermal Determination of Absorption Coefficients in Optically Dense Fluids: Application to Oleic Acid and Water at CO Laser Wavelength, *Appl. Spectrosc.* **49**, 1485-1489 (1995)
- 13 Favier J.P., Bicanic D., Bovenkamp P. van de, Chirtoc M. and Helander P., Detection of Total Trans Fatty Acids Content in Margarine: an Intercomparison Study of GLC, GLC + TLC, FT-IR and Optothermal Window (Open Photoacoustic Cell) *Anal. Chem.* **68**, 729-733 (1996)
- 14 Hale G.M. and Query M.R., Optical Constants of Water in the 200-nm to 200-nm Wavelength Region, *Appl. Optics* **12**, 555-563 (1973)
- 15 *Biochemical Analysis Food Analysis*, Boehringer Mannheim GmbH Biochemica, Germany (1986)
- 16 Vonach R., Kellner R. and Lippitsch M., A Phosphate Sensor for Soft-Drinks Based on IR Spectroscopy, *Proceedings Eurofood VIII*, Vienna, Austria (1995).

3.4

Compact, Open and General Purpose Cell of Variable Effective Pathlength: Direct Absorption Measurement of SO_4^{2-} in Water

based on

Jan Paul Favier, Dane Bicanic, Mihai Chirtoc and Per Helander

Fresenius J. Analytical Chemistry **355**, 357-358 (1996)

Abstract

The use of an optothermal window (OW) was proposed for the direct (no need for sample preparation) spectroscopic, non-destructive measurement of SO_4^{2-} in water at 1078 cm^{-1} . The presently determined limit of detection (LOD) of 1 mmol/L is comparable to that provided by CO_2 laser photoacoustic spectroscopy, but about one order of magnitude superior to that obtainable by the ATR method.

Introduction

Many samples of environmental, nutritional and biochemical interest require the examination in aqueous solution. Yet, the use of traditional as well as new spectroscopic methods (specific for analytes to be measured) at infrared (IR) wavelengths, is not straightforward due to the intrinsically strong absorption of water in this region. The problems related to very short cell pathlengths when working with such samples are partly alleviated by attenuated total reflection spectroscopy (ATR). Although in the principle ATR provides a simple means for obtaining spectra of liquids, their quality is influenced by factors such as sample surface texture and refractive index. Furthermore, distinct differences are observed between ATR and transmission spectra, mainly caused by the effect of wavelength dependent penetration depth (being smaller at shorter wavelengths) of the radiation into the sample.¹ These problems are avoided by the OW method, the feasibility of which has been demonstrated previously^{2,3} when measuring absolute absorption coefficients of strongly absorbing and pure liquids at shorter wavelengths.

This paper reports on a first use of the OW method for the *direct* measurement (at 1078 cm^{-1}) of SO_4^{2-} concentrations in aqueous solutions. The main objective of the undertaken study was to estimate the analytical potential of this candidate spectroscopic method, and to compare it to that of ATR. Sulfate was chosen as a test analyte because of its generally recognized role in environmental and agricultural sciences.⁴

Basic concepts

The new approach implies a modulated laser radiation passing through a transparent disk with a liquid sample atop. The heat generated in the sample due to the absorption of the radiation, diffuses into the window (ZnSe disk 1.5 mm thick, 20 mm diameter) causing its periodic expansion that is sensed by a piezoelectric detector bonded to the rear side of the disk. For a "thermally thick" sample making a good thermal contact with the sensor being itself "thermally thick", there exists a simple relationship² between the magnitude of the OW signal and the product of the absorption coefficient β of the sample and the thermal diffusion length μ . The effective pathlength of the sample is determined by μ and can be controlled by varying the modulation frequency.

Experimental

Mechanically chopped CO_2 laser radiation (200 mW and 223 Hz) passed through a 1.5 mm diameter diaphragm before reaching the OW cell. A series of aqueous SO_4^{2-} solutions was prepared ($(\text{NH}_4)_2\text{SO}_4$ and CuSO_4 Merck). The OW signal was measured by a lock-in amplifier and then normalized to the incident laser power. The OW cell was calibrated at 953

cm^{-1} using distilled water ($\beta=792 \text{ cm}^{-1}$)⁵ as a reference sample; under the given experimental conditions $\beta\mu$ is 1.1.

Results and Conclusions

The calibration curve for SO_4^{2-} in distilled water is shown in Fig. 1. The linearity of the normalized OW signal is observed overall concentration range spanning more than two orders of magnitude. The measured background signal due to the absorption of the distilled water is high (corresponding to β of 520 cm^{-1}) and limits at present the sensitivity for SO_4^{2-} to 1 mmol/L. This value, close to that reported by another IR photoacoustic experiment,⁶ exceeds the LOD of ATR by nearly one order of magnitude.⁷ The non-spectroscopic methods such as nephelometry, ion chromatography and titration,^{8,9} capable of better SO_4^{2-} LOD's all have an indirect character.

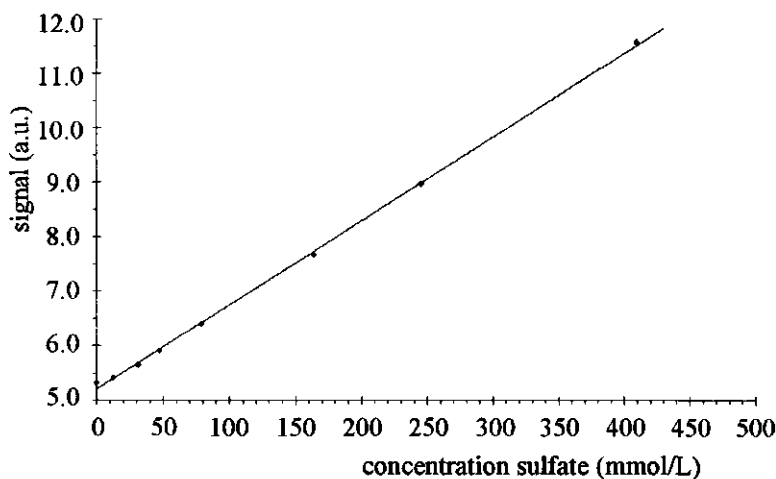


Figure 1 The normalized OW signal at 1078 cm^{-1} plotted versus concentration of SO_4^{2-} in distilled water. The solid curve represents the best fit ($r=0.9996$)

The compact and open OW cell, does not only require small quantities of sample for analysis, but it is also easy to load and clean. Possible interferences¹⁰ due to the presence of other anions (in particular PO_4^{3-}) in solution were not investigated here; yet their overall effect on the OW signal is expected to be comparable to that observed with ATR and IR spectroscopy.

Although the present LOD obtained with the OW is not sufficient for purposes of trace analysis, the moderate sensitivity of the OW method and its applicability for direct, on-line work, makes it suitable for monitoring higher SO_4^{2-} contents. Examples are found in studies of SO_4^{2-} to H_2S reduction due to the reaction of anaerobic micro-organisms, combating the

corrosion in concrete, process control in pharmaceutical, dye and textile industries, monitoring of SO_4^{2-} as a plant nutrient in the soil-less growth of many crops, etc.

The use of both the differential concept and the coated optics in designing a new OW cell is expected to further improve the LOD. Finally, the OW approach is not restricted to the IR region since one and the same OW can be universally used provided however the window transparency is guaranteed and the excitation of the analyte can be achieved.

References

- 1 Osland R.C.J., Principles and Practices of Infrared Spectroscopy, Pye Unicam Limited, Cambridge (1985)
- 2 Helander P., A Method for the Analysis of Optothermal and Photoacoustic Signals, *Meas. Sci. Technol.* **4**, 178-185 (1993)
- 3 Bicanic D., Chirtoc M., Chirtoc I., Favier J.P. and Helander P., *Appl. Spec.* **49**, 1485-1489 (1995)
- 4 Sonneveld C. and Straver N., Nutrient Solutions for Vegetables and Flowers Grown in Water or Substrates, Serie: Voedingsoplossingen glastuinbouw no 8 ISN 116174 (1988)
- 5 Hale G.M. and Query M.R., Optical Constants of Water in the 200-nm to 200-nm Wavelength Region, *Appl. Opt.* **12**, 555-563 (1973)
- 6 Kanstad S.O. and Nordal P.E., Infrared Photoacoustic Spectroscopy of Solids and Liquids, *Opt. Comms.* **29**, 413-422 (1981)
- 7 Application Manual Miran 1A, Foxboro, Bristol Park MA USA (1985)
- 8 Fresenius W., Quentin K.E. and Schneider W., Water Analysis, Springer-Verlag Berlin Heidelberg New York (1988)
- 9 Die chemische Untersuchung von Wasser, Merck, Darmstadt (1992)
- 10 Cross A.D. and Jones R.A., An Introduction to Practical Infrared Spectroscopy 3rd ed. London Butterworth (1969).

4 Thermal Characterization of Different Samples

4.1 Thermal Diffusivity of Hard Boiled Candy Obtained by Photothermal Beam Deflection and Standard Photopyroelectric Method

4.2 Photopyroelectric (PPE) Measurement of Thermal Diffusivity in Low Density Polyethylene (LDPE) and Polyvinyl Chloride (PVC) Foils

4.1

Thermal Diffusivity of Hard Boiled Candy Obtained by Photothermal Beam Deflection and Standard Photopyroelectric Method

Jan Paul Favier, Dorin Dadarlat, Jürgen Gibkes, Cornelius van den Berg, and Dane Bicanic
accepted by Instrumentation Science & Technology

Abstract

Two different photothermal techniques, photopyroelectric (PPE) and photothermal beam deflection (PTBD) method were used for the thermal characterization of a glassy sugar system, commercially available hard boiled candy. Thermal diffusivities at room temperature obtained by both techniques were comparable (i.e. 14.7×10^{-8} and $12.0 \times 10^{-8} \text{ m}^2\text{s}^{-1}$ for PPE and PTBD respectively). In addition, the PPE technique was also used to measure temperature dependence of the thermal diffusivity in the -30°C to 70°C temperature range. The glass-rubber transition, underwent by the sample in this temperature range was observed and compared to results obtained by differential scanning calorimetry (DSC) experiment.

Introduction

Thermal and optical characterization of foodstuffs are important for their industrial manufacture, development and improvement, prediction of stability, quality assessment, and other aspects. With regard to manufacturing and assessing the stability of sugar candies, data associated with phase transitions (melting and glass-rubber transitions) are of particular importance.^{1,2}

Thermal properties of these products allow one to predict heat transfer rates during the manufacturing process. Assuming constant values of thermal properties during heating and cooling cycles is an oversimplifying approach. At present, one computes thermal diffusivity from values for thermal conductivity, specific heat, and mass density.^{1,2} While the specific heat can be estimated with reasonable accuracy from the product composition, the thermal conductivity and mass density generally must be determined by experiment. Thermal properties are known to alter significantly during glass and other phase transitions, and as such are used to determine transition temperatures.³

Hard boiled candies are mainly amorphous materials in the glassy state; they are solidified liquids (with an extremely high viscosity) supporting their own weight. Typical properties of such sugar glasses are their brittleness and transparency. These qualities are decisive textural and optical characteristics for sweets. The extremely slow changes occurring in the glassy state are often referred to as physical ageing.¹

Water is a perfect plasticizer for glassy sugar systems, and its content strongly affects the glass transition temperature (T_g) of the product. Generally, T_g of amorphous food components has been recognized as one of the major factors in controlling the shelf life of low-moisture and frozen foods.¹ For hard boiled candies, T_g is above room temperature.

Recently, two new photothermal (PT) methods, i.e. photopyroelectric (PPE)⁴⁻⁷ and photothermal beam deflection (PTBD)^{8,9} were proposed for calorimetric investigation of foodstuffs. In the PPE method, the amount of heat developed in a sample, induced by the absorption of a modulated radiation, is measured with a pyroelectric sensor.^{10,11} Various PPE configurations were proposed in order to study thermal properties and/or phase transitions in foods.⁴⁻⁶ Among these, the so called "standard geometry", with sensor and sample both thermally thick and an optically opaque sample, proved the most suitable, because the temperature behavior of all sample thermal parameters can be obtained from a single measurement. On the other hand the PTBD zero crossing method is a well established laser based technique for thermal diffusivity measurements of biological and solid materials (with a typical accuracy of 5%).¹²⁻¹⁴

Due to unavailability of literature data of thermal parameters for sugar systems such as candies, the zero crossing PTBD and PPE method were applied in this study to determine the thermal diffusivity of hard boiled candy. The influence of temperature on thermal diffusivity, and the glass transitions were investigated in the -30°C to 70°C temperature range.

Principles of photothermal beam deflection method

The illumination of an absorbing sample by a periodically modulated focused laser beam (the pump beam) causes the periodic generation of heat. Propagation of thermal waves from the sample into the surrounding fluid can be described by appropriate heat diffusion equation. Since the refractive index of a fluid is temperature dependent, the generated spatial temperature gradient can be sensed by a second laser beam (the probe beam). As a result, the probe beam will be deflected as it traverses the heated region parallel to the surface of the sample.

The deflection is a vector having normal and transverse components that refer to deflections in a plane perpendicular and parallel to the surface of the sample. For strongly damped thermal waves, deflection signals are due to the contribution of heat originating within one thermal diffusion length μ_s (m) in the sample; the latter is given by

$$\mu_s = \sqrt{\frac{\alpha_s}{\pi f}} \quad (1)$$

where f (s^{-1}) is the modulation frequency and α_s is thermal diffusivity (m^2s^{-1}) of the sample, related to other thermal parameters by

$$\alpha_s = \frac{\kappa_s}{\rho_s c_s} \quad (2)$$

where κ_s , ρ_s and c_s are thermal conductivity ($\text{Wm}^{-1}\text{K}^{-1}$), density (kgm^{-3}) and mass specific heat ($\text{Jkg}^{-1}\text{K}^{-1}$) of the sample, respectively.

In order to accurately measure the thermal properties of the material sample, the probe beam should pass as close as possible (distances smaller than one thermal diffusion length in the fluid are acceptable) and parallel to its surface. If the distance between the probe beam and the surface of the sample becomes larger, the signal will be dominated by thermal properties of the surrounding fluid (mostly air).

A straight line is obtained when the zero crossing distance is plotted versus \sqrt{f} .¹²⁻¹⁴ The obtained slope m is related to the thermal diffusivity as

$$m = \sqrt{\gamma\pi\alpha_s} \quad (3)$$

and allows for its direct calculation. In Eq. (3) γ is 1.44 for opaque, thermally thick samples and 1 for transparent samples as well as for opaque, thermally thin samples. The PTBD technique is not described in more detail here, because of its limited practicability compared to the PPE method.

Principles of the photopyroelectric method

In the standard PPE configuration, the radiation impinges on the front surface of the sample, while the pyroelectric sensor, itself in a good thermal contact with the rear side of the sample, measures its temperature variation. A sensor or a sample are said to be thermally thick when their geometrical thickness' are larger than the thermal diffusion lengths in the materials.

If in the standard configuration the sample and sensor are both thermally thick and the sample is optically opaque, the amplitude S and the phase ϕ of the PPE signal are given by the following equations¹⁵

$$S = S_0 \times \frac{e^{-l_s \sqrt{\frac{\pi f}{\alpha_s}}}}{\epsilon_s \left(\frac{\epsilon_m}{\epsilon_s} + 1 \right) \left(\frac{\epsilon_p}{\epsilon_s} + 1 \right)} \quad (4)$$

and

$$\phi = -l_s \sqrt{\frac{\pi f}{\alpha_s}} \quad (5)$$

In Eq. (4), S_0 is an instrumental constant depending on the intensity of the incident radiation, the chopping frequency, thermal, electrical and geometrical parameters of the sensor, and ϵ is the thermal effusivity defined as $\sqrt{\kappa\rho c}$. The subscripts p, s and m refer to the pyroelectric sensor, sample and medium in front of the sample (air in the case discussed here), respectively. The Eq. (5) suggests that the phase ϕ of the PPE signal depends solely on the thermal diffusivity of the sample, allowing for its direct and absolute measurement, providing l_s and f are known.

Experimental section

The experimental set-up used for PTBD measurements of thermal diffusivity of candies is a modified version of the apparatus described previously.^{9,16} The major difference is that the probe beam (Spectra Physics 126, HeNe laser) bounces on the surface of the sample. It first passes through the neutral density glass filter (1% transmission; the filter is required to avoid saturation of the position sensitive quadrant detector) before reaching a 50 mm plano-convex converging lens (focusing is necessary to reduce the probe beam diameter). The probe beam is then defocused

behind the sample using another 50 mm plano-convex lens; the detection takes place with a sensitive quadrant diode. The output signal from the diode was fed into an ITHACO 3961B lock-in amplifier coupled to a personal computer. The same computer also provided the stepwise increasing voltage output used to drive the mirrors (lock-in signals were measured at each mirror setting).

The experimental set-up used for PPE investigations was discussed in extenso elsewhere;⁴ only some details are presented here. The PPE cell is a cold-finger based system, allowing the operation at temperatures below and above that of the ambient.⁵ The typical temperature variation rate was 1°C per minute with an acquisition at each 0.1°C. The pyroelectric sensor was a 300 µm thick single crystal of LiTaO₃. The opacity of the sample was achieved by placing a thin (10 µm) blackened Al foil atop of it. Thin layers of silicon grease between Al foil, sample and sensor provided a good thermal contact. A 5 mm diameter diaphragm in front of the sample prevented direct illumination of the sensor. The signal from the detector was processed with a Stanford Research SR 850 lock-in amplifier. The radiation source was a 30 mW Melles Griot diode laser chopped electronically by the internal oscillator of the lock-in amplifier, and a personal computer was used for data acquisition.

Initially, a frequency scan was performed at room temperature in order to find the range of appropriate modulation frequencies that satisfy the requirements imposed for this SPPE configuration (thermally thick regime for the sample and sensor) and to obtain an absolute calibrating value for the thermal diffusivity at room temperature.

Commercially available hard boiled candies (20×20×15 mm³, type LONKA) were used as test samples. Typically, they contain about 65% sucrose, 30% glucose syrup solids and less than 4% water. For the PPE experiments samples (0.5-1.0 mm thick, area about 10×10 mm²) were cut from the middle of the candy (flatness and uniform thickness of the samples are obligatory).

Duplicate samples (approximately 20 mg) of the same sugar candy in 20 µl aluminum cups were scanned at 5 and 10 Kmin⁻¹ in Perkin Elmer DSC-2, provided with computerized data acquisition. An empty cup was used as a reference. The results of PPE investigations of phase transitions were compared to these obtained by DSC.

Results and discussions

Using the experimental procedure described above, PTBD transverse signals were recorded at various chopping frequencies. An average of 50 successive measurements was taken as representative for each position of the pump laser beam. The candy was assumed transparent for the pump laser radiation, and the PTBD experiment was repeated three times. The average value for the thermal diffusivity calculated by linear regression from *m* values, 0.6198, 0.5765 and 0.9893 mm²s⁻¹ respectively, is 12×10⁻⁸ m²s⁻¹ (standard deviation $\sigma = 7 \times 10^{-8}$).

As to the PPE measurements, a frequency scan of the phase of the PPE signal allows one (Eq.(5)) to obtain the value for thermal diffusivity at room temperature. The results obtained for a 900 μm thick sample are presented in Fig. 1 (curve '+' and 'o'); The slopes of -4.05 and -4.27 give an average α of $14.7 \times 10^{-8} \text{ m}^2/\text{s}$ ($\sigma = 1 \times 10^{-8}$) which agrees rather well with the value obtained by PTBD.

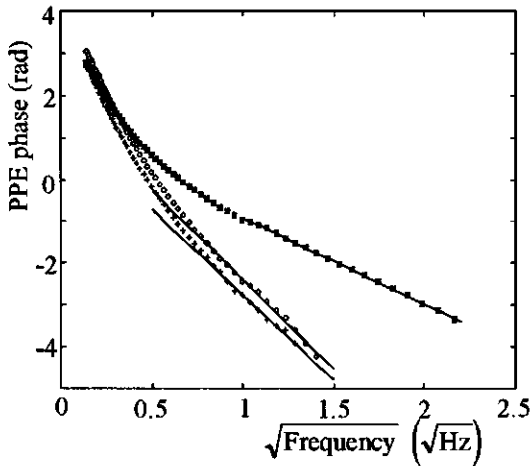


Figure 1 The phase of the PPE signal plotted versus square root of frequency, (+) sample 900 μm thick not heated; (o) sample 900 μm thick heated up to 30°C; (*) sample 400 μm thick heated up to 70°C

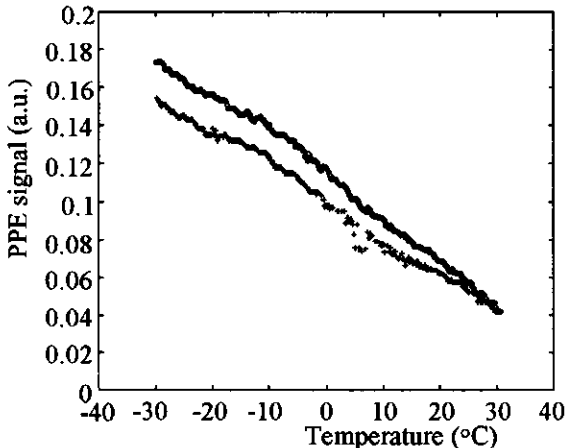


Figure 2 The magnitude of the photopyroelectric signal amplitude plotted versus temperature, (+) heating and (o) cooling

As seen in Fig. 1, the requirement for thermally thick sample imposed that the modulation frequencies must be larger than 1 Hz. Consequently, 1.5 Hz was used in the temperature scan. At this frequency the Al foil and silicon grease layers are thermally very thin and do not influence the results. When the measured data were processed the temperature dependence of the PPE signal obtained from the unloaded sensor was used for normalization;^{4,5} in such a way the temperature dependence of the pyroelectric coefficient and electrical capacitance of the sensor are eliminated.

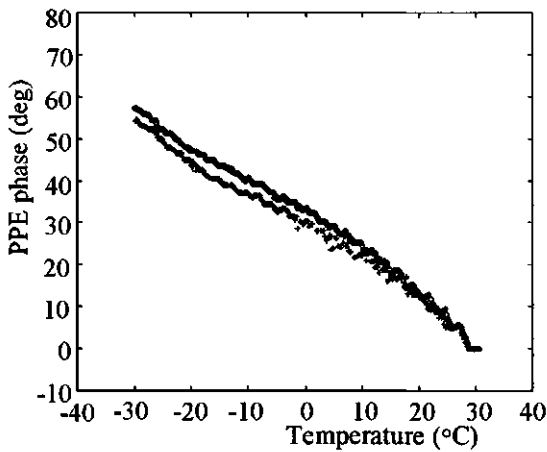


Figure 3 The phase of the photopyroelectric signal plotted versus temperature, (+) heating and (o) cooling

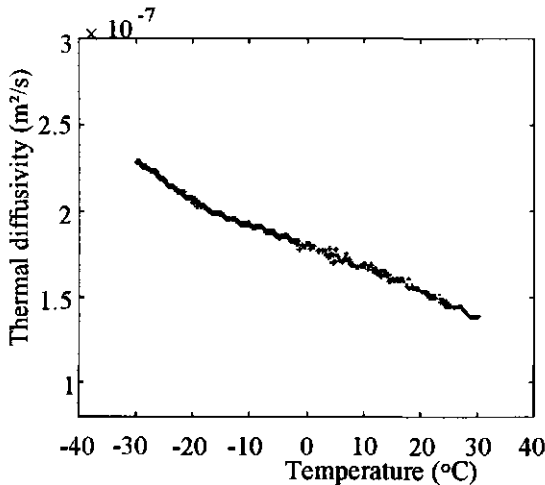


Figure 4 Thermal diffusivity versus temperature, for a sample thickness of 900 μm ; (+) heating and (o) cooling

As the temperature of the candy was varied from -30°C to 30°C , the thermal diffusivity decreased monotonically with increasing temperature. The heating-cooling process was reversible (see Figs. 2 and 3 for the amplitude and phase of the PPE signal and Fig. 4 for the thermal diffusivity). After several repeated cooling-heating cycles, the same room temperature value for α (in the error limit) was obtained, using the frequency scan method too (see Fig. 1, curve '*' with a slope of -2.05 and thickness of $400\ \mu\text{m}$; α of $12.0 \times 10^{-8}\ \text{m}^2\text{s}^{-1}$).

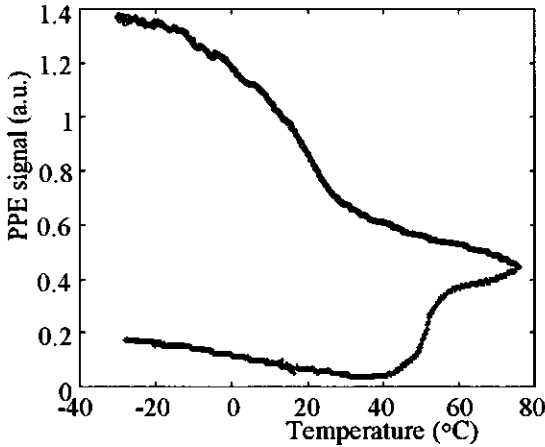


Figure 5 The temperature dependent amplitude of the photopyroelectric signal plotted versus temperature; (+) heating and (o) cooling

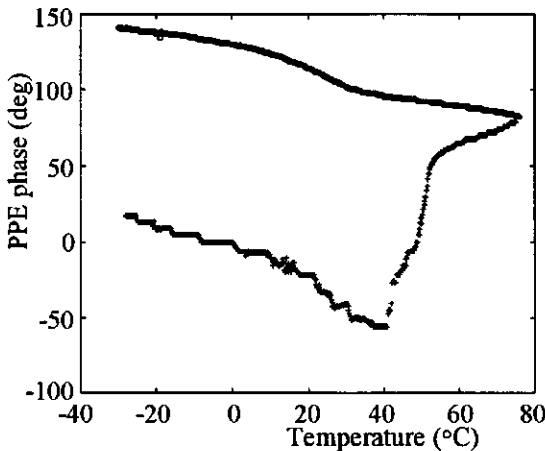


Figure 6 The phase of the photopyroelectric signal plotted versus temperature; (+) heating and (o) cooling

As the temperature exceeded 40°C, the candy undergoes a glass-rubber transition, i.e. a supercooled melting. The results for the amplitude and the phase of the PPE signal are presented in Figs. 5 and 6. The increase in amplitude and phase observed on cooling, was due to the reduced sample thickness (400 μm) during melting (see also strong increase heating trace). The DSC measurements also confirmed the existence of a glass transition (Fig. 7) at 30°C (midpoint, corrected for scan speed). This transition was reproducible, only the first heating showed a small overshoot peak in the DSC trace at the end of glass transition (Fig. 7), which is indicative for aging relaxation of the glass. The negative slope of the DSC trace is commonly observed for comparable sugar systems. Above 32°C the sample became a supercooled melt with fluid properties (crossing point of slopes in Fig. 8). However, at the time scale of measurement the sample became liquid near 40°C, where its thickness changed spontaneously.

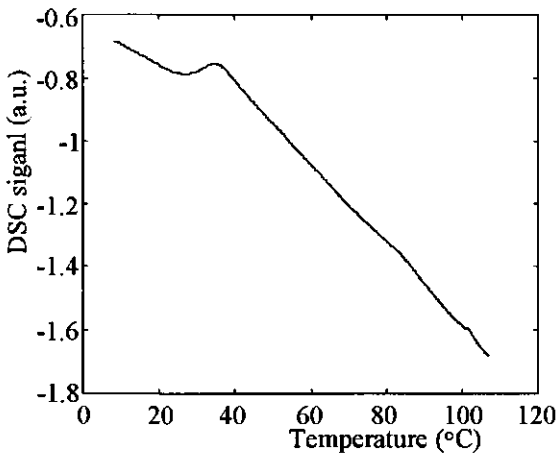


Figure 7 The DSC signal versus temperature

The width of the glass transition region is rather wide (approximately 8 centigrades from onset to endset, scan speed 5 Kmin^{-1}). At 10°C the trace started to deviate from the baseline, which is close to the first change in the slope found by PPE measurements (Figs. 5-8).

Despite an excessive thermal treatment, the value of thermal diffusivity at the room temperature remained practically the same (Fig. 1, curve '*'). Additional heating-cooling cycles (-30°C to 60°C) showed a well reproducible monotonous decrease of α for increasing temperature (Fig. 8), with comparable room temperature value (Fig. 1, curve '* is reproducible). These facts lead to the following conclusions: (i) temperature changes up to 30°C did not influence the thermal properties of the candy; the thermal diffusivity displays a gradual, reproducible decrease (from 2.4×10^{-7} to $1.4 \times 10^{-7} \text{ m}^2\text{s}^{-1}$) with increasing temperature.

(ii) Physical ageing, as a quality parameter, could not be determined from a room temperature frequency scan (the room temperature value of the thermal diffusivity remained the same), however physical ageing could be detected by a PPE temperature scan. This was due to the fact (also confirmed by DSC) that the initial heating (up to 70°C), always produces a relaxation of the glass.

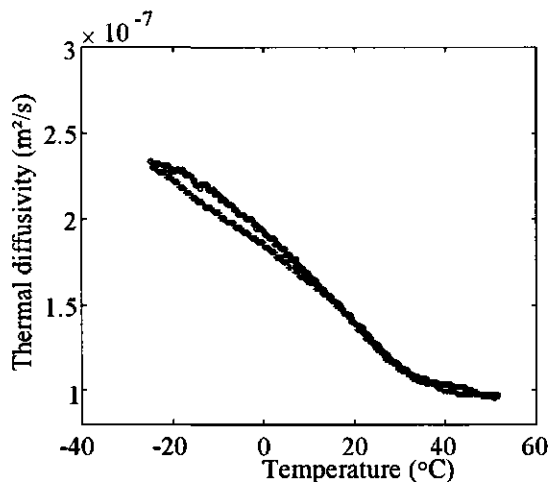


Figure 8 Thermal diffusivity versus temperature for a 400 µm thick sample; (+) heating and (o) cooling

An important remark concerns the use of Eq.(4). The amplitude of the PPE signal depends on two sample related thermal parameters (i.e. thermal diffusivity and effusivity). If a literature value of a second thermal parameter (at room temperature) would be available, the measurements of amplitude of the PPE signal could be calibrated. Consequently, the temperature dependence of all thermal parameters could be computed. Unfortunately, no quantitative information about the thermal parameters during the melting process could be obtained because the thickness of the sample changed in an uncontrollable manner.

In conclusion, two new photothermal techniques (PTBD and PPE) were used to obtain previously unreported value for thermal diffusivity of a hard boiled candy at room temperature. It was demonstrated that the PPE method was capable of measuring temperature dependence of the thermal diffusivity and to detect phase transitions in such sugar systems and the results were confirmed by DSC measurements. The occurrence of a glass phase transition, can be correlated with the thermal history of the sample.

Acknowledgments

One of the authors (D. Dadarlat) acknowledges the receipt of a visiting scientific fellowship from the Dutch Organization for Scientific Research (NWO, The Hague) that made this work

possible. The research described here is also supported by EC program Inco Copernicus (proposal ERBIC 15CT961003)

References

- 1 Roos Y.H., *Phase Transitions in Foods*, Academic Press, San Diego (1995)
- 2 Mohsenin N.M., *Thermal Properties of Foods and Agricultural Materials*, Gordon and Breach Scientific Publishers, New-York, London, Paris (1980)
- 3 Slade L. and Levine H., *CRC Crit. Rev. Food Sci. Nutr.* **30**, 115-360 (1991)
- 4 Dadarlat D., Bicanic D., Visser H., Mercuri F. and Frandas A. Photopyroelectric Method for Determination of Thermophysical Parameters and Detection of Phase Transitions in Fatty Acids and Triglycerides. Part I: Principles, Theory and Instrumentational Concepts, *J. Amer. Oil Chem. Soc.* **72**, 273-279 (1995)
- 5 Dadarlat D., Bicanic D., Visser H., Mercuri F. and Frandas A. Photopyroelectric Method for Determination of Thermophysical Parameters and Detection of Phase Transitions in Fatty Acids and Triglycerides. Part II: Temperature Dependence of Thermophysical Parameters. *J. Amer. Oil Chem. Soc.* **72**, 281-287 (1995)
- 6 Dadarlat D., Bicanic D., Gibkes J., Kloek W., Dries I. van den and Gerkema E., Study of Melting Processes in Fatty Acids and Oils Mixtures. A Comparison of Photopyroelectric (PPE) and Photopyroelectric Observations of Melting Differential Scanning Calorimetry (DSC), *Chem. Phys. Lipids* **82**, 115-123 (1996)
- 7 Bicanic D., Dadarlat D., Gibkes J., Chirtoc M., Favier J P and Gerkema E., The Photopyroelectric Approach to Thermal Characterization of Liquid and Pasty Foodstuffs and an Optothermal Accessory for Obtaining Infrared Spectra of Optically Dense Fluids, *Acta Chim. Slov.* **42**, 153-173 (1995)
- 8 Brown S.M., Baesso M.L., Shen J. and Snook R.D., Thermal Diffusivity of Skin Measured by Two Photothermal Techniques, *Anal. Chim. Acta* **282**, 711-719 (1993)
- 9 Brown S.M., Bicanic D. and van Asselt K., Photothermal Beam Deflection Measurement on Agricultural Produce, *J. Food Eng.* **28**, 211-223 (1996)
- 10 Mandelis A. and Zver M.M., Theory of Photopyroelectric Spectroscopy of Solids, *J. Appl. Phys.* **57**, 4421-4430 (1985)
- 11 Chirtoc M. and Mihailescu G., Theory of the Photopyroelectric Method for Investigation of Optical and Thermal Materials Properties, *Phys. Rev. B* **40**, 9606-9617 (1989)
- 12 Sell J.A., *Photothermal Investigation of Solids and Fluids*, Academic Press Inc., Boston (1988)
- 13 Bertolotti M., Li Voti R.L., Liakhou G. and Sibilica C., On the Photodeflection Method Applied to Low Thermal Diffusivity Measurements, *Rev. Sci. Instr.* **64**, 1576-1583 (1993)

- 14 Bertolotti M., Li Voti R.L., Liakhou G., Sibilia C., Reply to Comments on the Photothermal Method Applied to Low Thermal Diffusivity Measurements, *Rev. Sci. Instr.* **66**, 277 (1995)
- 15 Marinelli M., Mercuri F. and Zammit U., Pizzoferrato R., Scudieri F., Dadarlat D. Photopyroelectric Study of Specific Heat, Thermal Conductivity and Thermal Diffusivity of Cr_2O_3 at the Neel Transition, *Phys. Rev. B* **49**, 9523-9537 (1994)
- 16 Gibkes J., Dadarlat D., Favier J.P., Bicanic D., Bein B. and Gerkema E., Thermal Diffusivity Measurement of Selected Metals, Technical Graphites and Magnetic Materials: Zero Crossing Points and Phase Methods Versus Photopyroelectric Technique- an Intercomparison Study, *Prog. Nat. Sci.* **6**, S273-277 (1996).

4.2

Photopyroelectric Measurement of Thermal Diffusivity (-30 to 70°C) in Low Density Polyethylene (LDPE) and Polyvinyl Chloride (PVC) Foils

Jan Paul Favier, Dorin Dadarlat, Klaas Jan Riezebos, Cornelius Van den Berg, Dane Bicanic and Edo Gerkema

Abstract

The PPE technique in the standard configuration was used to measure the temperature dependence of thermal diffusivity of some low density polyethylene and polyvinyl chloride foils used for food packaging purposes. The glassy phase transitions observed in these plastics within -30 to 70°C range, caused a 7-20% increase of thermal diffusivity. Additional measurements by differential scanning calorimetry confirmed the validity of PPE results.

Introduction

Due to a wide applicability of plastics, research on these materials constitutes an important topic for a number of years.¹ Among these, low density polyethylene (LDPE) and polyvinylchloride (PVC) are especially important because of their use for packaging applications (food and other products) and other purposes (hardware items, toys, etc.). The most widely studied are mechanical (tensile and yield strength, elongation, Young's modulus, burst, impact and tear strengths, stiffness, flex resistance, coefficient of friction, blocking) and other physical and chemical properties (optical features, permeability to gases and water, density, heat sealability, resistance to light, heat and cold) and aging behavior.^{2,3}

Investigations concerning thermal parameters of plastics, and in particular of thermal diffusivity, conductivity and effusivity were rarely reported.³ The magnitude and the temperature behavior of these quantities have a great importance especially when plastics are produced and in applications where high and low temperatures are involved (i.e. packaging and storage of fresh products). Moreover, the information provided by classical calorimetric techniques is usually "discontinuous", that is to say data are collected in increments of 10-20°C. Consequently, this implies a possibility for failing to detect an anomalous behavior.³

In this paper we propose a new calorimetric method, the photopyroelectric (PPE) technique, to measure the temperature dependence of thermal diffusivity, α , for one LDPE and two PVC foils all used as food packaging materials. The PPE method is capable of providing a continuous information on α within the temperature range of interest.

Basically, the PPE method is concerned with the detection of temperature changes developed in an light absorbing sample when exposed to modulated radiation. The pyroelectric sensor is placed in a good thermal contact with the sample.^{4,5} The quantity measured in a PPE experiment is the photopyroelectric voltage (generated by the pyroelectric sensor), that has both amplitude and phase both depending on the thermal parameters of the sample. Various experimental configurations and PPE cell geometries were proposed for calorimetric studies, and many types of materials (magnetics, ferroelectrics, superconductors, foodstuffs, raw agricultural and biological products) were investigated.⁶⁻⁹ Due to its ability to provide the temperature dependence of thermal parameters, the PPE method can also be used to detect phase and glass transitions as well as other anomalous behavior of materials.⁷⁻⁹ This paper reports the results obtained in a PPE study from LDPE and PVC films and compares them to those obtained by differential scanning calorimetry (DSC).

Theory

Plastics films are optically opaque, constant thickness and flat what make suitable for PPE investigations. The most suitable PPE geometry is the standard (back) configuration with

thermally thick sample and sensor.⁶ In such scheme the front surface of the sample is exposed to the modulated light, while the pyroelectric sensor (glued to the rear side of the sample with a coupling fluid) measures the temperature variation of the sample. A given medium is called "thermally thick" if its geometrical thickness, l_s , is larger than the thermal diffusion length, μ , defined as

$$\mu = \sqrt{\frac{2\alpha_s}{\omega}} \quad (1)$$

where ω is the angular modulation frequency and α_s is the thermal diffusivity of the sample. The latter is related to other thermal parameters, thermal conductivity, κ_s , effusivity, ε_s , and volume specific heat, C_s , through the relationships

$$\kappa = C_s \alpha_s \quad \text{and} \quad \varepsilon = \sqrt{C_s \kappa_s} \quad (2)$$

Marinelli et al.⁶ demonstrated that for optically opaque sample and thermally thick sensor and sample, (with the sensor working in a voltage or current mode), the amplitude and the phase of the complex PPE signal are described by

$$S = S_0 \times \frac{e^{-l_s \sqrt{\frac{\omega}{2\alpha_s}}}}{\varepsilon_p + \varepsilon_s} \quad (3)$$

and

$$\varphi = -l_s \sqrt{\frac{\omega}{2\alpha_s}} \quad (4)$$

where S_0 is a calibration factor depending on the radiation intensity, geometrical, electrical and thermal parameters of the sensor. Subscripts p and s in above equations refer to the pyroelectric sensor and sample, respectively.

The phase of the PPE signal depends only on α_s , allowing for its direct and absolute measurement (provided the sample thickness l_s is known). The expected φ versus \sqrt{f} dependence is linear, and the slope m of this plot is related to α_s through:

$$\alpha_s = -\pi \times \left(\frac{l_s}{m}\right)^2 \quad (5)$$

Experiment

The experimental procedure, the apparatus and PPE cell design were extensively discussed elsewhere;^{7,8} only the specific details for the experimental setup used in this study are given

here. The PPE cell is a cold finger and allows measurements both below and above room temperature. The radiation source was a diode laser (Melles Griot, 830 nm) electronically modulated by the internal oscillator of the lock-in amplifier (Stanford Research SR 850) which was used to process the signal from the detector (300 μm thick single crystal of LiTaO_3). The scan rate of the temperature was about $0.5^\circ\text{Cmin}^{-1}$ with acquisitions each 0.1°C . The operating temperature ranged from -30 to 70°C . The investigated samples included a LDPE (167 μm thick; Gent, Belgium) and two PVC foils (160 and 90 μm thick; 4P, Forschung Germany) all manufactured for packaging practice. The irradiated foil area was about 20 mm^2 .

The opacity of samples was achieved by blackening the 10 μm thick Al foil glued (with silicon grease) to the front surface of the sample. The same silicon grease was also used to obtain a good thermal contact between the sample, sensor and the cold finger. For modulation frequencies used in this experiment the Al foil and the silicon grease layers are thermally very thin and their properties do not affect the measured data (for example, at 9 Hz, the thermal diffusion length in Al is about 2 mm).

A frequency scan was made at room temperature in order (i) to calibrate the phase of the PPE signal, and (ii) to find the optimal range of modulation frequencies that satisfy the condition imposed by the special PPE case (thermally thick regime for the sensor and sample). The heating and cooling procedures were always performed in the same fashion, i.e. the sample was initially cooled down to -30°C and then heated to 70°C before cooled to room temperature again.

A Perkin Elmer DSC-2 equipped with computerized data acquisition and analysis was used for differential scanning calorimetry (DSC) experiments.^{10,11} The reported curves were obtained from samples consisting of a stack of six layers in 60 μl sealed stainless steel cups. This was necessary to obtain sufficient heat effect. All DSC plots show the first and second heating runs; the scan speed was 10°Cmin^{-1} .

Results and discussion

The thickness of the foils was measured (with a micrometer) before the frequency scans and after completion of the PPE measurements and no changes due to the heating were observed. The frequency scans before heating are shown in Figs. 1-3 (curve '+'); the room temperature values of the thermal diffusivity are 6.7×10^{-8} , 3.2×10^{-8} , $5.5 \times 10^{-8}\text{ m}^2\text{s}^{-1}$ for LDPE, PVC (90 μm) and PVC (160 μm), respectively. These values agree rather well with literature data.^{3,12-15}

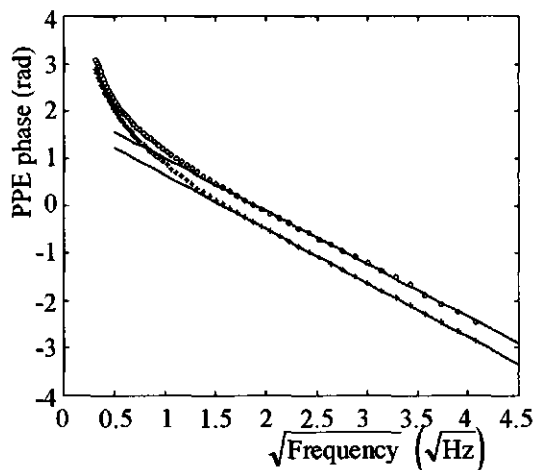


Figure 1 The phase of the PPE signal obtained from 167 μm thick LDPE foil plotted versus the square root of frequency. (+) before and (o) after heating

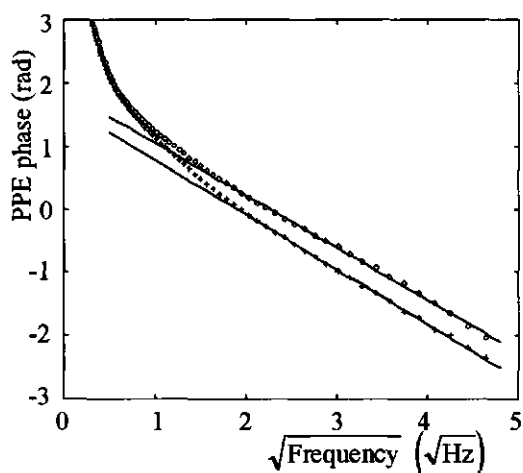


Figure 2 The phase of the PPE signal obtained from 90 μm thick PVC foil plotted versus the square root of frequency. (+) before and (o) after heating

At the same time, Figs. 1-3, indicate that frequencies exceeding 3 Hz are suitable for temperature scans. The frequency of 9 Hz was used for LDPE and PVC (160 μm) samples, while 12 Hz was used for the thinner PVC (90 μm) foil.

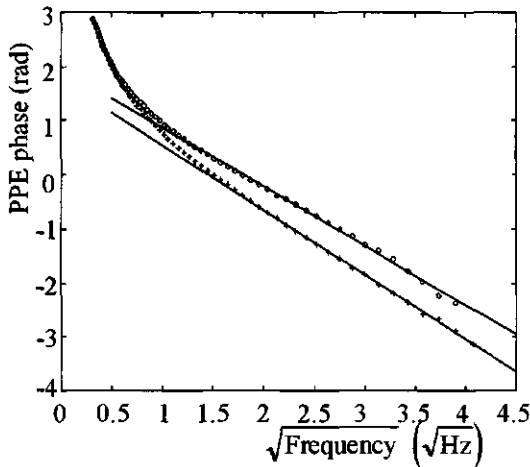


Figure 3 The phase of the PPE signal obtained from 160 μm thick PVC foil plotted versus the square root of frequency. (+) before and (o) after heating

LDPE 160 μm

The temperature dependence scan of the phase of the PPE signal, in -30 to 70°C range, is shown in Fig. 4. The initial heating produces a pronounced decrease of the phase for temperatures as high as 50 to 60°C . The material undergoes a relaxation just before the onset of the melting transition, which implies melting of crystallites and molecular rearrangement followed by an increase of the phase.

Transposing the temperature behavior of the phase into that of thermal diffusivity (Eq. (4)), one obtains results shown in Fig. 6. Apparently, heating affects the thermal diffusivity at room temperature. The value found by cooling the sample, is in agreement with the value of $7.2 \times 10^{-8} \text{ m}^2\text{s}^{-1}$ found with the frequency scan (Fig. 1, curve 'o').

This finding was also confirmed by results of DSC measurements, (Fig. 5), where a tiny exothermal event (dip at 41°C , Fig. 5) is followed by an endothermal (peak at 55°C , Fig. 5) enthalpy relaxation which precedes the melting of crystalline parts of LDPE. The PPE measurement comprised the relaxation event but not the melting. Since the measured heat effects are relatively small, the slope of the baseline appears strongly negative due to magnification (this is true for all DSC measurements).

Depending on the amount of plasticizers, polyethylene generally has a glass-rubber transition around -110°C . However, the melting of polyethylene occurred over tens of degrees centigrade ending at 112°C . This is due to the melting of nanoscale crystallites, a process having a considerably decreased melting point, in succession of their size. Reported DSC measurements include the range of initial melting.

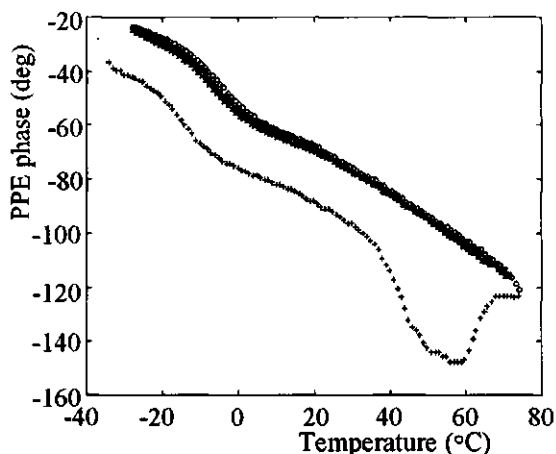


Figure 4 The phase of photopyroelectric signal plotted versus temperature, (+) heating and (o) cooling. Several runs were made to prove the absence of changes

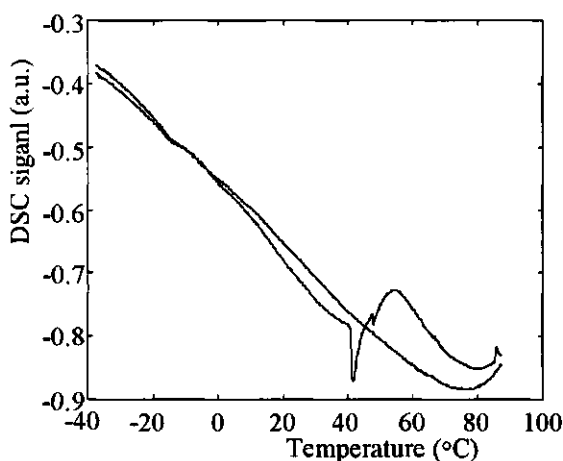


Figure 5 DSC signals of LDPE 167 μm (13.48 mg) plotted versus temperature. The first scan shows the exo- and endothermal peaks

Following the initial heating, successive cooling-heating cycles (with PPE) exhibited the same trend: i.e. no transition was observed (Fig. 4 and confirmed by DSC, Fig. 5). The second DSC trace was recorded after heating the sample up to 120°C (beyond the melting transition). No influence of the scan speed on DSC results from this sample could be found.

No change in thermal properties as a result of aging was observed either. A PPE experiment performed with the same sample after one month yielded the same results as before. The relaxation event can most probably be ascribed to the film manufacturing process and not to aging.

Intercomparison of DSC and PPE results showed (Figs. 4-6) that the PPE technique is more sensitive than the DSC method for obtaining thermal properties. Only a single layer of foil is needed here to obtain the result, as compared to six layers necessary to observe the thermal event using the DSC method.

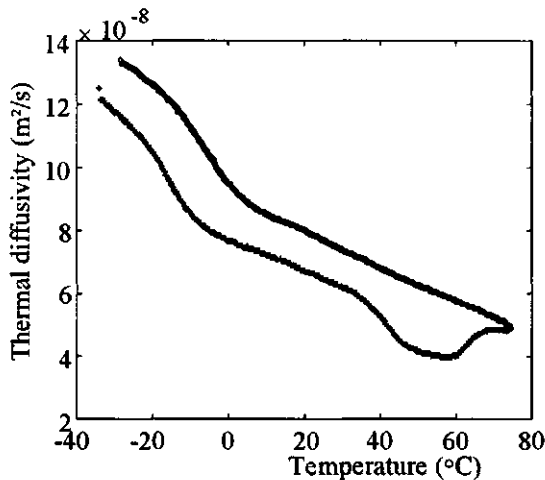


Figure 6 Thermal diffusivity versus temperature, for LDPE 167 μm ; (+) heating and (o) cooling

PVC 90 μm

The glass-rubber transition and the melting point of PVC are near 90°C and 212°C respectively. Depending on the amount of plasticizer, the position of the glass transition appears to vary over 10°C or more. The first observable weakening often occurs already above 40°C. Reported DSC measurements cover the range up to (PVC 90 μm) and well beyond (PVC 160 μm) the glass-rubber transition.

The temperature behavior of thermal diffusivity for the PVC foil (90 μm) is shown in Fig. 7, the shape resembles that of LDPE. The room temperature value of $3.8 \times 10^{-8} \text{ m}^2 \text{ s}^{-1}$ for α after heating of PVC was also confirmed by the frequency scan made at later stage (Fig. 2, curve 'o').

During the initial heating the DSC results show enthalpy relaxation events linked to the glass transition (Fig. 8). The different peaks probably originate from delayed thermal events in the stack of different layers. The second heating run showed a small glass transition at 80°C (uncorrected for scan speed). The results obtained from the thick PVC film (160 μm) were more pronounced.

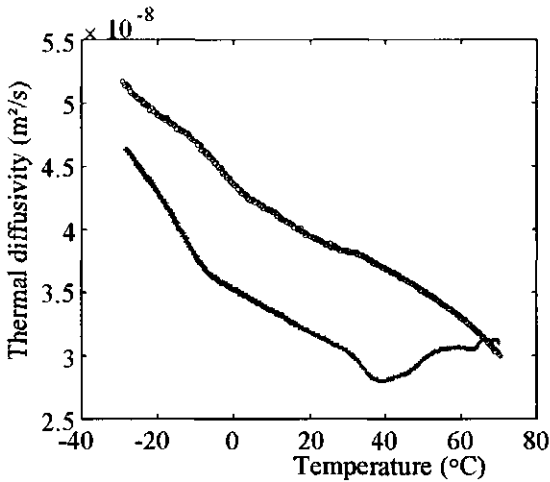


Figure 7 Thermal diffusivity versus temperature, for PVC 90 μm ; (+) heating and (\circ) cooling

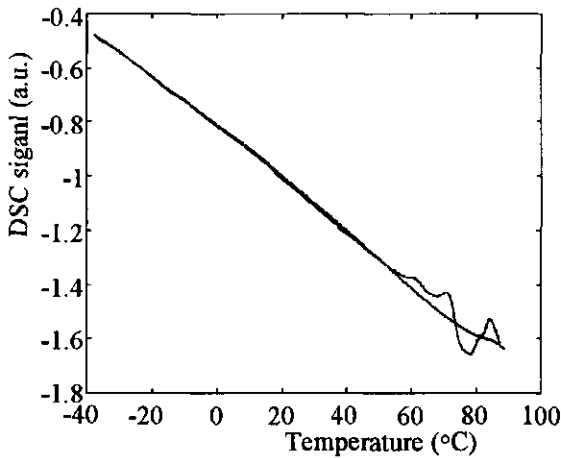


Figure 8 The DSC signal for PVC 90 μm (18.77 mg) against temperature; results of the first and second run. The trace associated with the first run showed thermal events

PVC 160 μm

For this material, the initial heating suggests (Fig. 9) two minima concerning the temperature behavior of thermal diffusivity, the first at -15°C and the second at about 50°C . The room temperature value for α after the initial heating is in agreement with $6.7 \times 10^{-8} \text{ m}^2\text{s}^{-1}$ found from frequency scan (Fig. 3, curve ' \circ '). The first anomaly was not observed in DSC experiments. The second anomaly at 50°C is associated with the onset of the relaxation prior to the glass transition as indicated by DSC measurements (Fig. 10). At subsequent cooling-heating cycles, the temperatures at which anomalies took place appears shifted to higher

values. As far as we are concerned the most important minimum for packaging applications is that close to 0°C existing after the initial heating cycle.

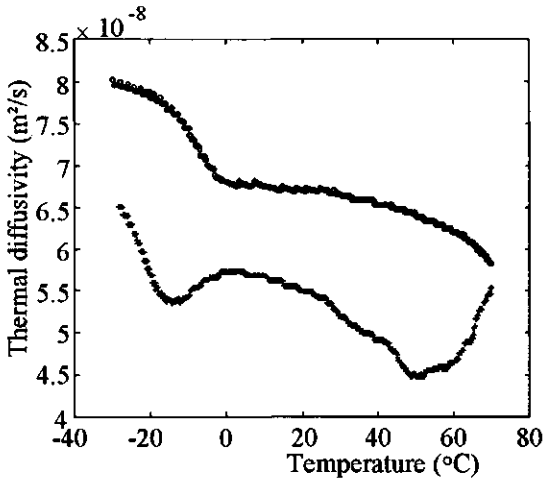


Figure 9 Thermal diffusivity versus temperature, for PVC 160 μm ; (+) heating and (o) cooling

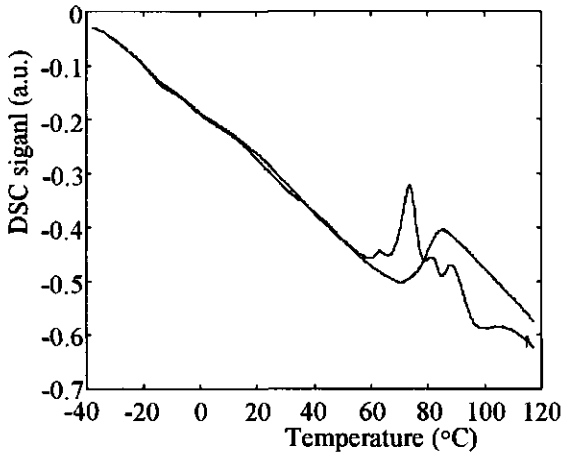


Figure 10 The DSC signal of PVC 160 μm (34.06 mg) plotted versus temperature (results of the first and second run). The first trace exhibit endothermal events, while the second trace shows a stable glass transition around 80°C

The thermal events observed in the first DSC heating run (Fig. 10) occur at the onset of the glass-rubber transition caused by enthalpy relaxation. The three successive peaks observed are most probably due to a poor thermal contact within the six layers stack. After heating to temperatures beyond the glass-rubber transition, repeated DSC runs show a stable glass

transition at 75°C (corrected for scan speed 4.5°C at 10 min). The glass transition region with the onset at 69°C is spread over 12°C. No influence of aging on the glass transition could be found, even after 10 weeks. Since the glass transition observed at 75°C is considerably lower than the expected 90°C for pure PVC, the investigated foil probably contained an appreciable amount of plasticizer.

Conclusions

The PPE method was used to study the temperature dependence (-30 to 70°C) of thermal diffusivity of selected plastic foils. The latter was found dependent on thermal history of sample. After the initial heating (up to 70°C) the thermal diffusivities of foils were significantly higher (7-20%) and remained constant during successive heating-cooling cycles. A possible explanation for this observation are structural changes (i.e. glass transitions) taking place in the material during thermal annealing. The thermal diffusivity values found for LDPE and PVC are comparable to data found in literature.

An interesting observation was the appearance of a minimum in the thermal diffusivity for the 160 µm thick PVC foil at low temperatures. Although not very pronounced, the occurrence of this minimum can be beneficial when using the material for packaging applications.

The PPE method was shown more practical and sensitive than the standard DSC. Except for the low temperature thermal event in foils the results of PPE measurements were generally confirmed by DSC method. An explanation for this phenomena could be the freezing of capillary water in the material.

One final remark concerns the use of Eq. (3). If one is interested to obtain values of all thermal parameters (C , κ or ϵ), the PPE signal can be calibrated with a thermal parameter (at room temperature); the complete temperature behavior can then be calculated. It was demonstrated⁷ that the inverse (front) PPE configuration with thermally thin sensor and thick sample is a useful approach to obtain thermal diffusivity of a sample at room temperature. Consequently, by combining these two configurations, the PPE method becomes independent of any other method or literature data. Unfortunately, this approach cannot be used for foils because of their small thickness.

References

- 1 Bershtein V.A. and Egorov V.M., *Differential Scanning Calorimetry of Polymers*, Physics, Chemistry, Analysis, Technology, Ellis Horwood, West Sussex (1994)
- 2 Bakker M. and Eckroth D., *The Wiley Encyclopedia of Packaging Technology*, Wiley & Sons New York (1986)
- 3 Brandrup J. and Immergut E.H., *Polymer Handbook* 3rd ed., Wiley, New York (1989)

- 4 Chirtoc M. and Mihailescu G., Theory of the Photopyroelectric Method for Investigation of Optical and Thermal Materials Properties, *Phys. Rev. B* **40**, 9606-9617 (1989)
- 5 Mandelis A. and Zver M.M., Theory of Photopyroelectric Spectroscopy of Solids, *J Appl Phys* **57**, 4421-4430 (1985)
- 6 Marinelli M., Mercuri F., Zammit U., Pizzoferrato R., Scudieri F. and Dadarlat D. Photopyroelectric Study of Specific Heat, Thermal Conductivity and Thermal Diffusivity of Cr_2O_3 at the Neel Transition, *Phys. Rev. B* **49**, 9523-9537 (1994)
- 7 Dadarlat D., Bicanic D., Visser H., Mercuri F. and Frandas A., Photopyroelectric Method for Determination of Thermophysical Parameters and Detection of Phase Transitions in Fatty Acids and Triglycerides. Part I: Principles, Theory and Instrumentational Concepts, *J. Amer. Oil Chem. Soc.* **72**, 273-279 (1995)
- 8 Dadarlat D., Bicanic D., Visser H., Mercuri F. and Frandas A., Photopyroelectric Method for Determination of Thermophysical Parameters and Detection of Phase Transitions in Fatty Acids and Triglycerides. Part II: Temperature Dependence of Thermophysical Parameters, *J. Amer. Oil Chem. Soc.* **72**, 281-287 (1995)
- 9 Dadarlat D., Bicanic D., Gibkes J., Kloek W., Dries I. van den and Gerkema E., Study of Melting Processes in Fatty Acids and Oils Mixtures: A Comparison of Photopyroelectric (PPE) and Photopyroelectric Observations of Melting Differential Scanning Calorimetry (DSC), *Chem. Phys. Lipids* **82**, 115-123 (1996)
- 10 Höhne G.W.H., Hemminger W. and Flammersheim H.-J., Differential Scanning Calorimetry: An Introduction for Practitioners, Springer-Verlag, Berlin (1996)
- 11 Hatley R.H.M., Franks F. and Green M., A Novel Data Acquisition, Retention and Examination System (Dares) for Differential Scanning Calorimetry, *Thermochimica Acta* **156**, 247-252 (1989)
- 12 Leite N.F., Cella N., Vargas H. and Miranda L.M.C., Photoacoustic Measurement of Thermal Diffusivity of Polymer Foils, *J. Appl. Phys.* **68**, 3025-3027 (1987)
- 13 Rantala J., Wei L., Kuo P.K., Jaarinen J. and Thomas R.L., Determination of Thermal Diffusivity of Low-Diffusivity Materials Using the Mirage Method with Multiparameter Fitting, *J. Appl. Phys.* **73**, 2714-2723 (1993)
- 14 Merté B., Korpiun P., Lüscher E., and Tilgner R., Thermal Diffusivity of Polymer Foils as a -Semicrystalline PETP and PE- as a Function of Drawings, *J. de Physique* **6** suppl. Colloq. C6, C6 463-467 (1983)
- 15 Mansanares A.M., Vargas H., Galembeck F., Buijs J. and Bicanic D., Photoacoustic Characterization of a Two-Layer System, *J. Appl. Phys.* **70**, 7046-7050 (1991).

Summary, Conclusion and Outlook

A rapidly increasing number of photothermal (PT) techniques has had a considerable impact on agriculture and environmental sciences in the last decade. It was the purpose of the work described here to develop and apply new PT techniques in this specific field of research.

Chapter 1 is a general introduction with an overview of PT techniques used in this research. Two different photoacoustic (PA) techniques used for optical characterization of a variety of condensed phase samples are discussed in chapters 2 and 3. The possibilities for thermal characterization of samples are described in chapter 4.

In chapter 2 classical PA spectroscopy with microphone detection was used to obtain spectra in the visible region (350-700 nm) of powdered (light scattering) food samples such as flours, coffee and spices (chapter 2.1). The outcome of these experiments suggest the feasibility of PA spectroscopy for quality control in the food-processing industry. Another PA cell was designed (chapter 2.2) and used in the IR region (10 μm). The final PA experiment was concerned with study of various carboxylic acids, alcohols and alkanes at 3.39 μm (chapter 2.3).

The feasibility of optothermal window (OW) method, an elegant approach to determine the optical absorption coefficient of condensed phase samples is described in chapter 3. The method was not only extended to 9-11 μm but also proved capable of investigating opaque samples (liquids and gel) which are otherwise not amenable to conventional IR spectroscopies.

The content of trans fatty acids in several margarine samples was measured with the OW technique and its performance compared to that of GLC, GLC + TLC and FTIR. The data obtained with the different methods were generally in a good agreement. The improved OW cell resulting in substantial reduction of the background signal, was then used to study extra virgin olive oil (chapter 3.2) adulterated by known adulterants (sunflower oil (4.5%) and safflower oil (6%)). The achieved limit of detection (LOD) was comparable to those reported in literature for other techniques (FTIR-ATR, GLC, HPLC and mass spectroscopy).

Many biological samples contain water that itself exhibits a strong absorption in IR. Quantitative measurements on such specimens are all but trivial. The new OW sensor was shown capable of direct and quantitative measurements (chapter 3.3 and 3.4) of lactose, corn starch and sulfate in water. The performance of the OW method was slightly inferior to that of FTIR. On the other hand, unlike the OW method, FTIR-ATR could only provide quantitative results for corn starch samples. As to the study of sulfate in water, the limit of detection (1 mmolL^{-1}) achieved with the OW method is one order of magnitude better than that of ATR.

In the fourth and last chapter, two different PT techniques (photopyroelectric method and photothermal beam deflection) were used for thermal characterization of a candy (a model for a glassy sugar system) and different packaging materials. The thermal diffusivity of a candy at room temperature found by PPE and PTBD was 14.7×10^{-8} and $12.0 \times 10^{-8} \text{ m}^2\text{s}^{-1}$ respectively. In addition, the PPE technique in the standard configuration, was used to measure temperature dependence of the thermal diffusivity in the -30°C to 70°C temperature range. The glass-rubber transition, underwent by the sample in this temperature range was observed and compared to the results obtained by differential scanning calorimetry (DSC).

The PPE technique was also used to obtain the temperature behaviour of thermal diffusivity of low density polyethylene and polyvinylchloride foils (used for packaging purposes). Such behavior was found dependent on the thermal history of the sample. The "untreated" foils exhibit values for thermal diffusivity that were consistently lower (7-20%) than those obtained for the same samples when heated to 70°C . The increase in thermal diffusivity is associated with structural changes (i.e. glass transitions) taking place in the material during thermal annealing. Additional measurements by differential scanning calorimetry (DSC) confirmed the validity of PPE results. It was shown that the PPE method is more sensitive than the standard DSC in detecting changes in thermal parameters.

Finally, the PPE method allows one in principle to obtain the temperature behavior of all static and dynamic thermal parameters provided one of the remaining thermal parameters (thermal conductivity, thermal effusivity and volume specific heat) is available at a given temperature.

Outlook

Results of a research described in this thesis show the feasibility of PT techniques for applications to a wide range of condensed phase samples. The methods used here constitute only a part of techniques developed and used in our laboratory. The low-cost and compact OW device is easy to handle and moreover offers the possibility for on-line studies of optically opaque and thermally thick samples that are normally not accessible by other techniques. It is anticipated that development of infrared diode lasers will increase the potential of the OW method because desired wavelengths characterized by the highest spectral contrast will become available. The sensitivity of the OW method was shown comparable to that of FTIR and therefore additional developments might eventually make the OW approach a candidate technique for quantitative analysis throughout the entire infrared region. The analytical potential of PT schemes becomes more obvious when they are used as detectors in combination with separation techniques such as GLC, HPLC or capillary electrophoresis.

The potential of photopyroelectric technique was demonstrated by obtaining thermal diffusivity values for different kind of samples. The PPE method is able to provide data on aging effect, structural stability and crystalline polymorphism. The technique is fast, sensitive and reproducible, requires small amounts of sample for analysis while providing more information than existing, classical methods used currently in thermal research. The only drawback of PPE is the necessity for good thermal contact between sample and sensor. When one is interested to obtain thermal diffusivity data in a non-contact manner the photothermal beam deflection (zero crossing method) is a valuable tool. Accurate (5% error) determination of thermal diffusivity is achievable due to intrinsically low errors in measurement of frequency and of zero crossing position.

In conclusion, based on the results of the work described here, one can anticipate that in the years to come the PT methods, alone or combined with existing techniques, will most likely play a more important role for variety of applications in agricultural and environmental sciences.

Samenvatting

Het hier beschreven promotieonderzoek gaat over nieuwe ontwikkelingen op het gebied van fothermische meettechnieken. De meest bekende is de fotoakoestische spectroscopie, welke door A.G. Bell is beschreven in 1880. Hij transporteerde geluid met behulp van licht over een afstand van 213 meter; hij was daarmee zijn tijd ver vooruit! Deze techniek werd een wetenschappelijke curiositeit, die een snelle dood stierf, maar een renaissance beleefde in de jaren 70. De verbeterde elektronica en de introductie van de laser droegen bij tot de nieuwe ontwikkelingen. De feitelijk doorbraak was de Rosencwaig-Gersho-theorie, die het mogelijk maakte om fothermische signalen op een eenvoudige manier te interpreteren.

Het basisprincipe van de fotoakoestiek berust op een omzetting van licht in geluid. Moleculen die lichtenergie absorberen komen in een aangeslagen toestand en kunnen terugkeren naar hun begintoestand door energie, in dit geval warmte aan de omgeving af te staan. Er zal lokaal een kleine opwarming zijn ($<0.001^{\circ}\text{C}$!!!!!!), en als men het licht met een bepaalde frequentie moduleert (aan-uit-aan-uit), zal de absorptie en opwarming met dezelfde frequentie plaatsvinden. Als een medium opwarmt zal dit uitzetten, met als gevolg een volume vergroting, wat beschouwt kan worden een drukgolf, welke gemeten kan worden met een microfoon.

Bell liet het licht door een roterende schijf met gaten vallen op een monster (gas, vloeistof of vaste stof). Het geluid dat Bell met een stethoscoop hoorde, had dezelfde frequentie als wanneer het zonlicht door de gaatjes in de schijf op het monster scheen. Ook vond hij dat de signaalsterke afhankelijk was van de lichtsterkte en de absorptie van het licht door het monster.

Een ander fothermisch effect, dat iedereen kent, is het "mirage effect": de zinderingen, die je bij mooi heet zomer weer boven het asfalt ziet. Door de warmte is de brekingsindex niet constant, waardoor lichtstralen niet rechtdoor gaan, maar worden afgebogen. De techniek die gebruikt maakt van het mirage effect heet fothermische deflectie en maakt gebruik van twee lasers. De eerste laser zorgt voor opwarming en de verandering in de brekingsindex, de tweede laser tast dit gebiedje af en wordt afgebogen. Om dit nauwkeurig te meten is goede en gevoelige elektronica nodig.

Deze fothermische technieken verschillen nogal van de conventionele transmissie spectroscopie. Bij de traditionele methode valt een bundel licht door een monster, waarna een detector meet welk deel van het licht er door komt. Dit wordt vergeleken met een referentie, zodat de absorptie van het monster kan worden berekend. Als nu al het licht wordt geabsorbeerd, meet de detector niets en kan er dus geen uitspraak worden gedaan over de absorptie. De oplossing is dan om de meetcel kleiner te maken, zodat het licht er nog wel

doorheen kan. Dit levert uiteraard problemen op als de cel te klein wordt. Wanneer het monster weinig absorbeert, geeft dit ook een probleem voor de detector: omdat er bijna 100% van het licht doorheen komt, is het niet te onderscheiden van de referentie. Sterk lichtverstrooiende monsters als poeders en suspensies lenen zich ook niet voor transmissie spectroscopie, omdat al het licht wordt gereflecteerd, zodat het de detector, die achter het monster staat, niet kan bereiken. Fotothermische spectroscopie kent al deze problemen niet.

De bedoeling van dit onderzoek was het ontwikkelen en toepassen van deze fotothermische technieken op zogezegd "moeilijke" monsters, die, zoals het woord al zegt, moeilijk te meten zijn met traditionele apparatuur.

Fotothermische technieken voor de bepaling van optische eigenschappen van materialen

Klassieke fotoakoestiek is gebruikt om optische verschillen aan materialen te meten. Voor veel levensmiddelen is de kleur een belangrijke kwaliteitsfactor. Daarom zijn in het zichtbare gebied van het spectrum verschillende soorten meel gemeten. Niet alleen de kleur (wit, geel of groen) van het meel kon gemeten worden, maar ook waren er verschillen te zien tussen fijn en minder fijn gemalen meel.

De optische verschillen zijn meestal klein en moeilijk te meten in het zichtbare deel van het spectrum. Daarom is er een nieuwe fotoakoestische cel gebouwd die het mogelijk maakte om in het infrarood te meten. Waarom infrarood? In theorie is infrarood spectroscopie de ideale methode om de samenstelling van monsters te meten omdat alle biologische en organische verbinding een karakteristiek infraroodabsorptie spectrum hebben, dat terug te voeren is op de moleculaire structuur. Deze "vingerafdrukken" van verbindingen maken het mogelijk om ze van elkaar te onderscheiden en onafhankelijk van elkaar te meten.

Een nieuwe fotoakoestische techniek, het "optothermische venster", is ontwikkeld om in het infrarood te meten. Hiermee kan niet alleen de mate van absorptie worden bepaald maar ook op een eenvoudige manier de absorptiecoëfficiënt. Het meetprincipe is vergelijkbaar met die van fotoakoestiek. De optothermische cel bestaat uit een infrarood transparant venster met daarop een kristal dat een stroom afgeeft op het moment dat daar warmte of druk opkomt. Het infrarode licht gaat door het venster waarop het monster ligt en dat de straling absorbeert. De warmte die in het monster ontstaat diffundeert naar het venster waardoor dit een beetje uitzet. De akoestische golf die dan ontstaat wordt dan gemeten m.b.v. het kristal.

Zoals hiervoor staat geschreven heeft iedere verbinding zijn eigen vingerafdruk in het infrarood. Door de juiste absorptiepiek(en) te kiezen, kan het optothermisch venster gebruikt worden om de legio toepassingen, die er zijn, te meten: de concentratie van transvetzuren in margarine, de echtheid van olijfolie en de concentratie van lactose, maiszetmeel en sulfaat in

water. De nieuwe techniek is vergeleken met andere moderne meettechnieken en bleek vaak net zo gevoelig. Het grote voordeel van deze sensor is dat hij relatief goedkoop is en makkelijk te bedienen en schoon te maken.

Fotothermische technieken voor de bepaling van thermische eigenschappen van materialen

Fotothermische technieken kunnen, behalve voor de bepaling van optische kwaliteiten, ook heel goed gebruikt worden om thermische eigenschappen van materialen te bepalen. In het laatste deel van dit onderzoek zijn de fotopyroelektrische methode en de fotothermische deflectie techniek gebruikt om de warmtevereffeningscoëfficiënt te berekenen. Deze parameter bepaalt hoe makkelijk warmte zich verdeelt in een monster (bijvoorbeeld de maat voor de snelheid waarmee een ei in kokend water de temperatuur van het water heeft gekregen). De fotopyroelektrische methode kan de warmtevereffeningscoëfficiënt bij verschillende temperaturen (-40 tot 80 °C) meten. Het is niet alleen interessant om de vereffeningscoëfficiënt te meten bij verschillende temperaturen, maar op deze manier is het ook mogelijk fase-overgangen te bestuderen, bijvoorbeeld het smeltgedrag van vetten. Hier is deze techniek gebruikt om naar een glasovergang te kijken in een snoepje, wat als model staat voor een suikersysteem. Momenteel wordt veel onderzoek verricht naar glasovergangen in levensmiddelen, omdat die van groot belang zijn voor de houdbaarheid. Met de fotopyroelektrische methode kon de glasovergang goed gemeten worden. De resultaten zijn vergeleken en bevestigd met een conventionele methode, namelijk differentiële scanning calorimetrie.

Als laatste is met deze twee methoden gekeken naar plastics: PVC en LDPE. Deze folies worden gebruikt voor verpakkingsmateriaal en ook hier is het van belang te meten wat de thermische parameters zijn bij verschillende temperaturen. Bij deze metingen was er echter een groot verschil tussen de twee gebruikte technieken. De fotopyroelektrische methode bleek veel gevoeliger en nauwkeuriger dan de differentiële scanning calorimetrie.

Dankwoord

Kersvers in dienst als AIO kon ik gaan inpakken; we moesten verhuizen van Duivendaal naar het nieuwe schip op de Dreijen. Het ging allemaal niet soepel maar dat kwam vooral doordat het gebouw nog niet af was en het er lawaaiig was. Een ander probleem was dat het nog negen maanden zou duren voor het lab klaar zou zijn en we de 'boel' konden gaan schoonmaken en opbouwen. De bibliotheek was een toevluchtsoord; ik heb nog nooit zoveel gelezen als toen. Uiteindelijk lagen we in een veilige haven, mede omdat we omgeven waren door 'schepen' met gelijke lading.

In de afgelopen jaren genoot ik van de grote vrijheid die ik kreeg en van de congressen die ik kon bezoeken in China, VS, Guadeloupe, Slovenië en Duitsland. Het was een goede tijd maar daarentegen miste ik wel mede AIO's die voor een kritische massa konden zorgen.

Tijdens mijn promotieonderzoek heb ik regelmatig het gevoel gehad: waar doe je het eigenlijk allemaal voor. Wat ik wel heb ervaren is dat je het niet alleen doet. Een groot aantal mensen zijn direct of, minstens zo belangrijk, indirect betrokken geweest bij het totstandkomen van dit promotieboekje.

Allereerst wil ik Dane bedanken. Hij stond altijd voor me klaar en had eindeloos veel ideeën. Daarnaast ken ik geen begeleider die een manuscript de volgende dag gecorrigeerd teruggeeft. Voor zijn snelheid en vechtlust ('nooit opgeven') heb ik dan ook grote bewondering. Als een Don Quichot vecht hij tegen 'the monkeys' voor het behoud van natuurkundig onderzoek binnen Wageningen.

Professor dr. J. Reuss wil ik bedanken voor de inhoudelijke discussies die we aan het eind gevoerd hebben en welke een duidelijke bijdrage hebben geleverd in het uiteindelijke resultaat.

Om onderzoek te verrichten heb je 'spullen' nodig en dan zijn werkplaatsen onontbeerlijk. Kees, niet alleen jouw kennis, maar ook jouw inzicht in de problematiek, speelden een doorslaggevende rol in het onderzoek. Ook de medewerkers van de fijn-mechanische werkplaats en de glasblazerij zijn van onschatbare waarde geweest voor het onderzoek.

In de *natuurkundegang* gebeurde veel, maar ik denk dat het koffie drinken het belangrijkste ritueel was. De vele buitenlandse gastmedewerkers brachten naast gezelligheid in het lab ook nieuwe kennis, die de productiviteit van het werk ten goede kwam. My word of thanks to Stephen, Nicu, Mladen, Mihai, Jürgen, András, Thomas, Ótto and Angela.

Een belangrijke rol was ook weggelegd voor clubjes als 'de Jeugd', 'Unitas Lunch Groepje', 'Rhine Town Tigers' en 'de Moleculairs'. Zij waren vooral belangrijk voor de mentale opvang en de *reset* van de geest. Hockey is een gezelligheidssport en met RTT hebben we een grote reputatie opgebouwd. De Moleculairs hebben een speciaal plekje, omdat zij als geen ander weten wat dit werk inhoudt!

Janine ik wil je hier bedanken voor alles wat jij voor mij betekend hebt en zult betekenen. Koos en Gusta, jullie interesse en mening zijn altijd erg belangrijk voor mij geweest.

Curriculum Vitae

Jan Paul Favier werd op 6 juli 1967 geboren te Leiden. In 1985 behaalde hij het eindexamen Atheneum aan de Samenwerkingsschool te Waddinxveen. Aansluitend startte hij de studie moleculaire wetenschappen aan de toenmalige Landbouwhogeschool in Wageningen. Tijdens de doctoraalstudie volgde hij de fysisch-chemische oriëntatie en koos als hoofdvakken: fysische- en colloïdchemie en natuurkunde. De stage periode werd doorgebracht aan het isotopen instituut van de Hongaarse academie van wetenschappen, Budapest, Hongarije. In 1991 behaalde hij het doctoraalexamen.

Vervolgens trad hij in 1992 in dienst, als assistent in opleiding, bij het fotoakoestisch laserlab bij de vakgroep agrotechniek en -fysica van de landbouwuniversiteit te Wageningen. De resultaten van dit onderzoek hebben tot dit proefschrift geleid. Tijdens zijn promotie-onderzoek heeft hij 2 maanden gewerkt bij Department of Physical Chemistry, Cambridge University in Engeland.

List of Publications

- Favier J.P., Dadarlat D., Gibkes J., Van den Berg C., Bicanic D., Thermal diffusivity of hard boiled candy Obtained by Photothermal Beam Deflection and Standard Photopyroelectric Method, accepted in *Instrum. Sci. Technol.* (1997)
- Favier J.P., Bicanic D., Iersel M. van, Helander P., The optothermal approach to a real time monitoring of glucose content during fermentation by brewers' yeast, accepted in *J. Biochem. Biophys. Methods* (1997)
- Favier J.P., Bicanic D., Dóka O., Chirtoc M., Helander P., Optothermal detection of infrared radiation-induced absorption in aqueous solutions of carbohydrates: lactose and corn starch, *J. of Agriculture & Food Chemistry* **45**, 777-780 (1997)
- Bicanic D., Franco M., Gibkes J., Gerkema E., Favier J.P. and Jalink H., Applications of photoacoustic and photothermal non-contact methods in selected areas of environmental and agricultural sciences, Chapter 5, in *Life and Earth Sciences "Progress in Photoacoustic and Photothermal Science III"*, A. Mandelis (ed.), SPIE Optical Engineering Press, Washington DC. (1997)
- Favier J.P., Iersel M. van, Dóka O., Koenderman I., Schouten F., Asselt K, van, Bicanic D. and Helander P., Applications of a universal optothermal window detector for samples of agricultural purpose, *Progress in Natural Sciences* **6**, S562-564 (1996)
- Gibkes J., Dadarlat D., Favier J.P., Bicanic D., Bein B. and Gerkema E., Thermal diffusivity measurement of selected metals, technical graphites and magnetic materials: zero crossing points and phase methods versus photopyroelectric technique-an intercomparison study, *Progress Natural Sciences* **6**, S273-277 (1996)
- Favier J.P., Bicanic D., Chirtoc M., Helander P., Compact, open and general purpose cell of variable effective pathlength: direct absorption measurements of SO_4^{2-} in water, *Fresenius J. Analytical Chemistry* **355**, 357-358 (1996)
- Favier J.P., Bicanic D., Bovenkamp P. van de, Chirtoc M., Helander P., Determination of total trans fatty acids content in margarine: an intercomparison study GLC, GLC + TLC, FTIR and optothermal window (open photoacoustic cell), *Analytical Chemistry* **68**, 729-733 (1996)
- Bicanic D., Chirtoc M., Chirtoc I., Favier J.P., Helander P., Photothermal determination of absorption coefficients in optically dense fluids: application to oleic acid and water at co laser wavelengths, *Applied Spectroscopy* **49**, 1485-1489 (1995)
- Bicanic D., Dadarlat D., Gibkes, J, Chirtoc M., Favier J.P., Gerkema E., The photopyroelectric approach to thermal characterization of liquid and pasty foodstuffs and on optothermal

- accessory for obtaining infrared spectra of optically dense fluids, *Acta Chimica Slovenica*, **42**, 153-173 (1995)
- Bicanic D., Chirtoc M., Chirtoc I., Veldhuizen B. van, Favier J.P., Helander P., New technique for measuring absorption coefficients of strongly absorbing liquids: optothermal study of sunflower oil, oleic acid and its chloroform solutions at 3.39 microns, *Spectroscopy Letters* **28**, 101-110 (1995)
- Favier J.P., Bicanic D., Asselt K. van, Miklos A., Organic compounds measured with infrared (3.39 μm) photoacoustics, *J. de Physique IV* **4**, 495-497 (1994)
- Bicanic D, Chirtoc M, Chirtoc I, Vanveldhuizen B., Favier J.P., Helander P., Harryvan J., Cozijnsen J., Lubbers M., New approach in determining absorption coefficients of strongly absorbing liquids: optothermal studies sunflower oil, oleic acid (and its chloroform solutions) at 3.39 microns, *J. de Physique IV* **4**, 487-490 (1994)
- Favier J.P., Buijs J., Miklós A., Lorincz A., Bicanic D: Photoacoustic characterization of different food samples, *Zeitschrift für Lebensm.-Untersuchung und-Forschung* **199**, 59-63, (1994)
- Favier J.P., Miklós A. and Bicanic D., New and versatile photoacoustic for studies of powdered specimens across broad spectral range, *Acta Chimica Slovenica*, **40**, 115-122 (1993)
- Buijs J., Favier J.P., Dóka O. and Miklós A., Photoacoustic signal generation and spectra of powders, *Springer Series in Optical Sciences Vol 69*, Photoacoustic and Photothermal Phenomena III, page 168-170, editor D. Bicanic, Springer-Verlag Berlin, Heidelberg, New York (1992)
- Norde W. and Favier J.P., Structure of adsorbed and desorbed proteins, *Colloid and Surfaces* **64**, 87-93 (1992)
- Strauss E., Favier J.P., Bicanic D., Asselt K. van, Lubbers M., Sensitive colorimetric determination of ammonium ion in water by laser photothermal detection, *The Analyst*, **116**, 77-79 (1991)
- Bicanic D., Favier J.P., Strauss E., Lubbers M. and Fleuren G., Low-cost colorimetric measurement of phosphate trace levels in water and soil solutions by the collinear photothermal beam deflection method, *Internat. J. Environ. Anal. Chem.*, **38**, 623-628 (1990)
- Bicanic D., Strauss E., Favier J.P., Miklós A., Torfs P. and Lubbers M., Photothermal colorimetry of phosphorus and ammonium in aqueous phase for use in the agricultural practice, *Springer Series in Optical Sciences, Vol 62*, Photoacoustic and Photothermal Phenomena II, 445-447, editors: J.C. Murphy e.a., Springer-Verlag, Heidelberg (1990)